

Hysteresis Modeling of Wood Joints and Structural Systems

by

Greg C. Foliente

Thesis submitted to the Faculty of the
Virginia Polytechnic Institute and State University
in partial fulfillment of the requirements for the degree of

MASTER OF SCIENCE

in

Civil Engineering

APPROVED :



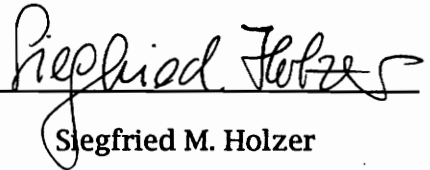
Mahendra P. Singh, Co-chairman



Raymond H. Plaut, Co-chairman



J. Daniel Dolan



Siegfried M. Holzer

June, 1993

Blacksburg, Virginia

C.2

LD
5655
V855
1993
F6441
C.2

Hysteresis Modeling of Wood Joints and Structural Systems

by

Greg C. Foliente

Committee Co-chairs: Mahendra P. Singh and Raymond H. Plaut

Civil Engineering

(Abstract)

Difficulties in characterizing the dynamic behavior of wood structures have hindered investigations into their performance under dynamic loading. Because of this, wood structures are treated unfavorably in seismic design codes, even though past damage assessment surveys after seismic events indicated generally satisfactory performance. To allow investigations into their performance and safety under dynamic loading, the energy dissipation mechanisms of wood joints and structural systems must be known and the hysteretic behavior modeled properly. This thesis presents a general hysteresis model for wood joints and structural systems, based on a modification of the Bouc-Wen-Baber-Noori (BWBN) model. The hysteretic constitutive law, based on the endochronic theory of plasticity and characterized by a single mathematical form, produces a versatile, smoothly varying hysteresis that models previously observed behavior of wood joints and structural systems, namely, (1) nonlinear, inelastic behavior, (2) stiffness degradation, (3) strength degradation, (4) pinching, and (5) memory. The constitutive law takes into account the experimentally observed dependence of wood joints' response to their past history (i.e., the input and response at earlier times, or memory). Practical guidelines to estimate the hysteresis parameters of any wood joint or structural system are given. Hysteresis shapes produced by the proposed model are shown to compare reasonably well with experimental hysteresis of wood joints with: (1) yielding plate, (2) yielding nails, and (3) yielding bolts. To demonstrate its use, the proposed model is implemented in a nonlinear dynamic analysis program for single-degree-of-freedom (SDF) systems. System response from arbitrary dynamic loading, such as cyclic or earthquake-type loadings, can be computed.

Three SDF wood systems are subjected to the Loma Prieta accelerogram to obtain their response time histories. Advantages of using the proposed model over currently available models in nonlinear dynamic analysis of more complex systems are identified. A multidegree-of-freedom shear building model incorporating the proposed hysteresis model is formulated but not implemented on a computer.

Acknowledgements

I wish to express my gratitude to Drs. Mahendra P. Singh and Raymond H. Plaut for co-chairing my Master's committee. My interest in structural dynamics and earthquake engineering was heightened by the teaching and research of Dr. Singh. I have learned a lot from him. Dr. Plaut provided support in various aspects of this work. I am also grateful to Drs. J. Daniel Dolan and Siegfried M. Holzer for serving in my committee and for their comments.

Some of the researchers responsible for the original model, that forms the basis for the present work, were very cooperative and helpful. I thank Dr. Y.-K. Wen of the University of Illinois at Urbana-Champaign, Dr. R.H. Sues of Applied Research Associates, Inc. in Raleigh, North Carolina and Dr. M.N. Noori of Worcester Polytechnic Institute in Massachusetts. The encouragement and information provided by Dr. Noori are deeply appreciated.

This project was funded by the U.S. Department of Agriculture's National Research Initiative, Competitive Grants Program for Forest and Rangeland Renewable Resources. Dr. Thomas E. McLain served as my initial supervisor. I treasure the opportunity of being associated with him.

I am especially indebted to my wife, Tomoko, for her encouragement and abiding love. I am extremely blessed to have such a patient and supportive wife. Finally, I thank my parents and brothers, who have always been a constant source of love and support.

“The fear of the Lord is the beginning of wisdom, and knowledge of the Holy One is understanding.”

- Proverbs 9:10

Table of Contents

List of Figures	ix
Notation	xii
1 Introduction	1
1.1 General	1
1.2 Objectives	2
1.3 Thesis Overview	5
2 Literature Review	7
2.1 General	7
2.2 Basic Concepts of Structural Dynamics	8
2.2.1 Introduction	8
2.2.2 Equation of Motion	9
2.2.3 Damping and Energy Dissipation	11
2.3 Wood Structures and Components	14
2.3.1 Behavior of Wood Structural Systems	14
2.3.2 Hysteretic Characteristics	17
2.4 Hysteresis Models	20
2.4.1 Models for General Dynamic Analysis	20
2.4.2 Current Models for Wood Systems	24
2.4.3 Comments	30
2.5 Summary	33
3 Hysteresis Modeling	35
3.1 General	35

3.2	Approach to Modeling	36
3.3	Mechanical Model	36
3.4	The Bouc-Wen-Baber-Noori Model	38
3.4.1	Background	38
3.4.2	Equation of Motion and Constitutive Relations	40
3.4.3	Hysteresis Shape Properties	41
3.4.3.1	Parameters A and α	41
3.4.3.2	Parameters β and γ	43
3.4.3.3	Parameter n	45
3.4.4	Strength and Stiffness Degradation and Pinching	48
3.4.5	Model Limitation	57
3.5	Pinching of Wood Systems	57
3.5.1	Experimental Observations	57
3.5.2	Pinching Function Development	60
3.6	Summary	61
4	Dynamic Modeling of Wood Structures	64
4.1	General	64
4.2	Proposed Model for Wood Structural Systems	64
4.2.1	Model for SDF Systems	64
4.2.2	Model for MDF Systems	67
4.2.2.1	Shear Building Model	67
4.2.2.2	Alternatives to the Shear Building Model	73
4.3	Parameter Estimation	75
4.4	Comparison With Experimental Hysteresis	76
4.5	Potential	78
4.6	Summary	79
5	Nonlinear Dynamic Analysis	81

5.1	General	81
5.2	Preliminary Considerations	82
5.2.1	Governing Equations	82
5.2.2	Overview of Numerical Solution Methods	82
5.2.3	Solution Approach	84
5.3	Response to General Cyclic Loading	84
5.4	Time History Analysis	89
5.4.1	Ground Accelerogram	89
5.4.2	Seismic Response	89
5.4.2.1	Trussed-frame Building	91
5.4.2.2	Building with Plywood Shear Walls	91
5.4.2.3	Heavy Timber Building	96
5.5	Comments	96
5.6	Summary	99
6	Conclusions and Recommendations	101
6.1	Summary and Conclusions	101
6.2	Recommendations for Future Work	102
	Bibliography	105
	Vita	114

List of Figures

1.1	Block scheme of the dynamic analysis process	3
1.2	Typical load-displacement relations	4
2.1	A linearly elastic-perfectly plastic single-degree-of-freedom system	10
2.2	Energy terms using absolute energy formulation (from Uang and Bertero 1990)	15
2.3	Some common structural systems	16
2.4	Typical hysteresis of wood subassemblies	18
2.5	Typical hysteresis loops for wood joints	19
2.6	Illustrations of hysteresis models for various structures	22
2.7	Hysteresis model proposed by Ewing et al. (1980) for wood diaphragms	25
2.8	Hysteresis model proposed by Kivell et al. (1981) for moment resisting nailed timber joints	26
2.9	Hysteresis models proposed for nailed sheathing-to-frame connections	28
2.10	Hysteresis model proposed by Ceccotti and Vignoli (1990) for moment resisting semi-rigid wood joints	29
2.11	Hysteresis models proposed by Japanese researchers	31
2.12	Hysteresis model proposed by Foschi and his associates (UBC 1993) for wood joints with dowel-type fasteners	32
3.1	Typical mechanical models for nonlinear systems	37
3.2	Hysteretic SDF system for wood structural systems	39
3.3	Nondegrading and non-pinching BWBN model: (a) $z-u$ plane, (b) F_T-u plane	44
3.4	Hysteresis loop behavior for $n=1$	46
3.5	Possible hysteresis shapes, $n=1$ (from Baber 1980)	47

3.6	Skeleton curves with varying n	49
3.7	Strength and stiffness degradation- effect of varying A	51
3.8	Strength degradation- effect of varying ν	52
3.9	Stiffness degradation- effect of varying η	53
3.10	Degradation effect using dz/du vs. z/z_u plot	54
3.11	Baber and Noori's (1986) pinching function effect (dz/du vs. z/z_u)	56
3.12	Hysteresis during partial loading-unloading	58
3.13	Pinching of wood systems (dz/du vs. z/z_u)	59
3.14	Behavior of the proposed pinching function for wood systems	62
4.1	SDF idealization of wood structural systems	66
4.2	MDF idealization of multi-storey wood buildings	69
4.3	Sakamoto and Ohashi's (1988) MDF idealization of multi-storey conventional Japanese houses	70
4.4	Hysteresis frame discrete hinge model (from Baber 1986b)	74
4.5	Hysteresis loops produced by the modified BWBN model	77
5.1	Loading types handled by the computer program	86
5.2	Cyclic loading patterns for tests of wood joints and structural systems	87
5.3	Modified BWBN response to general cyclic load	88
5.4	The Loma Prieta earthquake ground acceleration	90
5.5	Hysteresis response of a trussed-frame building to the Loma Prieta accelerogram	92
5.6	Response time histories of a trussed-frame building to the Loma Prieta accelerogram	93
5.7	Hysteresis response of a building with plywood shear walls to the Loma Prieta accelerogram	94
5.8	Response time histories of a building with plywood shear walls to the Loma Prieta accelerogram	95

5.9 Hysteresis response of a heavy timber building to the Loma Prieta ac-
celerogram 97

5.10 Response time histories of a heavy timber building to the Loma Prieta
accelerogram 98

Notation

The following variables and symbols are used in this thesis:

A	=	parameter that affects the tangent stiffness and ultimate hysteretic strength;
A_o	=	initial value of A ;
a_1, a_2, a_i	=	amplitude of cyclic excitation;
$[C]$	=	the damping matrix of a multidegree-of-freedom (MDF) system;
c	=	viscous damping coefficient;
c_i	=	viscous damping coefficient of i^{th} mass;
E_a	=	absorbed energy;
E_h	=	hysteretic energy;
E_i	=	input energy;
E_s	=	elastic strain energy;
E_{ξ}	=	damping energy;
$F(t)$	=	forcing function;
F_h	=	hysteretic restoring force;
F_T	=	total non-damping restoring force;
F_{T_y}	=	yield level of F_T ;
\mathbf{f}	=	vector of the dynamic actions;
$f(t), f_i(t)$	=	mass-normalized forcing function;
f_s	=	non-damping restoring force;
$h(z)$	=	pinching function;
$[H^\alpha]$	=	matrix that contains the hysteretic elements;
h_i^α	=	hysteretic coefficient of i^{th} element $[(1 - \alpha_i)k_i]$;
$\{I\}$	=	the influence vector;
$[K^\alpha]$	=	linear part of the stiffness matrix;

k	=	stiffness;
k_i, k_f	=	initial and final tangent stiffness, respectively;
k_i^α	=	linear spring coefficient of i^{th} element ($\alpha_i k_i$);
m	=	system mass;
m_i	=	mass of the i^{th} element;
n	=	hysteresis shape parameter that controls curve smoothness;
P	=	applied force;
p	=	constant that controls the rate of initial drop in slope;
Q_i	=	total restoring force of the i^{th} mass;
q	=	fraction of ultimate hysteretic strength, z_u , where pinching occurs;
\mathfrak{R}	=	differential operator;
r	=	total number of lumped masses in a MDF model;
$[M]$	=	the mass matrix of a MDF system;
$\text{sgn}(\cdot)$	=	the signum function;
t, t_i	=	time;
\mathbf{u}	=	vector of system response;
u	=	relative displacement of the mass with respect to the base displacement;
\dot{u}	=	relative velocity of the mass with respect to the base velocity;
\ddot{u}	=	relative acceleration of the mass with respect to the base acceleration;
u_g	=	earthquake ground displacement;
\ddot{u}_g	=	earthquake ground acceleration;
u_i	=	interstorey drift, or relative displacement between floors;
u_{max}	=	maximum relative displacement;
u_0	=	relative displacement at $z = 0$;
u_{pi}	=	peak displacement in i^{th} half cycle;
u_{pi-1}	=	peak displacement in $(i - 1)^{th}$ half cycle (note that this is the peak

	opposite and immediately before that in the i^{th} half cycle);
u_t	= absolute or total mass displacement ($u + u_g$);
u_y	= yield relative displacement;
y	= vector of global response of a single-degree-of-freedom (SDF) system;
y_i	= i^{th} element of response vector y ;
\dot{y}_i	= time derivative of y_i ;
$\{X\}$	= vector of relative displacements;
x_i	= relative displacement of the i^{th} mass with respect to the ground displacement;
\dot{x}_i	= relative velocity of the i^{th} mass with respect to the ground velocity;
\ddot{x}_i	= relative acceleration of the i^{th} mass with respect to the ground acceleration;
\ddot{x}_g	= ground acceleration;
\ddot{x}_i^A	= absolute acceleration ($\ddot{x}_i + \ddot{x}_g$);
$\{Z\}$	= vector of the hysteretic components of the displacements;
z	= hysteretic component of the displacement;
z_i	= hysteretic displacement of the i^{th} mass;
z_{p_i}	= peak z value in i^{th} half cycle;
$z_{p_{i-1}}$	= peak z value in $(i - 1)^{th}$ half cycle;
z_u	= ultimate value of z (or z at $\frac{dz}{du} = 0$);
α	= a weighting constant representing the relative participations of the linear and nonlinear terms ($0 < \alpha < 1$);
β	= hysteresis shape parameter;
γ	= hysteresis shape parameter;
δ_A	= constant that controls the rate of strength and stiffness degradation;
δ_{ij}	= Kronecker delta;
δ_η	= constant that controls the rate of stiffness degradation;
δ_ν	= constant that controls the rate of strength degradation;

δ_ψ	=	parameter specified for the desired rate of change of ζ_2 based on ε ;
ε	=	dissipated hysteretic energy;
$\dot{\varepsilon}$	=	the rate of change of dissipated hysteretic energy;
ζ_1	=	controls the magnitude of initial drop in slope, $\frac{dz}{du}$, ($\zeta_1 < 1.0$);
ζ_{1o}	=	measure of total slip;
ζ_2	=	controls the rate of change of the slope, $\frac{dz}{du}$;
η	=	stiffness degradation parameter;
η_i	=	value of η during the i^{th} half cycle;
λ	=	small parameter that controls the rate of change of ζ_2 as ζ_1 changes;
μ	=	ductility;
ν	=	strength degradation parameter;
ξ	=	viscous damping ratio;
ξ_o	=	linear damping ratio ($c/2\sqrt{k_i m}$);
ψ	=	parameter that contributes to the amount of pinching;
ω, ω_i	=	frequency of cyclic excitation;
ω_n	=	natural frequency of undamped oscillation;
ω_o	=	preyield natural frequency of the system ($\sqrt{k_i/m}$).

Chapter 1

Introduction

1.1 General

Wood structures are generally recognized to perform well in seismic zones. This is attributed to wood's high specific strength (high strength to weight ratio), redundancy of non-load bearing elements including the presence of non-engineered shear walls and diaphragms and unit action of the system when the components are adequately fastened. Favorable system geometry, e.g. symmetrical plan for earthquake and steep roof slope for wind, also contribute to its performance.

Wood construction does not, however, guarantee earthquake- and/or hurricane-resistant structures. Assessments of collapsed or damaged wood buildings after earthquakes and typhoons have identified common failure modes and their possible causes and solutions (Soltis 1984; Falk and Soltis 1988; Conner et al. 1987). Most of what we know about wood structural behavior under dynamic loading, however, comes from qualitative field data and/or limited experimental data, with little theoretical understanding of actual behavior. Difficulties in characterizing wood system behavior (e.g., sensitivity of material properties to the rate and duration of loading and inelastic and nonlinear behavior) have hindered investigations into their performance under dynamic loading. Because of this, wood structures are treated unfavorably in seismic design codes. Stringent and unclear code requirements put wood at a disadvantage in competing with other traditional construction materials, such as steel and concrete, for the engineered structures market. Methods for dynamic analysis of wood structures are needed to investigate the performance and safety of engineered wood systems.

A *dynamic analysis* or *dynamic response analysis* problem is one where the dynamic action (i.e., force) on a structural system— which is modeled mathematically by the assumed (or measured) mass, damping and stiffness properties of the actual system— is known and the corresponding system response is sought (Fig. 1.1). Accuracy of the computed response depends on the accuracy of the mathematical model used to describe the actual system. Thus, the model should provide as realistic a description of the actual structure's behavior as possible. With static monotonic loading, an appropriate load-displacement relation is normally sufficient to predict system response (Fig. 1.2a). With cyclic loading, the load-displacement trace produces *hysteresis* loops (Fig. 1.2b) caused by damping and/or inelastic deformation. (The area contained in the loop represents the *energy dissipated* by the structure.) Analytical modeling of an inelastic structure under dynamic loading ideally requires a force-displacement relation, or hysteresis model, that can produce the true behavior of the structure at all displacement levels and strain rates (Sozen 1974). Consequently, the energy dissipation mechanisms of wood joints and structural systems must be known and the hysteretic behavior modeled properly before we can accurately predict the overall system response of wood structures to dynamic loads.

Since (1) there are hundreds of combinations of materials and joint configurations in wood systems, and (2) wood-based products, fasteners and use of wood-based products continue to evolve, a general model is preferred over models derived from specific configurations. A completely empirical model will not only be expensive to obtain but may also be of limited use in dynamic analysis. A mathematical model, that simulates the general hysteretic features of wood systems, is preferred. Parameters of the new hysteresis model may be estimated from data obtained from previous tests of specific wood joints and assemblies.

1.2 Objectives

The objectives of the present work are to:

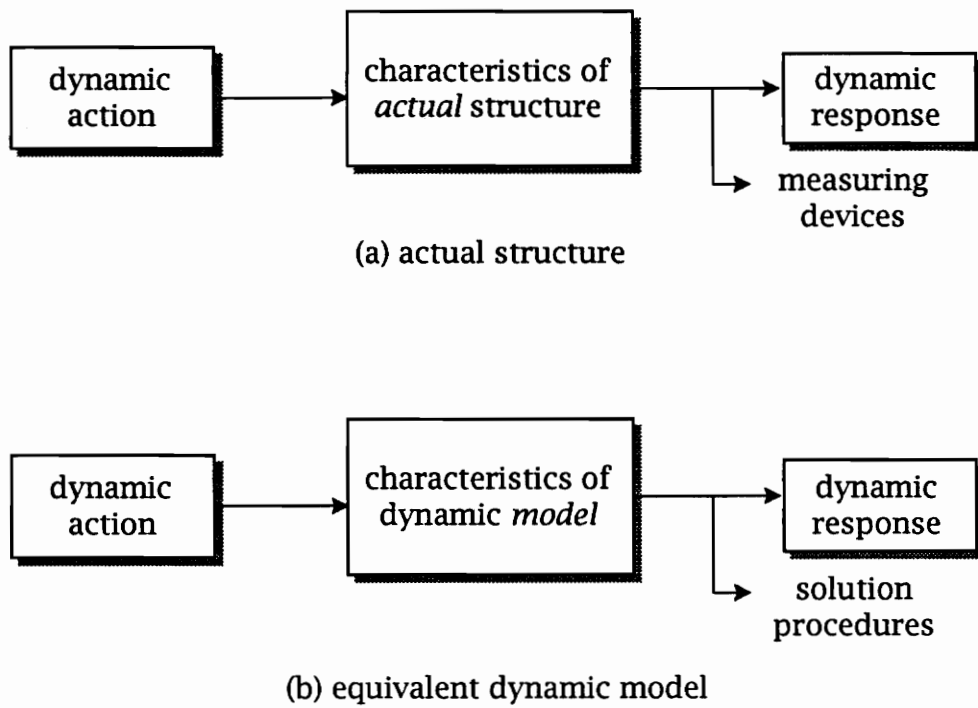
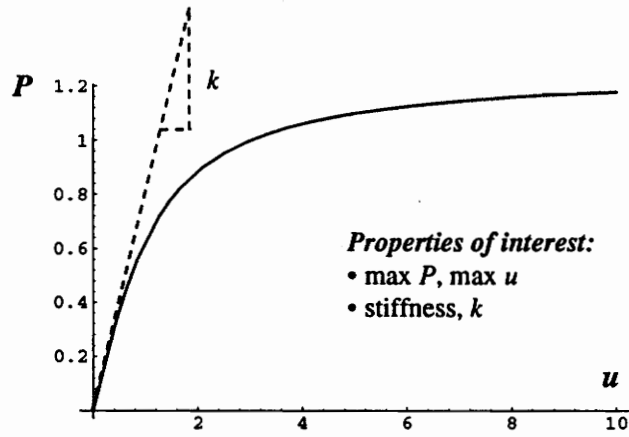
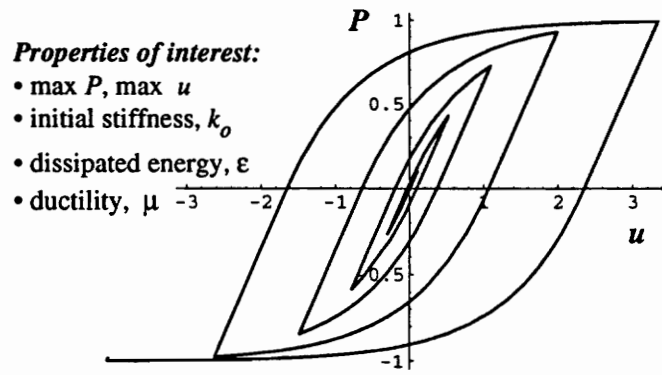


Figure 1.1: Block scheme of the dynamic analysis process



(a) due to monotonic loading



(b) due to cyclic loading

Figure 1.2: Typical load-displacement relations

1. develop a general hysteresis model that simulates experimentally observed behavior of wood joints and structural systems under cyclic loading, and
2. incorporate the hysteresis model into a dynamic analysis computer program to allow response computations of wood structural systems under arbitrary dynamic loading.

To fulfill these objectives, it is sufficient to limit the present analysis to a single-degree-of-freedom (SDF) wood system. The hysteresis model developed for a SDF system can also be used for a more refined analysis of wood structures and structural systems using multi-degree-of-freedom (MDF) models. It is also desired that a general set of rules for identifying hysteresis model parameters for common wood systems be established.

1.3 Thesis Overview

A review of literature related to basic concepts of structural dynamics, observed behavior of wood joints and structural systems, and hysteresis modeling is presented in Chapter 2. Characteristic features of hysteresis behavior of wood joints are identified and current hysteresis models that have been used and proposed for dynamic analysis of wood structures are also reviewed. In Chapter 3, the approach taken in modeling the general hysteretic behavior of wood joints and structural systems, and the form and properties of the proposed model are discussed. Generalization of the pinching capability of the Bouc-Wen-Baber-Noori (BWBN) model, to complete the proposed hysteresis model for wood, is presented. Chapter 4 gives a summary of the proposed hysteresis model for SDF systems, presents the formulation for MDF shear building models, introduces the topic of systems identification and provides a general set of rules for identifying hysteresis model parameters for wood systems. Model hysteresis is compared with experimental hysteresis of common wood joints. The new model is incorporated in a nonlinear dynamic analysis program. Chapter 5 describes

the program and presents time history analysis results of three hypothetical SDF wood buildings subjected to the Loma Prieta accelerogram. Finally, Chapter 6 presents a set of conclusions for the present study and recommendations for future work.

Chapter 2

Literature Review

2.1 General

Research on dynamic analysis of wood structures lags behind advances in general structural dynamics mainly because of (1) many factors affecting the collection of test data and (2) difficulties in characterizing the dynamic behavior of wood joints and structural systems. An international workshop on full-scale behavior of wood-framed buildings in earthquakes and high winds produced a document presenting the state-of-the-art and the specific research needs on the earthquake and wind performance of low-rise, light-framed wood construction (Gupta and Moss 1991). Summarizing the research needs in mathematical modeling of wood-framed buildings, Stalnaker and Gramatikov (1991) stressed the need for accurate hysteresis models for wood components, subcomponents and (both inter-element and inter-component) connections and for tests from which the model can be derived. The hysteresis model should be incorporated into a dynamic analysis procedure that would allow response computations of wood structures under dynamic loading. The need for various types of parametric studies was also identified.

The objectives of this chapter are to elaborate on the need to accurately model the hysteretic behavior of wood joints and structural systems and to discuss the basis and limitations of current models for wood. Literature on other topics related to the present work will be mentioned in other chapters and sections as needed. To provide a background on dynamic behavior of wood structures and structural systems, some basic terms and concepts used in structural dynamic analysis and modeling are first

introduced.

2.2 Basic Concepts of Structural Dynamics

2.2.1 Introduction

The mathematical expression, that describes the behavior of a structural system under dynamic loads, provides a quantitative expression of load-response relations. It may be written in the following synthetic form (Meirovitch 1985):

$$\mathfrak{R} \mathbf{u} = \mathbf{f} \quad (2.1)$$

where \mathfrak{R} is a differential operator, \mathbf{u} is the vector of the system response and \mathbf{f} is the vector of the dynamic actions. Three fundamental cases can be studied:

1. The operation performed by the operator \mathfrak{R} is known and the actions defined by the vector \mathbf{f} are also known. The problem requires the solution of dynamic response, described by vector \mathbf{u} . This is known as a *dynamic analysis* or *dynamic response analysis* problem.
2. When the operator \mathfrak{R} and the response \mathbf{u} are known, the problem requires the solution of action vector \mathbf{f} that produced the response \mathbf{u} . This is called an *action identification* or *action synthesis* problem.
3. When the vectors \mathbf{f} and \mathbf{u} are known, the problem is reduced to identifying the operator \mathfrak{R} . This is known as a *system identification* or *operator synthesis* problem.

Two concepts can be used to define dynamic loads: (1) *deterministic*, or (2) *non-deterministic* or *stochastic* or *random*. When loading is deterministic, the forcing function is assumed as a known function of time. Its time variation is completely known at each time instant. When loading is random, the forcing function is not completely known *a priori* and is, thus, defined statistically.

The present work deals with deterministic dynamic analysis of wood structures. But first, a mathematical model, that simulates the general hysteretic features of wood systems, needs to be defined.

2.2.2 Equation of Motion

Development of any mathematical model normally starts with the construction of an appropriate mechanical model of the actual system. In structural dynamics, a single-degree-of-freedom (SDF) mechanical model typically consists of the system mass, m , a dashpot with viscous damping coefficient, c , and a spring with stiffness, k (Fig. 2.1a).

The response of a SDF system to an earthquake ground motion will be analyzed. The SDF systems in Figs. 2.1a and b are assumed to behave in a linearly elastic-perfectly plastic fashion (Fig. 2.1c), with viscous damping.

The equation of motion for the system subjected to ground motion (Fig. 2.1a) is

$$m\ddot{u}_t + c\dot{u} + f_s = 0 \quad (2.2)$$

where m = mass, c = viscous damping coefficient, f_s = restoring force, $u_t = u + u_g$ = absolute (or total) displacement of the mass, u = relative displacement of the mass with respect to the ground motion, u_g = earthquake ground displacement, and dots designate time derivatives. In the linear elastic range, f_s may be expressed as ku , where k = stiffness (Fig. 2.1c).

Letting $\ddot{u}_t = \ddot{u} + \ddot{u}_g$, Eq. (2.2) may be rewritten as

$$m\ddot{u} + c\dot{u} + ku = -m\ddot{u}_g \quad (2.3)$$

With this equation, Fig. 2.1a is conveniently represented with the equivalent system in Fig. 2.1b having a fixed base and subjected to an effective horizontal dynamic force of magnitude $-m\ddot{u}_g$. Dividing Eq. (2.3) by m , we obtain the differential equation

$$\ddot{u} + 2\xi\omega_n\dot{u} + \omega_n^2u = -\ddot{u}_g \quad (2.4)$$

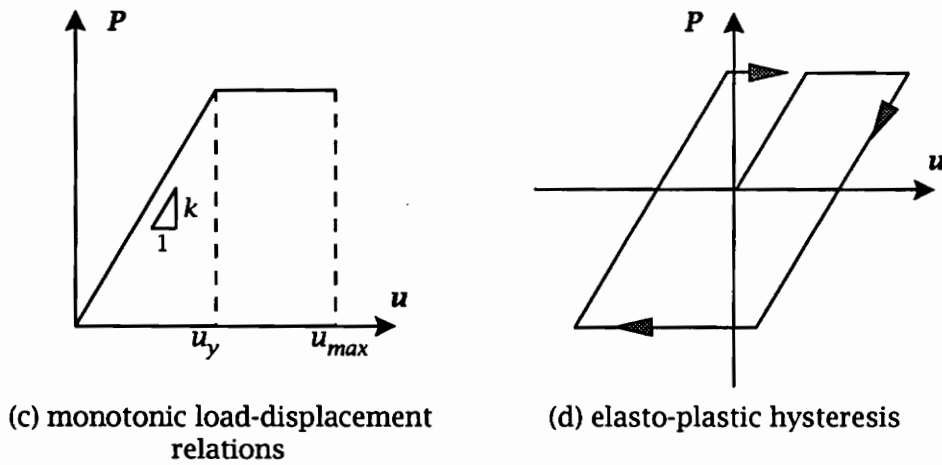
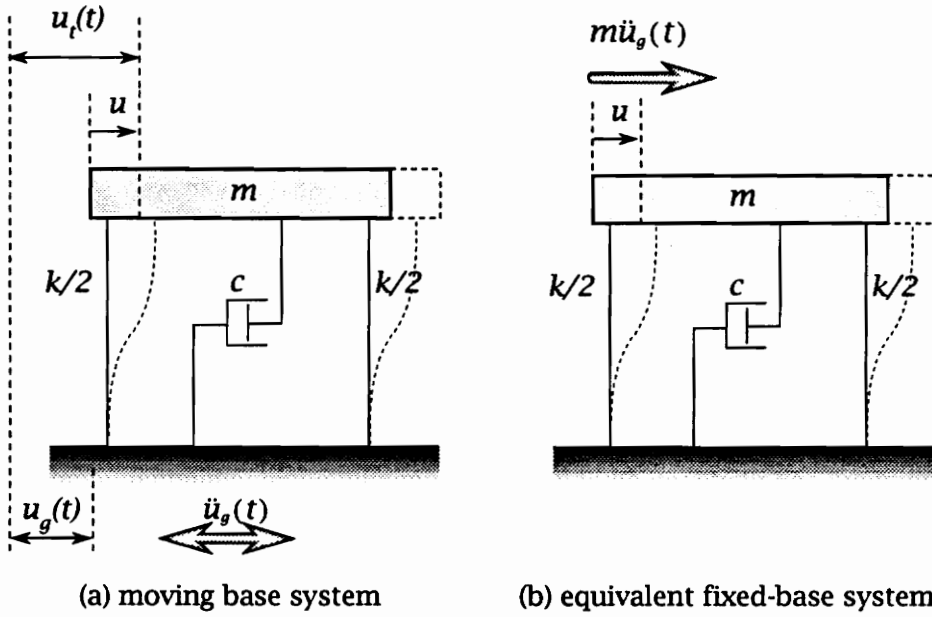


Figure 2.1: A linearly elastic-perfectly plastic single-degree-of-freedom system

where $\omega_n = \sqrt{k/m}$ and $\xi = c/(2m\omega_n)$. The *natural frequency* of undamped oscillation is ω_n . The product $2m\omega_n$ is known as *critical damping* and ξ is a nondimensional quantity known as the *viscous damping factor* or *damping ratio*. When $\xi > 1$, the system is *overdamped* and oscillation is absent. When $\xi = 1$, system damping, c , equals critical damping. For a given initial excitation, a critically damped system “tends to approach the equilibrium position the fastest” (Meirovitch 1986). Most structures have the case $0 < \xi < 1$, referred to as the *underdamped case*. When $\xi = 0$ (or $c = 0$), known as the *undamped case*, the structure oscillates infinitely unless acted upon by an external force.

From the static monotonic load-displacement diagram, Fig. 2.1c, *displacement ductility* is

$$\mu = \frac{u_{max}}{u_y} \quad (2.5)$$

where u_{max} is maximum displacement and u_y is yield displacement. With cyclic loading, the load-displacement trace produces *hysteresis* loops, shown in Fig. 2.1d, caused by damping and/or inelastic system behavior. The area contained within the loop represents the *energy dissipated* by the structure.

2.2.3 Damping and Energy Dissipation

Damping is the mechanism by which energy is removed from a vibratory system; it is the property responsible for the eventual decay of free vibrations and for the fact that the response of a vibratory system excited at resonance (i.e., cyclic excitation with frequency, $\omega = \omega_n$) does not grow without limit (Crandall 1970). The origin and mechanism of damping, however, is complex and difficult to comprehend. For instance, damping can be (Srinivasan 1982): (1) of viscous origin, where the damping force is proportional to the first power of velocity [as in Eqs. (2.2) and (2.3)]; (2) of aerodynamic origin, where the damping force is proportional to the square of the velocity; (3) of the Coulomb type, where the energy dissipated is constant in magnitude but changes direction with velocity (e.g., friction between dry sliding surfaces or interface effects in

structures); (4) hysteretic in nature, where energy dissipation is a function of the stress amplitude; (5) due to imperfect elasticity of vibrating bodies (i.e., internal friction); etc. Analytical study is difficult because in real engineering systems, damping is a heterogeneous mix of these various types of mechanisms.

To simplify vibration analysis, viscous damping is normally assumed. In cases where damping forces are not proportional to velocity and have significant effect on response, an *equivalent viscous damping* concept is sometimes used (e.g., Medearis and Young 1964). To obtain the equivalent viscous damping ratio for a system, it is necessary to obtain the amount of energy dissipated per cycle measured by the area enclosed by the hysteresis loop and to divide this by the maximum stored energy. The dissipated energy of the actual damping force is assumed to be equivalent to that of a viscous damping force, $-c\dot{u}$. If the restoring force needed to bring the system back to equilibrium state at any given displacement is linear in the absence of damping, the use of equivalent viscous damping ratio simplifies the analysis. But in the case of systems with nonlinear restoring force, e.g. wood structural systems, actual damping is underestimated by the equivalent viscous damping approach (Polensek 1988). Note that most reported values of damping ratio of wood joints and components in literature pertain to the equivalent viscous damping ratio.

References to damping in engineering literature should be clarified because different researchers use the term in slightly different ways. Some materials engineering researchers study damping as a nondestructive inspection tool to determine material properties while others use it as a macrostructural tool to investigate stress, strain and slip at interfaces within structural configurations and systems (Lazan 1968). They use the word damping to mean the total energy dissipation in a member, i.e. viscous and non-viscous types are combined. Researchers in structural dynamics, however, normally refer to viscous damping alone when they use the word damping. Energy dissipation is, thus, attributed to “damping” *and* inelastic deformation. This is based on the evaluation of energy equations derived from the equation of motion [Eq. (2.2)

or (2.3)].

Energy is *imparted* to a structure during seismic ground motion. The energy equations can be derived by using either Eq. (2.2) or (2.3) since both systems (Figs. 2.1a and b) give the same relative displacement. Many researchers used the derivation based on Eq. (2.3) in past studies. The choice of equation, however, may result in different definitions of input and kinetic energies. Uang and Bertero (1990) refer to the energy equation derived from Eq. (2.2) as “absolute” energy equation and that from Eq. (2.3) as “relative” energy equation. The absolute energy equations derived by Uang and Bertero are used in defining energy components.

By integrating Eq. (2.2) with respect to u from the time that ground motion excitation starts and replacing u by $(u_t - u_g)$, we obtain

$$\frac{m(\dot{u}_t)^2}{2} + \int c\dot{u}du + \int f_s du = \int m\ddot{u}_t du_g \quad (2.6)$$

The first term is the “absolute” kinetic energy (E_k),

$$E_k = \frac{m(\dot{u}_t)^2}{2} \quad (2.7)$$

because absolute velocity (\dot{u}_t) is used. The second term is the damping energy (E_ξ), which is always non-negative because

$$E_\xi = \int c\dot{u}du = \int c\dot{u}^2 dt \quad (2.8)$$

The third term is the absorbed energy (E_a), which is composed of recoverable elastic strain energy (E_s) and irrecoverable hysteretic energy (E_h):

$$E_a = \int f_s du = E_s + E_h \quad (2.9)$$

where $E_s = (f_s)^2/(2k)$.

The right-hand-side in Eq. (2.6) is the “absolute” input energy (E_i):

$$E_i = \int m\ddot{u}_t du_g \quad (2.10)$$

where $m\ddot{u}_t$ represents the inertia force applied to the structure which is the same as the total force applied to the structure foundation. Thus, E_i represents the work done by the total base shear at the foundation on the foundation displacement.

The absolute energy equation can be written as

$$E_i = E_k + E_\xi + E_a = E_k + E_\xi + E_s + E_h \quad (2.11)$$

The energy terms are illustrated in Fig. 2.2 for an elastic-perfectly plastic SDF system (with $\mu=5$ and $\xi=5\%$) subjected to the 1986 San Salvador earthquake (Uang and Bertero 1990).

2.3 Wood Structures and Components

2.3.1 Behavior of Wood Structural Systems

Wood structures consist of interacting components (or subassemblies) such as walls, floors, roofs and foundation that are fastened together by nails, bolts, steel straps and/or cleats forming a three-dimensional, highly indeterminate system. They normally incorporate some kind of lateral load resisting system that helps them to survive natural disasters, such as earthquakes and typhoons. The four most common systems, shown in Fig. 2.3a, are (Buchanan and Dean 1988): moment resisting frames, cantilever columns, diagonal bracing and shear walls. Horizontal bracing and/or diaphragm also contribute to a building's lateral load resistance. Typical light-frame residential wood buildings with diaphragm/shear and bearing wall construction (e.g., Fig. 2.3b) are not engineered.

Information from damage assessment surveys after natural disasters have traditionally served to indicate the performance of wood-framed buildings (Soltis 1984; Falk and Soltis 1988). Data from post-disaster surveys, however, are highly qualitative and do not provide complete information on the dynamic behavior of the buildings under inspection. Recently, full-scale tests on houses have been used to observe building

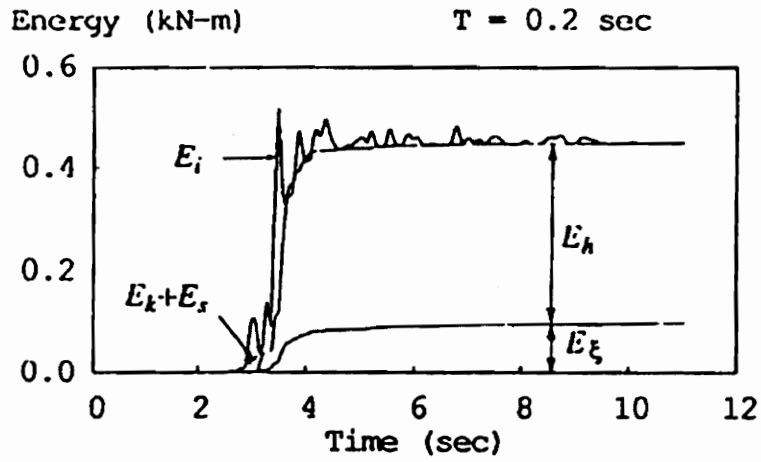
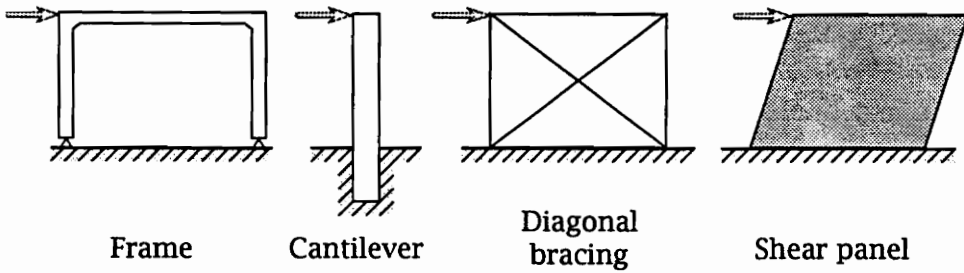
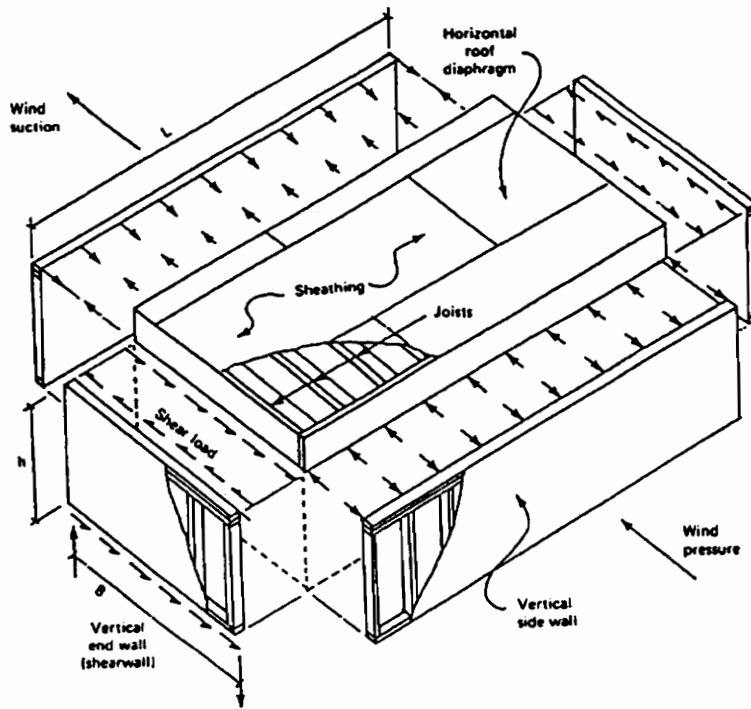


Figure 2.2: Energy terms using absolute energy formulation (from Uang and Bertero 1990)



(a) lateral load resisting systems



(b) typical wood diaphragm and shear wall construction (from Diekmann 1989)

Figure 2.3: Some common structural systems

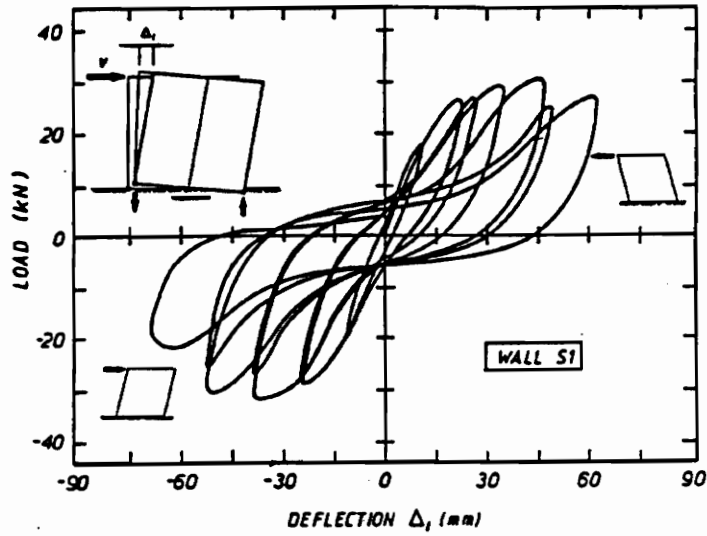
behavior and evaluate the failure mechanisms of the complete house and the major structural components. Three-storey wood houses have been tested in Japan under various types of loading including horizontal static, reverse cyclic and forced vibration (e.g. Yasumura et al. 1988, Hirashima 1988). Full-scale dynamic test of a 2-storey wood house using a 6-degree-of-freedom earthquake simulator has been performed in Greece (Touliatos 1989). Extensive reviews of full-scale testing around the world can be found in Gupta and Moss (1991).

Most available data are, however, based on tests of subassemblies such as shear walls (Medearis and Young 1964; Stewart 1987; Kamiya 1988; Dolan 1989; Filiatrault and Foschi 1991), diaphragms (Cheung et al. 1988; Polensek and Bastendorff 1979; Weyerhaeuser 1990) and truss systems (Gavrilović and Gramatikov 1991). A common observation from these tests is that the hysteresis trace of a wood subsystem or subassembly is governed by the hysteretic characteristics of its primary connection. Nailed sheathing behavior governs the hysteresis of shear walls and diaphragms (e.g., compare Figs. 2.4 and 2.5b); metal plate connections govern the hysteretic behavior of truss-frame systems. Dowrick (1986) also noted this when he collected cyclic test data of wood joints and structural systems in New Zealand, Japan and North America and examined common hysteresis loops for timber structures. Thus, we only need to characterize the hysteretic behavior of wood joints to characterize the behavior of wood structures and structural systems.

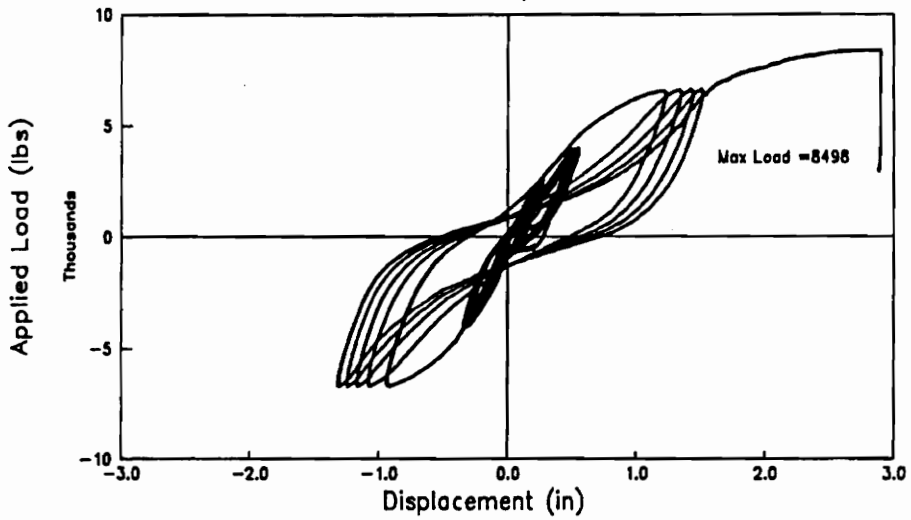
For analytical purposes, Dowrick classified the hysteresis loops for timber structures, based on their shape characteristics, into joints with: (1) yielding plate, (2) yielding nails, and (3) yielding bolts (Fig. 2.5). Similarities in the hysteresis shapes of the dowel-type fasteners, i.e. nails and bolts, can be seen in Figs. 2.5b and c.

2.3.2 Hysteretic Characteristics

Equation (2.5) shows that ductility is mathematically defined in terms of material yield behavior. This poses no problem for steel and some reinforced concrete



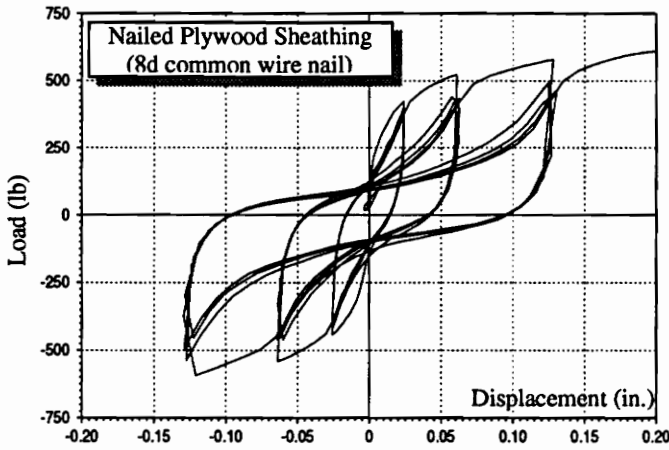
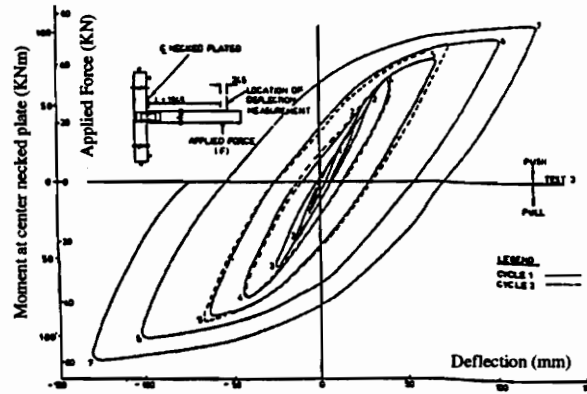
(a) plywood shear wall (from Stewart 1987)



(b) oriented strand board diaphragm (from Weyerhaeuser 1990)

Figure 2.4: Typical hysteresis of wood subassemblies

(a) joint with yielding plate
(from Dowrick, 1986)



(b) joint with yielding nail

(c) joint with yielding bolt
(from Dowrick, 1986)

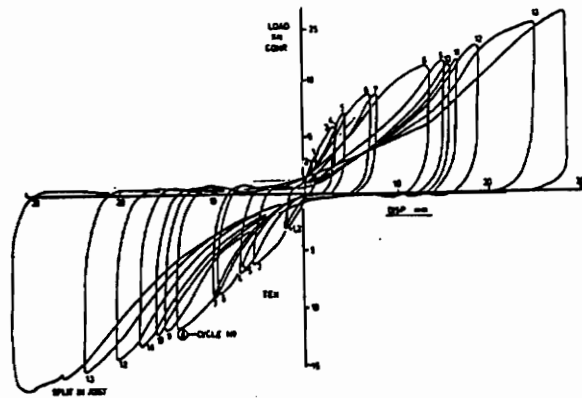


Figure 2.5: Typical hysteresis loops for wood joints

structures, but requires an alternative concept for timber structures since they do not demonstrate typical yield behavior.

Figure 2.5b shows hysteresis loops from static cyclic loading of a nailed plywood sheathing, typical of those observed in timber shear walls and diaphragms. Several characteristic features of cyclic response of these systems can be noted from the figure: (1) nonlinear, inelastic load-displacement relationship without a distinct yield point, (2) progressive loss of lateral stiffness in each loading cycle (will be referred to as *stiffness degradation*), (3) degradation of strength when cyclically loaded to the same displacement level (will be referred to as *strength degradation*), and (4) *pinched* hysteresis loops. A very important feature, not observed in the figure, is that the response of a wood joint, and possibly wood structures in general, at a given time depends not only on instantaneous displacement but also on its past history (i.e., the input and response at earlier times). This is known as *memory*. Whale (1988) observed that nailed or bolted timber joints under irregular short or medium term lateral loading have memory. In some tests, Dean et al. (1989) also noted the presence of initial slackness due to shrinkage clearances at bolt holes or deformation at supports.

Any hysteresis or constitutive model for timber structures should incorporate experimentally observed characteristics such as those given above.

2.4 Hysteresis Models

2.4.1 Models for General Dynamic Analysis

Analytical modeling of an inelastic structure under seismic loading requires a force-displacement relation that can produce the true behavior of the structure at all displacement levels and strain rates. This is a very stiff requirement considering that numerous factors contribute to the hysteresis behavior of different structural systems (Sozen 1974). Besides, most structural systems have hysteretic restoring forces that

are difficult to compute because the response depends not only on instantaneous displacement but also on its past history. Thus, simplified hysteresis models are used in practice to obtain estimates of bounds to dynamic response in the inelastic range. Some models incorporate strength and/or stiffness degradation and pinching in an attempt to more accurately represent actual system behavior. This is important because degradation might lead to progressive weakening and total failure of structures.

Some piecewise linear hysteresis models that were developed for reinforced concrete and steel structures to represent their earthquake response have also been used in seismic analysis of timber structures. A summary is shown in Fig. 2.6 and briefly presented below (Loh and Ho 1990):

- *Elasto-plastic model* (Fig. 2.6a)- is used for a linearly elastic-perfectly plastic system and normally applied to steel frame structures with large deformation capacities.
- *Bilinear model* (Fig. 2.6b)- has a finite positive stiffness slope after yielding to simulate the strain hardening characteristics of steel and reinforced concrete structures. The elasto-plastic model is a special case of the bilinear model.
- *Modified Clough model* (Fig. 2.6c)- has a bilinear primary curve and an unloading stiffness that is updated for each loop by an unloading stiffness degradation parameter.
- *Q-hysteresis model* (Fig. 2.6d)- is a modified bilinear hysteresis model incorporating stiffness degradation during load reversals.
- *Takeda model* (Fig. 2.6e)- is based on experimentally observed behavior of reinforced concrete members tested under lateral load reversals with axial load.
- *Slip model* (Fig. 2.6f)- is commonly used to model the pinching effects in reinforced concrete structures with large vertical stresses.

The elasto-plastic and bilinear models are probably the simplest and most widely

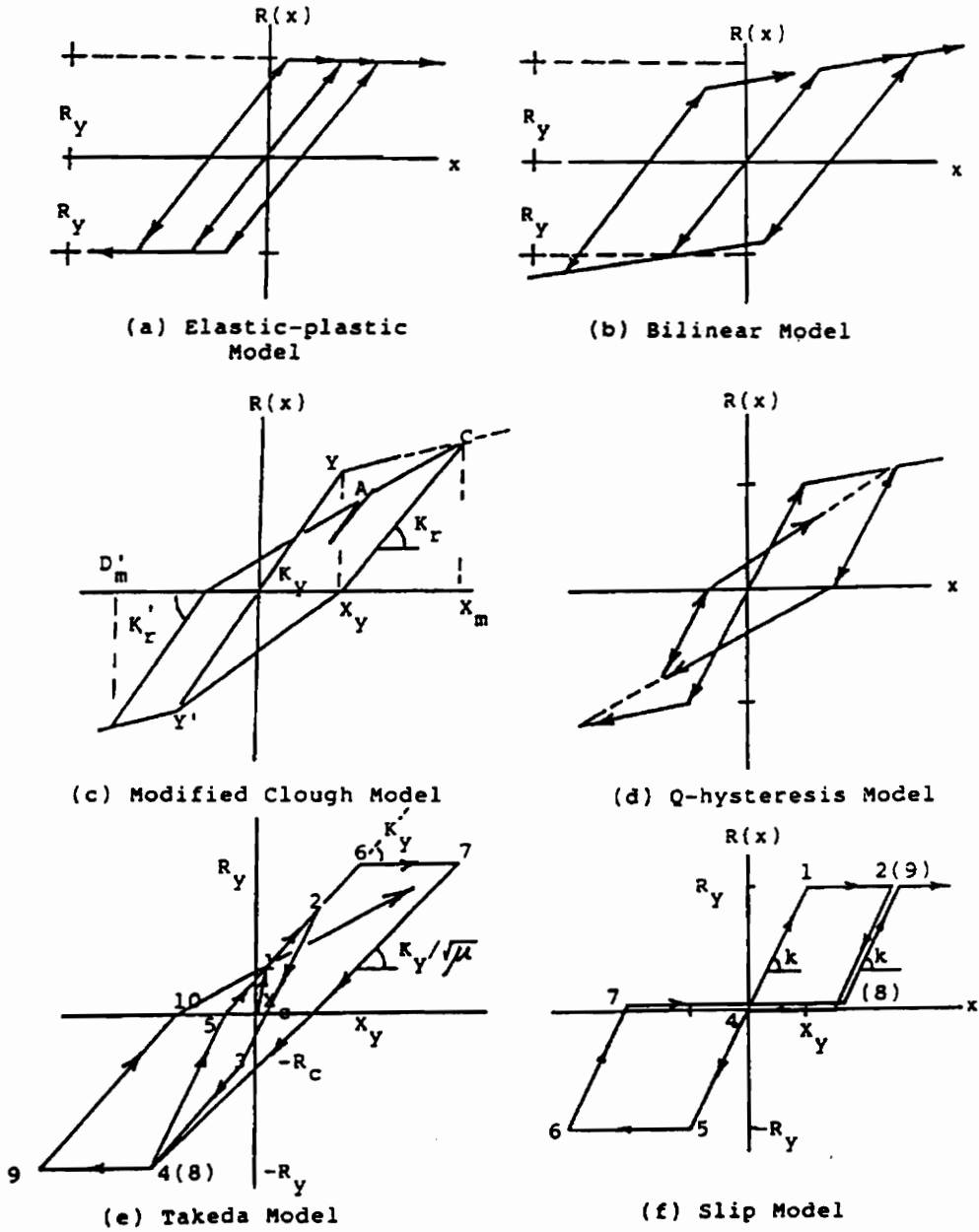


Figure 2.6: Illustrations of hysteresis models for various structures (from Loh and Ho 1990)

used in dynamic analysis of structures under complex deterministic and random excitations. But the exact solution for random vibration analysis, even for these simple models, has not been obtained. Previous researchers have used a variety of approximate solution techniques with varying degrees of success (Noori 1984). The main problem with the elasto-plastic and bilinear models is their inability to accurately represent actual material behavior. Other piecewise linear models that allow various forms of degradation, however, are computationally inefficient, especially for random vibration analysis, in that they require one to keep track of all stiffness transition points. Ideally, a hysteresis model should be given in a form suited for random vibration analysis to allow researchers to investigate structural performance under natural hazards, with the random characteristics of the loading modeled as random processes. Estimates of response statistics may then be used to design a structure based on accepted levels of safety, measured in terms of probability of failure.

Another commonly used model, with smoothly varying hysteresis loops, is the *Ramberg-Osgood* model. It is based on a simple function defined by three parameters: a characteristic or yield load, a characteristic or yield displacement and an exponent. When the exponent is equal to unity, the model is elastic and when it approaches infinity, the elasto-plastic case is obtained. It has been used in modeling structural steel members and connections and is most applicable for systems exhibiting stable, nondeteriorating hysteresis loops (Kaldjian and Fan 1968). But this is not suitable for random vibration analysis in its original form (Bhatti and Pister 1981). Jennings (1965), Iwan (1969) and Iemura (1977) have proposed variations of the Ramberg-Osgood model.

Other smoothly varying hysteresis models have been proposed (Iwan 1977; Bouc 1967) but one that has gained wide acceptance is Wen's (1976; 1980) modification of Bouc's model. The hysteretic restoring force is given by a nonlinear first order differential equation; thus, it is characterized by a single mathematical form. Baber and Wen (1981) extended the model to admit stiffness and/or strength degradation and applied it to analyze multidegree-of-freedom structures. Baber and Noori (1986)

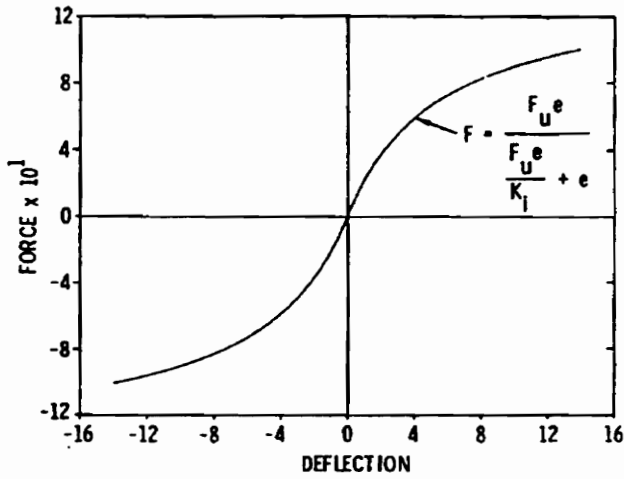
added pinching capability. The Bouc-Wen model has been studied and used by various researchers (e.g., Ang and Wen 1982, Casciati 1987, Maldonado et al. 1987, Sues et al. 1988 and Maldonado 1992 among others) to study various engineering problems. Detailed properties of this model will be discussed in the next chapter.

2.4.2 Current Models for Wood Systems

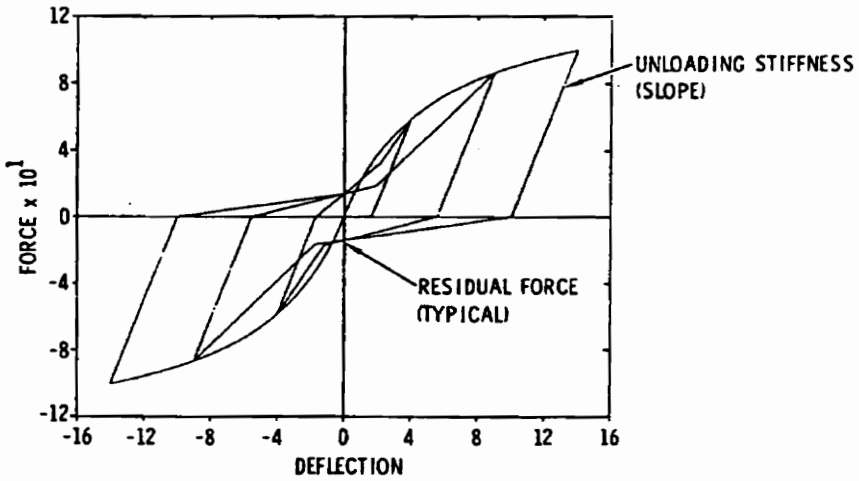
Ewing et al. (1980) developed a hysteresis model for wood diaphragms to perform seismic analysis of wood diaphragms in masonry buildings. The model follows the backbone curve shown in Fig. 2.7a. (A *backbone*, or *skeleton* or *load envelope*, curve is the curve resulting from joining the tips of the hysteresis, i.e. points of maximum load in a virgin loading path.) Based on observations of hysteresis data from Medearis and Young (1964), they used a trilinear path from the maximum deflection on the positive backbone curve to the maximum deflection on the negative backbone curve (Fig. 2.7b). The unloading slope and the residual force are specified to match experimental data.

Since wood joints govern the overall dynamic behavior of wood structures (Dowrick 1986; Stewart 1987; Dolan 1989; Polensek and Schimel 1991), many researchers used data obtained from tests of wood joints to develop hysteresis models for wood structures. Kivell et al. (1981) derived an idealized hysteresis model for moment resisting nailed timber joints (Fig. 2.8a) based on a modification of the Takeda model shown in Fig. 2.6e. The model follows a simple bi-linear backbone curve. Similar to the model by Ewing et al., a trilinear path connects maximum deflections in each half cycle. Kivell et al., however, defined the end points of the lines by a cubic function that passes through the maximum deflections. They used the model to perform dynamic analyses of two simple timber portal frames with nailed beam-to-column connections. The model displays some pinching but does not incorporate stiffness and strength degradation.

Lee (1987) used the hysteresis model earlier proposed by Polensek and Laursen (1984) for nailed plywood-to-wood connections to perform dynamic analyses of wood wall and floor systems using the finite element method. The model follows a trilinear



(a) Load-deflection envelope of the model



(b) Typical hysteresis loop produced by the model

Figure 2.7: Hysteresis model proposed by Ewing et al. (1980) for wood diaphragms

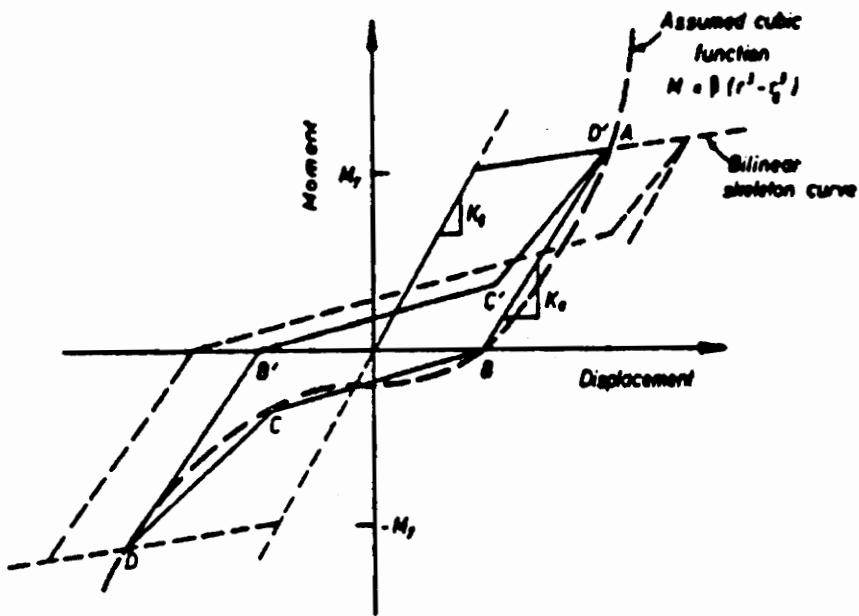


Figure 2.8: Hysteresis model proposed by Kivell et al. (1981) for moment resisting nailed timber joints

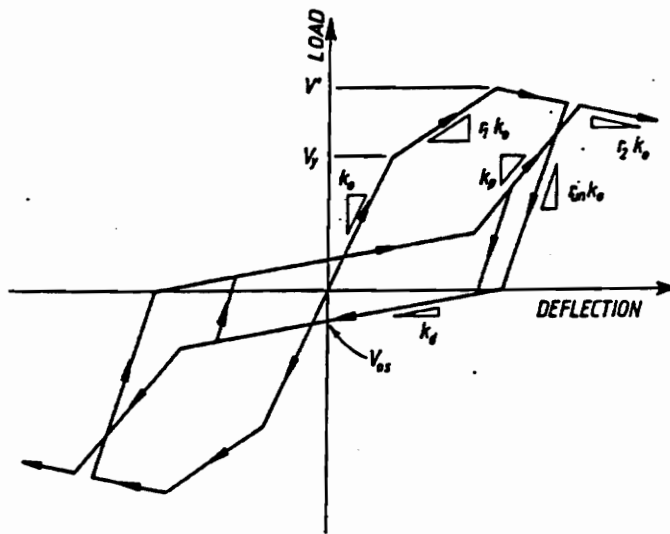
backbone curve. Similar to earlier models, the hysteresis trace between maximum deflections in each half cycle follows a trilinear path. The control points are, however, obtained using a statistical fit of test data. The model relies heavily on the type and size of the nail and the material properties of the side members. The regression equations used to define the control points have a very limited use.

Chou (1987) tested nailed plywood-to-wood connections under cyclic loading and investigated the experimental hysteresis shapes. He used a system of nonlinear Kelvin models in series and in parallel to model the hysteresis loops of the joint. Nail behavior was studied using a modification of the beam-on-elastic-foundation analysis. Nonlinear response was approximated by a linear step-by-step approach; that is, nonlinear response was considered as the sum of different linear responses under small increments of load. It is, however, unclear how Chou's model can be used for dynamic analysis of wood structural systems.

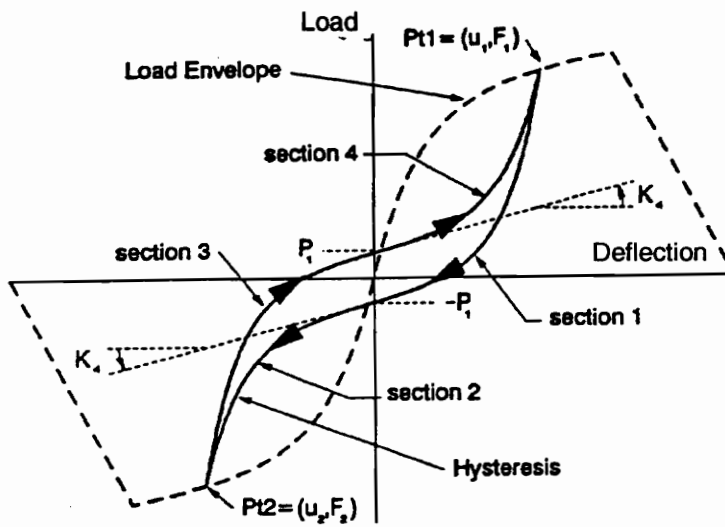
Stewart (1987) and Dolan (1989) modeled hysteresis in nailed sheathing-to-lumber connections. Stewart (1987) idealized pinching and stiffness degradation using a set of force-history rules to obtain the hysteresis shape shown in Fig. 2.9a. A key feature of Stewart's model is the option to include an initial slackness in the first loading cycle. Dean et al. (1989) noted the presence of initial slackness in tests of subassemblies caused by shrinkage clearances at bolt holes or deformation at supports. Dolan (1989) divided a hysteresis loop into four segments, each one defined by an exponential equation with four boundary conditions (Fig. 2.9b). This model was incorporated in a dynamic finite element model that predicts shear wall response to earthquakes.

Ceccotti and Vignoli (1990) developed a hysteresis model for moment-resisting semi-rigid wood joints that are normally used in glulam portal frames in Europe. It also models pinching and stiffness degradation (Fig. 2.10). A set of subroutines were written to define the new hysteretic element and were incorporated into the commercial nonlinear dynamic analysis program DRAIN-2D.

In Japan, several models have been used in dynamic analysis of Japanese wood



(a) from Stewart (1987)



(b) from Dolan (1989)

Figure 2.9: Hysteresis models proposed for nailed sheathing-to-frame connections

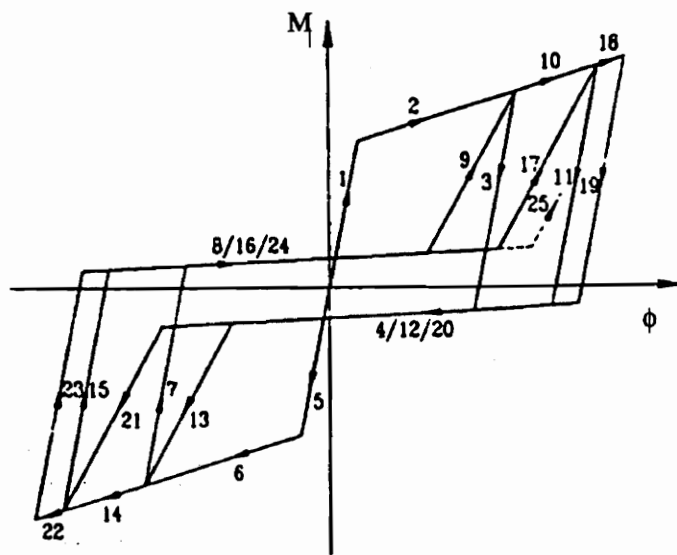


Figure 2.10: Hysteresis model proposed by Ceccotti and Vignoli (1990) for moment resisting semi-rigid wood joints

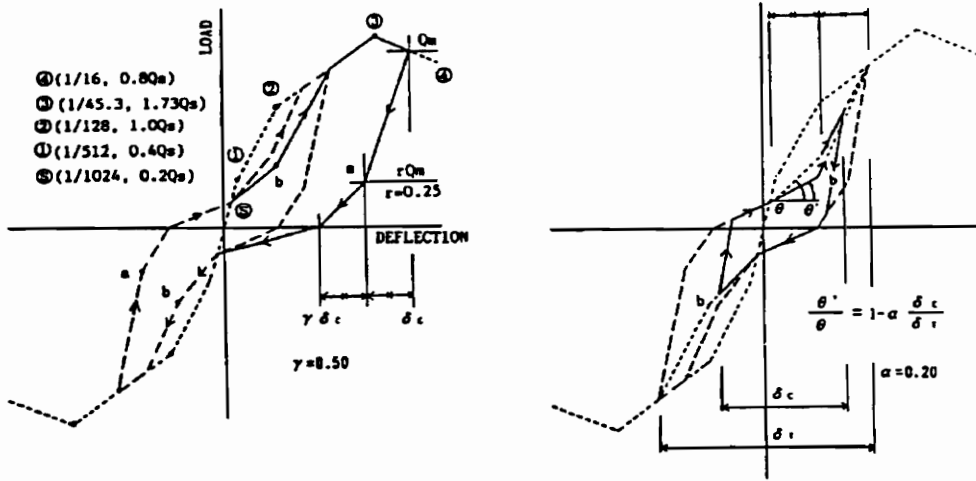
houses. Sakamoto and Ohashi (1988) proposed two hysteresis models for conventional Japanese wood houses. The first model consists of a parallel combination of bilinear element and slip element and the second model follows a trilinear path from the maximum deflection on the positive backbone curve to the maximum deflection on the negative backbone curve. The three control points were obtained from racking tests of shear walls (Fig. 2.11a). Kamiya (1988) proposed the model shown in Fig. 2.11b, which was developed from pseudo-dynamic tests of wood-sheathed shear walls. The model in Fig. 2.11c was proposed by Miyazawa (1990) for Japanese wood-framed construction.

For trussed-frame wood systems, Gavrilović and Gramatikov (1991) used a simple bilinear hysteresis model. The hysteresis trace between maximum deflections in each half cycle also follows a bilinear path.

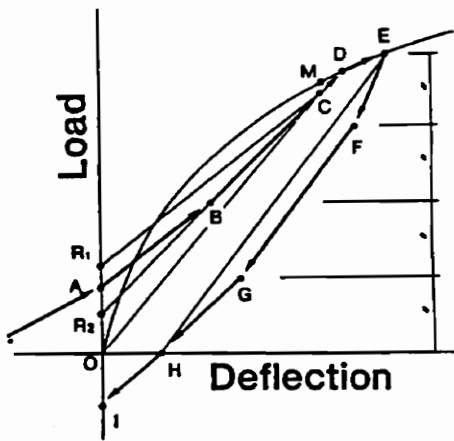
Foschi and his associates proposed a new hysteresis model for a single dowel-type fastener (Fig. 2.12). The analysis considered the fastener as an elasto-plastic beam on a nonlinear foundation (the wood support), and keeps track of the gap which forms between the beam and the support during load cycling (UBC 1993). The model was verified by cyclic testing of nails driven into spruce wood. Hysteresis parameters are obtained from basic characteristics of joint materials, namely, modulus of elasticity and yield point of the fastener and embedment properties of the side members.

2.4.3 Comments

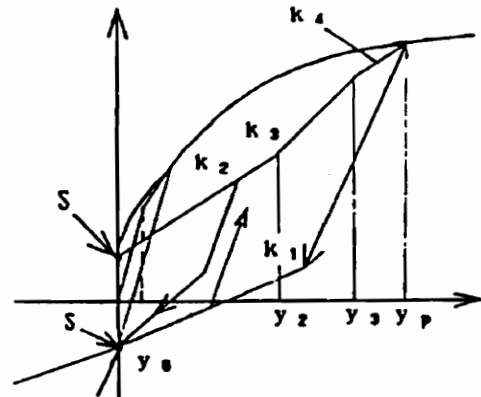
While the current models for wood satisfied some of the specific features of the joints that they meant to model, they may be inappropriate for joints with different configurations and material components. Since (1) there are hundreds of combinations of materials and joint configurations in wood systems, and (2) wood-based products, fasteners and use of wood-based products continue to evolve, a general model is preferred over models derived from specific configurations. A completely empirical model will not only be expensive to obtain but may also be of limited use in dynamic analysis. A mathematical model, meeting all the criteria given in section 2.3.2, is preferred.



(a) from Sakamoto and Ohashi (1988)



(b) from Kamiya (1988)



(c) from Miyazawa (1990)

Figure 2.11: Hysteresis models proposed by Japanese researchers

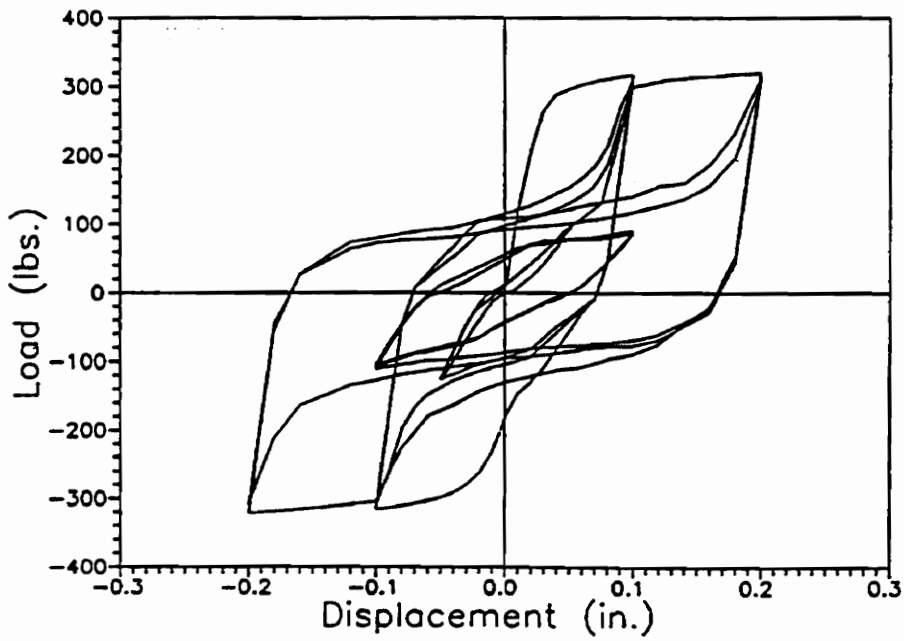


Figure 2.12: Hysteresis model proposed by Foschi and his associates (UBC 1993) for wood joints with dowel-type fasteners

Model parameters may be estimated from tests of representative wood joints or assemblies.

All the available models for wood systems use a complex set of force-history rules and are expressed in forms incompatible with available random vibration solution methods. For this reason, research on the dynamic analyses of wood structures has been limited to deterministic approaches and has lagged behind advances in general structural dynamics. Ideally, a hysteresis model for wood structures should be given in a form suited for both deterministic and random vibration analyses. The latter would allow researchers to investigate the performance of wood structures under natural hazards, with the loading modeled as random processes.

2.5 Summary

Basic terms and concepts used in structural modeling and dynamic analysis were presented to provide the necessary background for the present work. Cyclic tests on wood subassemblies and wood joints were reviewed. It was pointed out that the hysteresis trace of a wood subsystem or subassembly is governed by the hysteretic characteristics of its primary connection. Thus, we only need to characterize the hysteretic behavior of wood joints to characterize the behavior of wood structures and structural systems. Dowrick (1986) classified the hysteresis loops for timber structures, based on their shape characteristics, into joints with: (1) yielding plate, (2) yielding nails, and (3) yielding bolts. Based on experimental hysteresis, any hysteresis or constitutive model for timber structures should incorporate experimentally observed characteristics such as: (1) nonlinear, inelastic load-displacement relationship without a distinct yield point, (2) stiffness degradation, (3) strength degradation, (4) pinching, and (5) memory. Incorporating memory means that the model should be capable of predicting response at a given time based not only on instantaneous displacement but also on its past history (i.e., the input and response at earlier times).

Hysteresis models proposed for steel, concrete and wood structures were reviewed.

The models for wood were derived from specific joint configurations and were expressed using either a complex set of force-history rules or limited empirical relations. It was apparent that there is a need for a general hysteresis model that incorporates all the features given above. Such a model would permit response computations of a wide variety of wood structural systems under arbitrary dynamic loading and help in investigating the safety and performance of engineered wood structures.

Chapter 3

Hysteresis Modeling

3.1 General

Analytical modeling of an inelastic structure under seismic loading requires a force-displacement relation that can produce the true behavior of the structure at all displacement levels and strain rates. This is a very stiff requirement considering that numerous factors contribute to the hysteresis behavior of different structural systems (Sozen 1974). Besides, most structural systems, especially wood systems, have hysteretic restoring forces that are difficult to compute because the response depends not only on instantaneous displacement but also on its past history (referred to earlier as memory). The hysteresis model should take this into account while simulating other characteristic features of wood systems that have been identified in the previous chapter. It is important to incorporate strength and/or stiffness degradation and pinching to more accurately represent actual system behavior because degradation might lead to progressive weakening and total failure of structures.

A general hysteresis model for wood joints and structural systems that incorporates the hysteretic features that have been identified in the previous chapter will be presented. The smoothly varying Bouc-Wen hysteresis model and its extensions will be examined. A pinching, degrading model modified to more accurately model the hysteretic behavior of wood joints will be described.

3.2 Approach to Modeling

Generally, there are two possible approaches in obtaining a hysteresis model for wood systems: (1) by empirically fitting experimental data from cyclic tests of particular wood joints, or (2) by describing system behavior using an approximate mathematical model. Since (1) there are hundreds of combinations of materials and joint configurations in wood systems, and (2) wood-based products, fasteners and use of wood-based products continue to evolve, a general model is preferred over models derived from specific configurations. A completely empirical model will not only be expensive to obtain but may also be of limited use in dynamic analysis. A mathematical model, meeting the criteria given in section 2.3.2, is preferred. Model parameters may be estimated from tests of representative wood joints or assemblies.

3.3 Mechanical Model

In the previous chapter, a simple single-degree-of-freedom (SDF) mechanical model with system mass, m , a dashpot with viscous damping coefficient, c , and a spring with stiffness, k , was introduced. A brief background was also given on damping and energy dissipation. Here, the mechanical model for nonlinear wood systems is presented.

A nonlinear system can be represented by a dynamic mechanical model with: (1) linear spring and nonlinear damping- Coulomb type or aerodynamic type alone or in combination with viscous damping (Fig. 3.1a); (2) nonlinear spring and linear viscous damping (Fig. 3.1b); (3) nonlinear spring and nonlinear damping (Fig. 3.1c); (4) linear spring, linear viscous damping and nonlinear hysteretic element (Fig. 3.1d), or; (5) various combinations of (1) to (4). The choice of an appropriate mechanical model depends on the complexity of mathematical expression that describes the model and its compatibility with known solution techniques.

An efficient way to treat a nonlinear hysteretic system is to separate the source of nonlinearity in the system from any linear components. This results in a mechanical

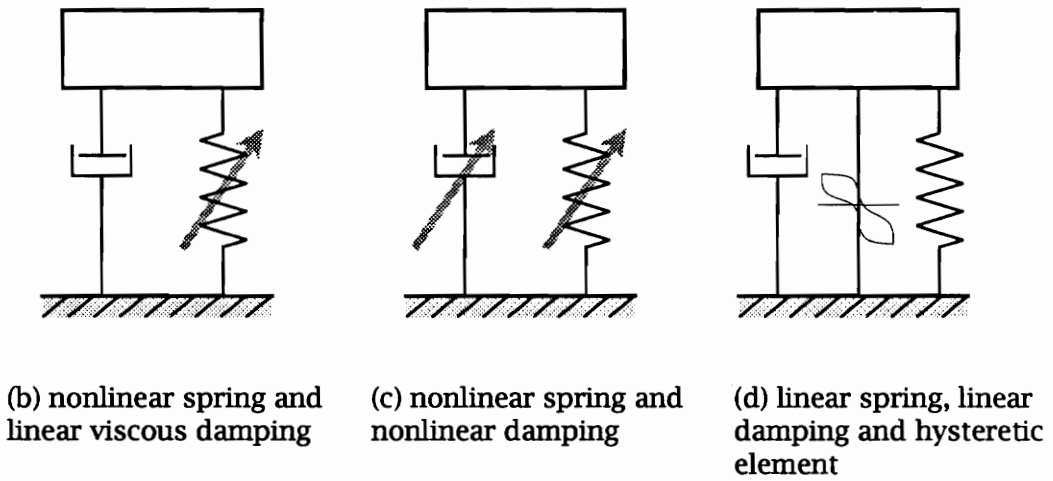
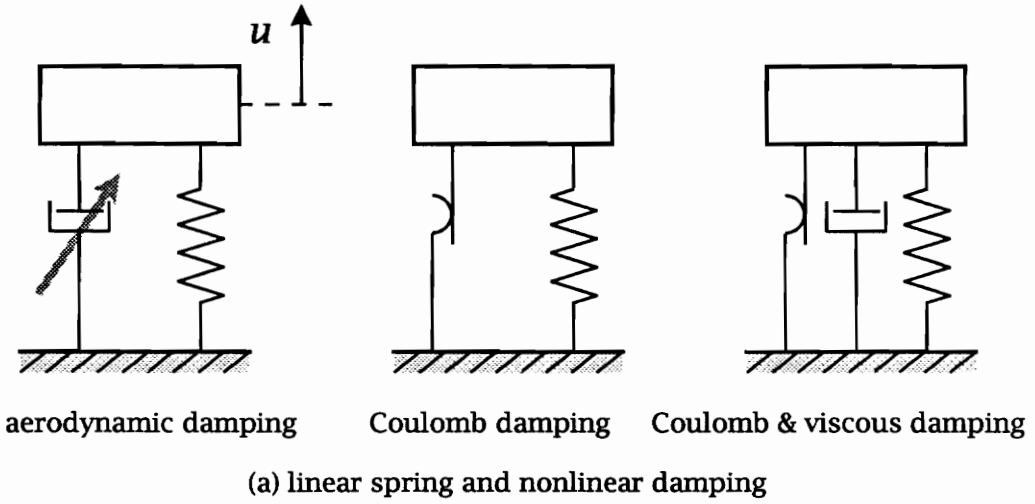


Figure 3.1: Typical mechanical models for nonlinear systems

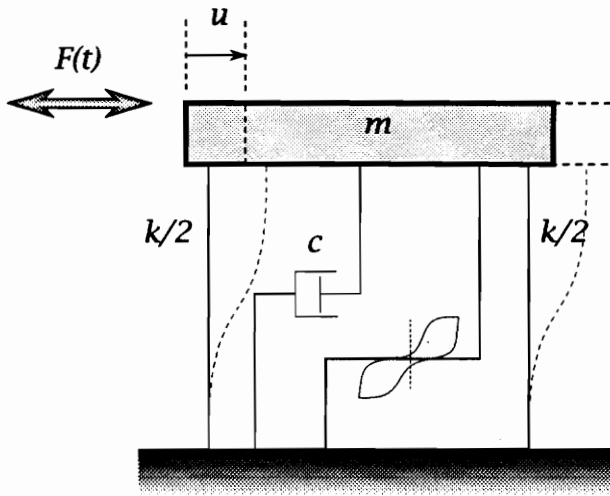
model with three parallel elements: (1) a linear viscous damping, (2) a linear spring and (3) a hysteretic element (Fig. 3.2a). This achieves two things: (1) analytical difficulty in treating the different sources of energy dissipation in the system is avoided since the non-viscous types are lumped together into the hysteresis element, and (2) standard values for the viscous damping ratio of linear wood systems can be used for analysis. Once the parameters of the hysteresis model are identified, dissipated hysteretic energy can be obtained from the hysteresis trace of the response.

3.4 The Bouc-Wen-Baber-Noori Model

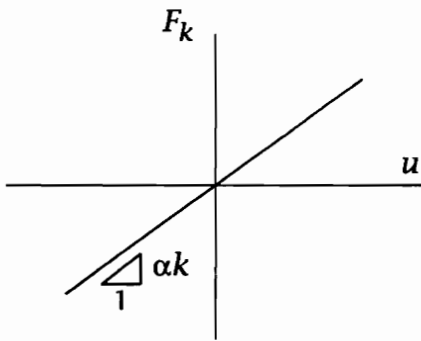
3.4.1 Background

Bouc (1967) suggested a versatile, smoothly varying hysteresis model for a SDF mechanical system under forced vibration. With the mechanical model shown in Fig. 3.2a, Wen (1976; 1980) generalized Bouc's hysteretic constitutive law and developed an approximate solution procedure for random vibration analysis based on the method of equivalent (or statistical) linearization. Baber and Wen (1981) extended the model to admit stiffness and/or strength degradation as a function of hysteretic energy dissipation and applied it to a multidegree-of-freedom system. Later on, Baber and Noori (1986) further extended the modified Bouc model by incorporating pinching while maintaining it in a form compatible with Wen and Baber and Wen's equivalent linearization solution. Response statistics obtained by the equivalent linearization technique were shown to reasonably approximate those obtained by Monte Carlo Simulation. The final model will be called the Bouc-Wen-Baber-Noori (BWBN) model in the present work.

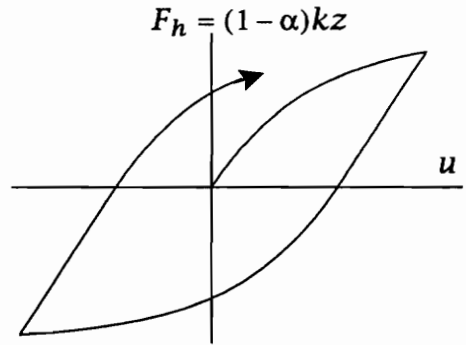
Many researchers have used the early form of the modified Bouc model in random vibration investigations of hysteretic systems. With the features added by Baber and Wen (1981) and Baber and Noori (1986), it has more closely approximated the hysteretic behavior of wood joints and structural systems. However, it needs further modification to be applicable in modeling general wood system behavior.



(a) schematic model



(b) non-damping linear restoring force component



(c) hysteretic restoring force component

Figure 3.2: Hysteretic SDF system for wood structural systems

Although one of the best features of the BWBN model is its continuous and mathematically tractable form that is suited for random vibration analysis, the present work will focus only on deterministic dynamic analysis (i.e., the forcing function is assumed as a known function of time).

3.4.2 Equation of Motion and Constitutive Relations

Considering the SDF hysteretic system in Fig. 3.2a, the equation of motion may be generally written as

$$m\ddot{u} + c\dot{u} + R[u(t), z(t); t] = F(t) \quad (3.1)$$

where dots designate time derivatives; $F(t)$ is the forcing function; the damping restoring force, $c\dot{u}$, is assumed linear and $R[u(t), z(t); t]$ is the non-damping restoring force consisting of the linear restoring force αku and the hysteretic restoring force $(1 - \alpha)kz$ (Figs. 3.2b and c). Dividing both sides of Eq. (3.1) by m , the following standard form is obtained:

$$\ddot{u} + 2\xi_o\omega_o\dot{u} + \alpha\omega_o^2u + (1 - \alpha)\omega_o^2z = f(t) \quad (3.2)$$

where the hysteretic displacement z is a function of the time history of u ; it is related to u through the following first-order nonlinear differential equation,

$$\dot{z} = h(z) \left\{ \frac{A\dot{u} - \nu(\beta|\dot{u}||z|^{n-1}z + \gamma\dot{u}|z|^n)}{\eta} \right\} \quad (3.3)$$

where,

$f(t)$ = mass-normalized forcing function,

ω_o = preyield natural frequency of the system ($\sqrt{k_i/m}$); k_i is initial stiffness ,

ξ_o = linear damping ratio ($c/2\sqrt{k_i m}$),

α = a weighting constant representing the relative participations of the linear and nonlinear terms ($0 < \alpha < 1$),

A = parameter that regulates the tangent stiffness and ultimate hysteretic strength,

- β, γ, n = hysteresis shape parameters,
 ν, η = strength and stiffness degradation parameters, respectively; if $\nu = \eta = 1.0$,
the model does not degrade ,
 $h(z)$ = the pinching function introduced by Baber and Noori (1986); if $h(z) = 1.0$,
the model does not pinch.

The hysteretic restoring force is given by the fourth term in Eq. (3.2) as $F_h = (1 - \alpha)\omega_0^2 z$. Since $[(1 - \alpha)\omega_0^2]$ is a time-invariant system property, the hysteretic restoring force will also be referred to as z from hereon.

Equation (3.3) defines the constitutive law, based on a modified “endochronic” model of the force-displacement relations. The hereditary restoring force model satisfies the requirement that the response depends not only on instantaneous displacement but also on its past history (referred to earlier as memory).

3.4.3 Hysteresis Shape Properties

Baber (1980) and Maldonado et al. (1987) examined in great detail the properties of the Bouc-Wen or Modified-Bouc model (i.e., the non-degrading, $\nu = \eta = 1.0$, and non-pinching, $h(z)=1$, model). To understand the effects of the model parameters on hysteresis shape, let us examine the parameters α, A, β, γ and n .

3.4.3.1 Parameters A and α

From Eq. (3.1), the total non-damping restoring force F_T is expressed as

$$F_T = k[\alpha u + (1 - \alpha)z]. \quad (3.4)$$

Recall that $\alpha k u$ is the linear restoring force (due to the spring element) and $(1 - \alpha)k z$ is the the hysteretic restoring force (due to the hysteretic element). The tangent stiffness to the nonlinear restoring force is obtained by differentiating F_T with respect to displacement u :

$$\frac{dF_T}{du} = k \left[\alpha + (1 - \alpha) \frac{dz}{du} \right] \quad (3.5)$$

where $\frac{dz}{du}$ is the tangent to the nonlinear path in the z - u plane. This is obtained by dividing both sides of Eq. (3.3) by \dot{u} (or $\frac{du}{dt}$),

$$\frac{dz}{du} = h(z) \left\{ \frac{A - \nu(\beta \operatorname{sgn}(\dot{u}) |z|^{n-1} z + \gamma |z|^n)}{\eta} \right\} \quad (3.6)$$

where $\operatorname{sgn}(\cdot)$ = the signum function. The ultimate value of z , or z_u , is obtained by setting $\frac{dz}{du}$ to zero and solving it for z to get

$$z_u = \left[\frac{A}{\nu(\beta + \gamma)} \right]^{1/n}. \quad (3.7)$$

Assuming that ν , β , γ and n do not change, this shows that A regulates the ultimate hysteretic strength, z_u .

To investigate the effect of A on the tangent stiffness in the z - u plane, set $\nu = \eta = 1.0$ and $h(z)=1$, and rewrite Eq. (3.6) as

$$\frac{dz}{du} = A - (\beta \operatorname{sgn}(\dot{u}) |z|^{n-1} z + \gamma |z|^n) \quad (3.8)$$

At the limit $z \rightarrow u \rightarrow 0$,

$$\left. \frac{dz}{du} \right|_{z=u=0} = A \quad (3.9)$$

This means that A sets the initial tangent stiffness. Eqs. (3.7) and (3.9), thus, show that increasing the value of A increases both the ultimate hysteretic strength, z_u , and the initial tangent stiffness, $\frac{dz}{du}$ at $z = u = 0$.

In the special case where $A=1$, a physical interpretation of the parameter α may be obtained. Substitute Eq. (3.9) into (3.5) to obtain the initial tangent stiffness, k_i , in the F_T - u plane,

$$k_i = \left. \frac{dF_T}{du} \right|_{z=u=0} = k[\alpha + (1 - \alpha) \cdot 1] \quad (3.10)$$

which gives

$$k_i = k. \quad (3.11)$$

At z_u , $\frac{dz}{du}=0$ and the final tangent stiffness, k_f , is

$$k_f = \left. \frac{dF_T}{du} \right|_{z=z_u} = k\alpha. \quad (3.12)$$

From Eqs. (3.11) and (3.12),

$$\alpha = \frac{k_f}{k_i}. \quad (3.13)$$

Thus, α is the ratio of the final tangent stiffness to the initial stiffness, when $A=1$.

The preceding discussion may also be extended to provide some insight into the relationship of hystereses in the F_T - u and the z - u planes. For illustration purpose, we will keep $A=1$. First, consider a half cycle in the z - u plane. After plotting the tangent stiffness lines at $z=0$, Eq. (3.9), and $z = z_u$, the hysteresis may be plotted as shown in Fig. 3.3a. When $A=1$, the “yield” displacement, u_y , corresponding to the intersection of the initial and final tangent stiffness lines, is numerically equal to z_u .

In the F_T - u plane, the yield force is

$$F_{Ty} = k[\alpha u_y + (1 - \alpha)z_u] \quad (3.14)$$

or

$$u_y = z_u = \frac{F_{Ty}}{k}. \quad (3.15)$$

As seen in Fig. 3.3b, F_{Ty} corresponds to the intersection of the initial and final tangent stiffness lines and not to the actual force in the hysteresis curve corresponding to u_y . Fig. 3.3 shows that the hysteresis may be plotted in either plane, since it can be easily mapped from one to the other. The present work will focus mainly on the hysteresis in the z - u plane.

3.4.3.2 Parameters β and γ

Focusing on the non-degrading, non-pinching BWBN model, the constitutive relations may be broken into four segments. Eq. (3.8) is expressed as four differential equations,

$$\frac{dz}{du} = A - (\beta + \gamma)z^n \quad z \geq 0, \dot{u} \geq 0 \quad (3.16)$$

$$\frac{dz}{du} = A - (\gamma - \beta)z^n \quad z \geq 0, \dot{u} < 0 \quad (3.17)$$

$$\frac{dz}{du} = A + (-1)^{n+1}(\beta + \gamma)z^n \quad z < 0, \dot{u} < 0 \quad (3.18)$$

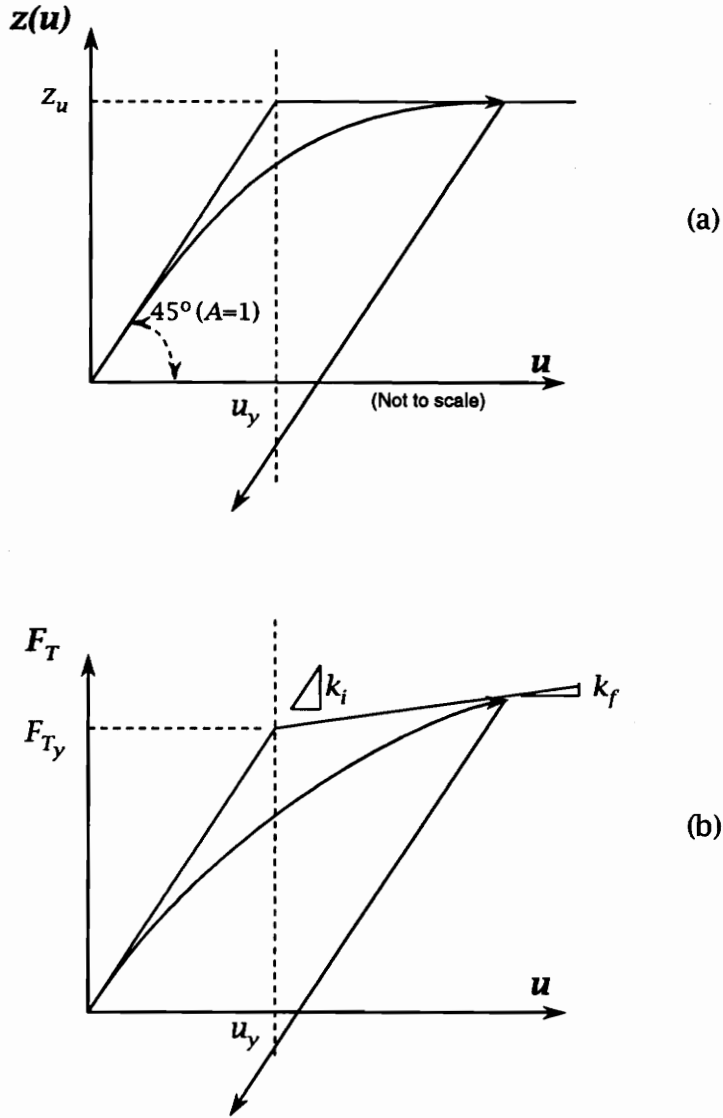


Figure 3.3: Nondegrading and non-pinching BWBN model: (a) z - u plane, (b) F_T - u plane

$$\frac{dz}{du} = A + (-1)^{n+1}(\gamma - \beta)z^n \quad z \leq 0, \dot{u} \geq 0 \quad (3.19)$$

Considering the simple case where $n = 1$, solutions to the above equations are plotted in Fig. 3.4, where u_o is the displacement at $z=0$, a quantity which varies from cycle to cycle. Eqs. (3.16) and (3.18) (Figs. 3.4a and c) are the *loading*, or outward, paths and Eqs. (3.17) and (3.19) (Figs. 3.4b and d) are the *unloading*, or inward, paths.

The equations for the loading paths may be combined and rewritten as

$$\frac{dz}{du} = A - (\beta + \gamma)|z|^n \quad z\dot{u} > 0 \quad (3.20)$$

Similarly, for the unloading paths,

$$\frac{dz}{du} = A - (\gamma - \beta)|z|^n \quad z\dot{u} < 0 \quad (3.21)$$

With these equations, it can be readily seen that when $\beta=0$, the two equations are the same and the loading and unloading paths coalesce into a single path. Although the path may remain nonlinear (when $n > 1$), it is nonhysteretic.

Examining the positive loading (Fig. 3.4a) and unloading (Fig. 3.4b) paths, it is observed that a variety of hysteresis shapes may be obtained by varying the values of A , β and γ . When $\beta < 0$, a negative dissipation energy is obtained. Since this cannot be physically realized, β should therefore always be positive, regardless of the value of γ . With this restriction, hysteresis shapes resulting from possible combinations of β and γ are shown in Fig. 3.5.

Depending on γ , a softening or hardening model may be obtained. A softening characteristic is obtained when the slope of the hysteresis path decreases with increasing $|z|$. A hardening model is obtained when the slope of the hysteresis path increases with increasing $|z|$. As seen in Fig. 3.5, positive γ tends to cause softening and negative γ tends to cause hardening, but the limiting behavior will remain softening unless $|\gamma| > |\beta|$ and $\gamma < 0$. To obtain a linear unloading path, set $\gamma = \beta$.

3.4.3.3 Parameter n

The effect of n on the skeleton curves of the hysteresis will be investigated in this

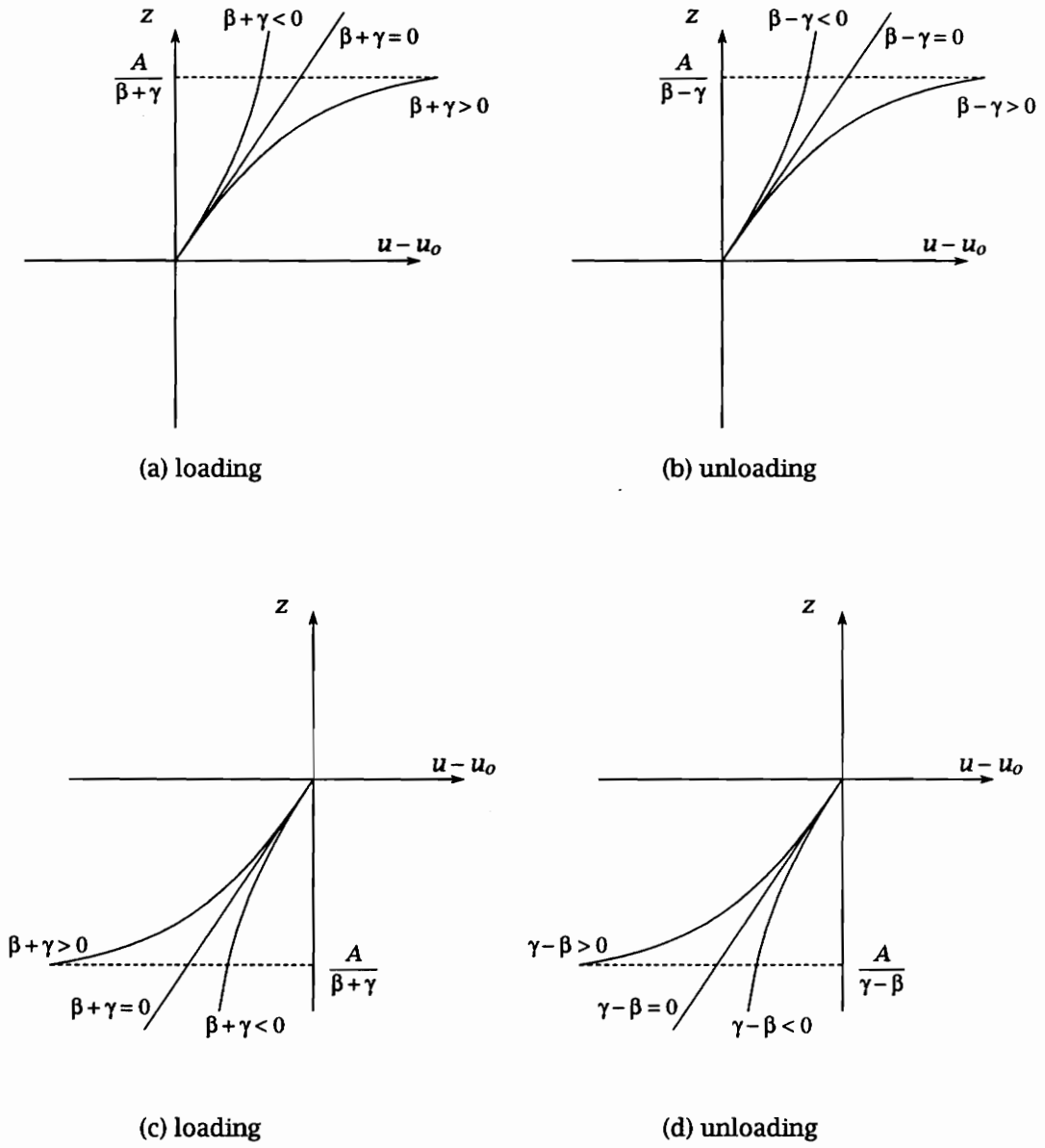


Figure 3.4: Hysteresis loop behavior for $n=1$

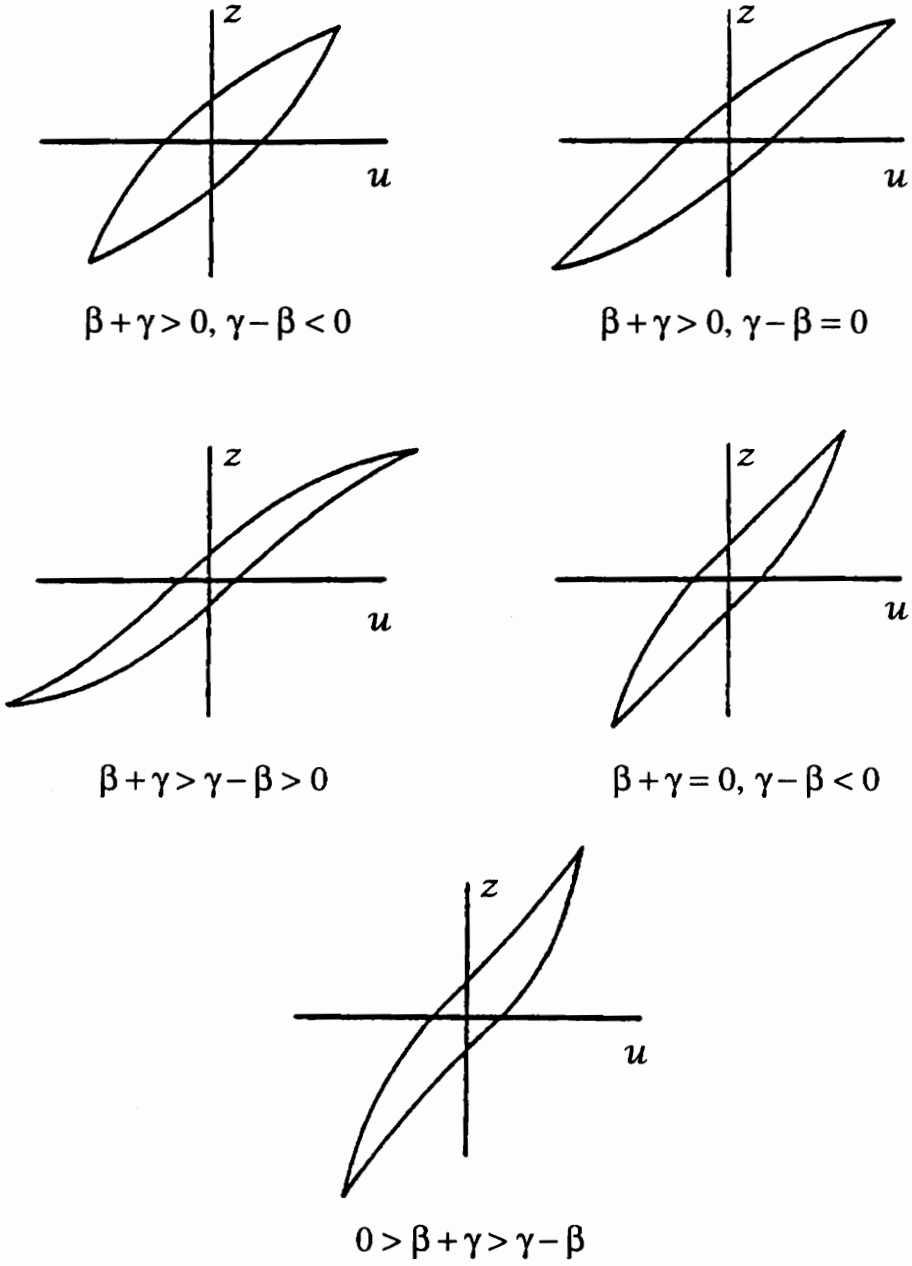


Figure 3.5: Possible hysteresis shapes, $n=1$ (from Baber 1980)

section. In Fig. 3.6, the skeleton curves for $n=1,3,6$ and 12 are shown for the case $A=1$, $\beta = \gamma = 0.5$. It can be seen that as n increases, the model approaches the elasto-plastic behavior. This can be shown analytically by examining the softening model, $(\beta + \gamma) > 0$. The loading path is given by Eq. (3.20). Considering the non-degrading case, $\nu=1$, and substituting for $(\beta + \gamma)$ from Eq. (3.7) into (3.20), we get

$$\frac{dz}{du} = A - A \left(\frac{z}{z_u} \right)^n . \quad (3.22)$$

When $z < z_u$, as $n \rightarrow \infty$, $(z/z_u)^n = 0$ and $\frac{dz}{du} = A$. Thus, the loading path for $0 < z < z_u$ is linear. When $z = z_u$, $\frac{dz}{du} = 0$ as before. This is a horizontal line.

The unloading path when $z > 0$ is defined by Eq. (3.21) and may be expressed as

$$\frac{dz}{du} = A - \left[A \left(\frac{\gamma - \beta}{\gamma + \beta} \right) \right] \left(\frac{z}{z_u} \right)^n \quad (3.23)$$

after some manipulation of Eq. (3.7) and substitution into (3.21). Again, as $n \rightarrow \infty$, the slope approaches a constant value A , which is the same as that for the loading path.

The foregoing shows that as $n \rightarrow \infty$, the hysteresis in the $z-u$ plane produces an elasto-plastic model. Following Fig. 3.3, this would produce a true bilinear hysteresis in the F_T-u plane, with $\alpha > 0$, and a true elasto-plastic hysteresis, with $\alpha \approx 0$.

3.4.4 Strength and Stiffness Degradation and Pinching

Degradation is controlled by defining the parameters ν and η as functions of the dissipated hysteretic energy given by

$$\varepsilon = \int_{u_o}^{u_f} F_h \cdot du = (1 - \alpha) \omega_o^2 \int_{u_o}^{u_f} z du = (1 - \alpha) \omega_o^2 \int_{t_o}^{t_f} z \dot{u} dt \quad (3.24)$$

Then, A , ν and η may be written as

$$\begin{aligned} A(\varepsilon) &= A_o - \delta_A \varepsilon \\ \nu(\varepsilon) &= 1.0 + \delta_\nu \varepsilon \\ \eta(\varepsilon) &= 1.0 + \delta_\eta \varepsilon \end{aligned} \quad (3.25)$$

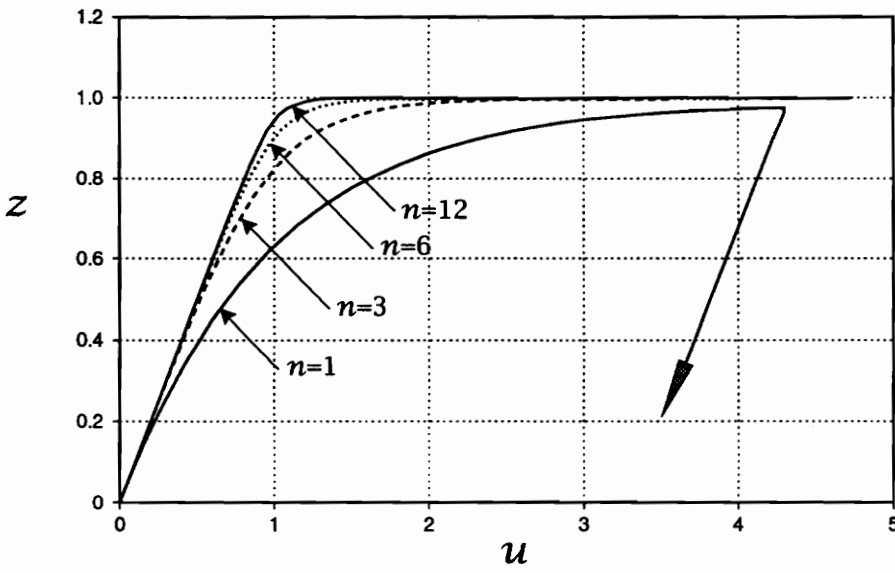


Figure 3.6: Skeleton curves with varying n

where A_0 is the initial value of A and the δ 's are constants specified for the desired rate of degradation. A value of $\delta = 0$ means no degradation. If A decreases (i.e., $\delta_A > 0$), both strength and stiffness degrade (Fig. 3.7). If ν increases (i.e., $\delta_\nu > 0$), strength alone degrades (Fig. 3.8). If η increases (i.e., $\delta_\eta > 0$), stiffness alone degrades (Fig. 3.9). Figures 3.10a, b and c show the effect of changing values of A , ν and η , respectively, using the stiffness, dz/du , vs. z/z_u plot. Note that each plot shows the positive z loading case only.

Sues et al. (1988) suggested an alternative stiffness degradation scheme similar to that of Clough for reinforced concrete elements (see Fig. 2.6c). The stiffness degradation parameter, η , is defined such that the value of A (which controls the initial loading slope of each hysteresis cycle) reflects the maximum deformation reached in the previous cycle. The desired displacement dependent stiffness degradation is achieved by

$$\eta_i = A_0 \frac{(u_{p_i} - u_{p_{i-1}})}{(z_{p_i} - z_{p_{i-1}})} \quad (3.26)$$

where,

- η_i = value of η during the i^{th} half cycle ,
- u_{p_i} = peak displacement in i^{th} half cycle,
- z_{p_i} = peak z value in i^{th} half cycle
- $u_{p_{i-1}}$ = peak displacement in $(i - 1)^{th}$ half cycle (note that this is the peak opposite and immediately before that in the i^{th} half cycle),
- $z_{p_{i-1}}$ = peak z value in $(i - 1)^{th}$ half cycle.

Sues et al. (1988) found Eq. (3.26) to adequately model the stiffness degradation observed in scale model tests of a reinforced concrete building and a reinforced concrete frame. Incorporating Eq. (3.26) with pinching (like the one that will be described next), the author, however, found that the rate of degradation increases too fast and out of control. The resulting model is practically useless. Thus, for a Bouc-Wen model that incorporates pinching, the energy-based stiffness degradation originally proposed by Baber and Wen (1981), and given in Eq. (3.25), is preferred.

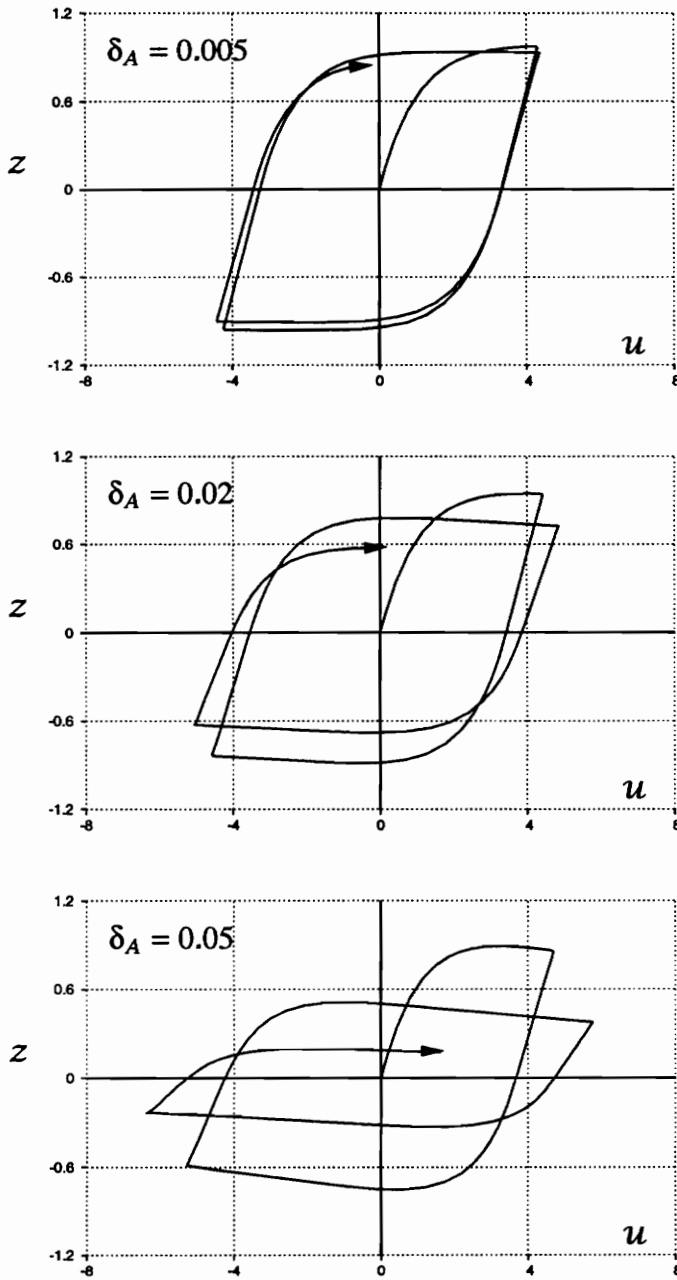


Figure 3.7: Strength and stiffness degradation- effect of varying A

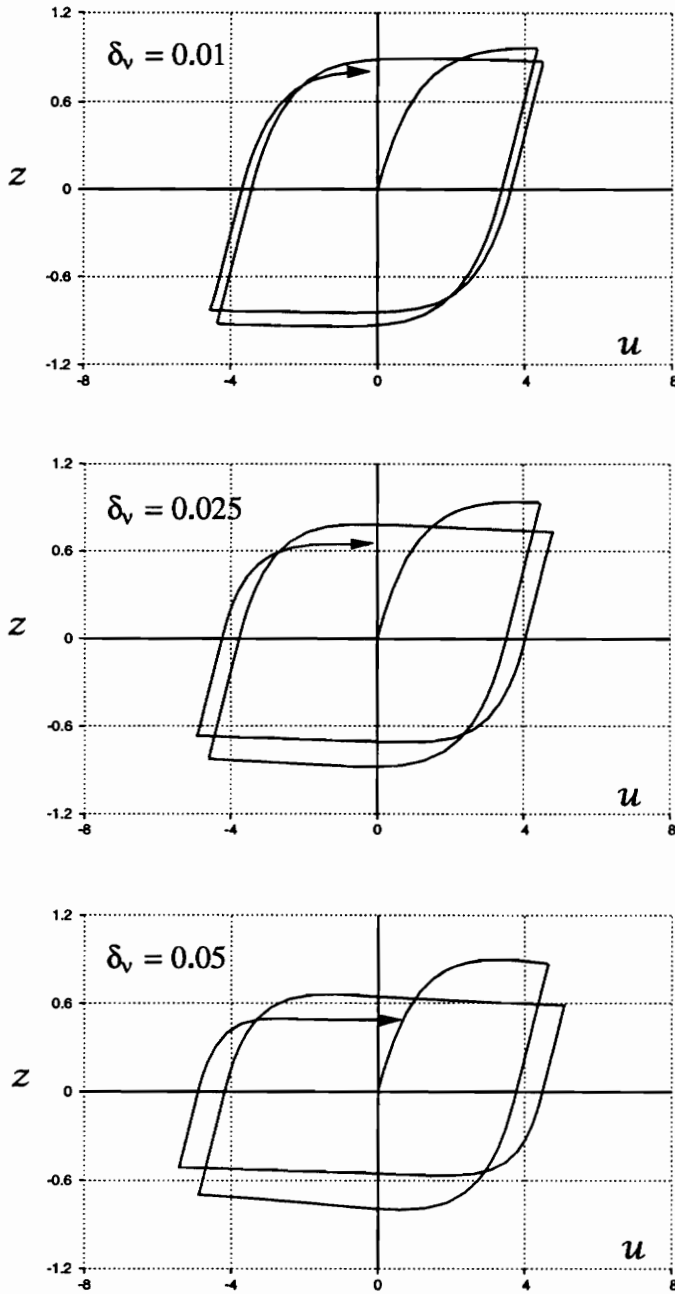


Figure 3.8: Strength degradation- effect of varying ν

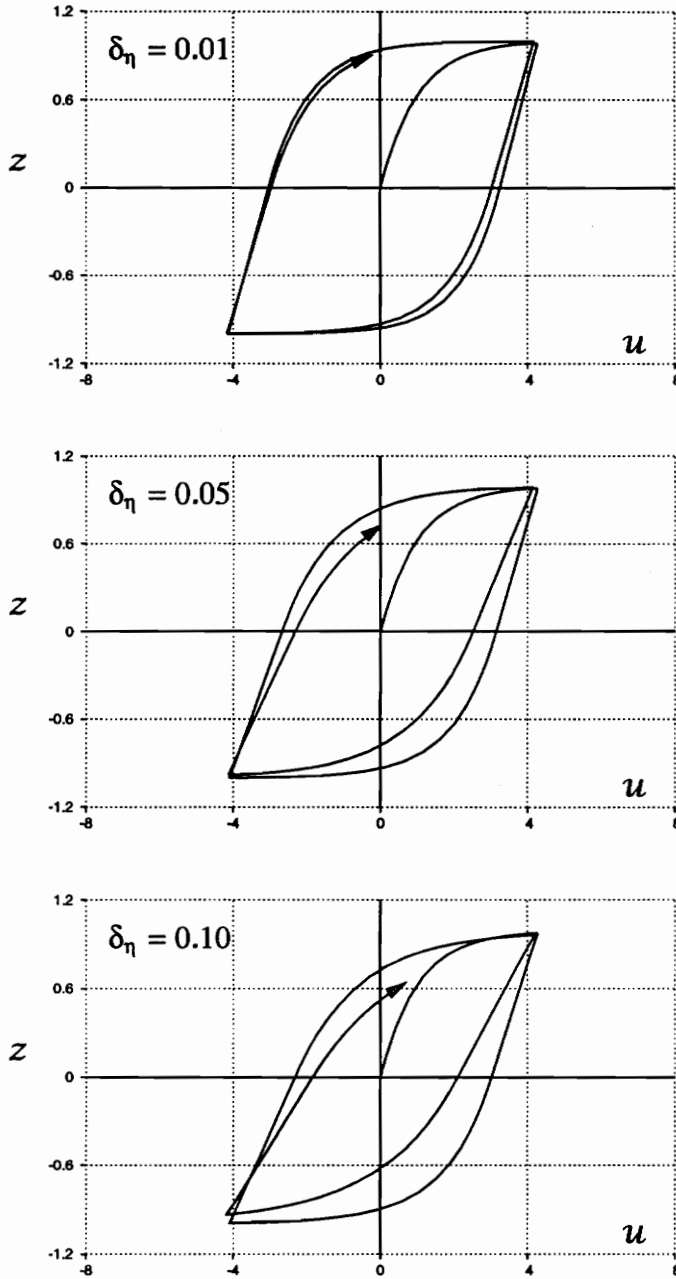
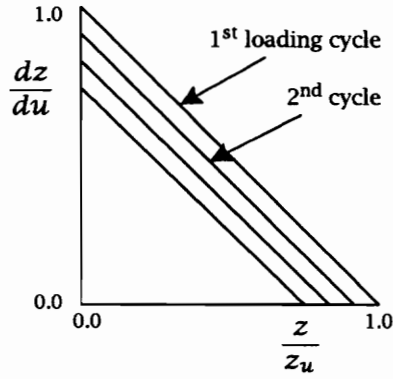
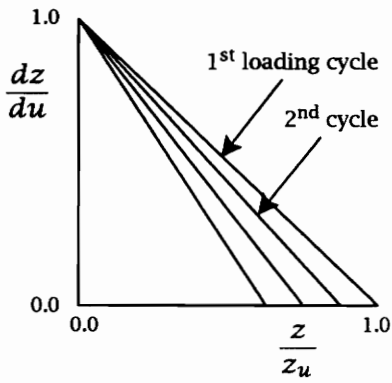


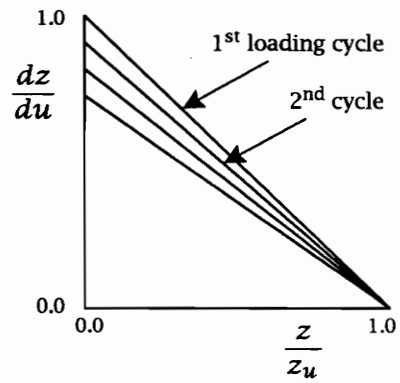
Figure 3.9: Stiffness degradation- effect of varying η



(a) only A is degrading



(b) only v is degrading



(c) only η is degrading

Figure 3.10: Degradation effect using $\frac{dz}{du}$ vs. $\frac{z}{z_u}$ plot

The pinching function, $h(z)$, originally proposed by Baber and Noori (1986), allows control of pinching severity and sharpness as functions of ε . It is defined by the following expressions (Baber and Noori 1986):

$$h(z) = 1.0 - \zeta_1 e^{(-z^2/\zeta_2^2)} \quad (3.27)$$

$$\zeta_1(\varepsilon) = \zeta_{1o} [1.0 - e^{(-p\varepsilon)}] \quad (3.28)$$

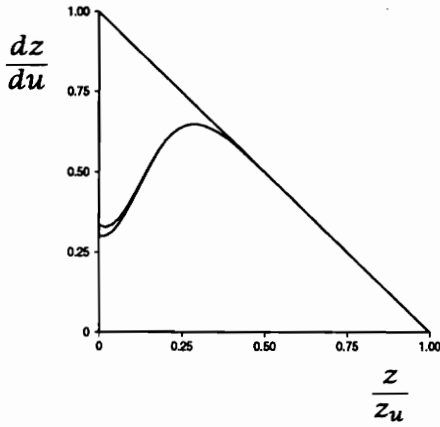
$$\zeta_2(\varepsilon) = (\psi_o + \delta_\psi \varepsilon) (\lambda + \zeta_1) \quad (3.29)$$

where,

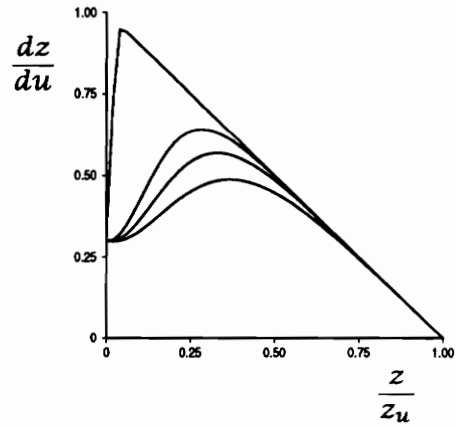
- ζ_1 = controls the magnitude of initial drop in slope, dz/du ; ($\zeta_1 < 1.0$),
- ζ_2 = controls the rate of change of the slope, dz/du ,
- ψ = parameter that contributes to the amount of pinching,
- δ_ψ = parameter specified for the desired rate of change of ζ_2 based on ε ,
- p = constant that controls the rate of initial drop in slope,
- ζ_{1o} = measure of total slip,
- λ = small parameter that controls the rate of change of ζ_2 as ζ_1 changes.

The pinching function effect can be seen from the plot of stiffness, dz/du , against z/z_u in the absence of degradation (Fig. 3.11). Fig. 3.11a shows that when ζ_1 varies while ζ_2 is kept constant, dz/du drops at the start of the second and successive loading cycles. Pinching is induced by forcing minimum tangent stiffness when $z=0$. Then, the stiffness increases relatively rapidly as z increases, slowing down as the original slope is approached. When ζ_2 is kept constant, the original slope is reached at the same level of z in all cycles. When ζ_2 is varied and ζ_1 is kept constant, the level of drop at the start of the second and successive loading cycles remains the same but the original slope is reached at increasing levels of z . Thus, it may be stated that ζ_1 controls the severity of pinching while ζ_2 controls the rate of pinching. Fig. 3.11c shows the pinching function effect when both ζ_1 and ζ_2 vary.

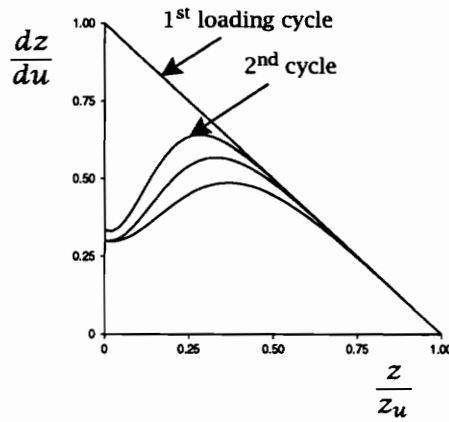
While Baber and Noori's pinching function improved the versatility and capability of the BWBN model, most wood joints and structural systems that show pinching behavior



(a) only ζ_1 varies (ζ_2 is constant)



(b) only ζ_2 varies (ζ_1 is constant)



(c) both ζ_1 and ζ_2 vary

Figure 3.11: Baber and Noori's (1986) pinching function effect (dz/du vs. z/z_u)

do not pinch at $z=0$ (e.g., Fig. 2.4). Thus, the pinching function should be modified. Section 3.5 will discuss the pinching behavior of wood systems and the development of an appropriate pinching function.

3.4.5 Model Limitation

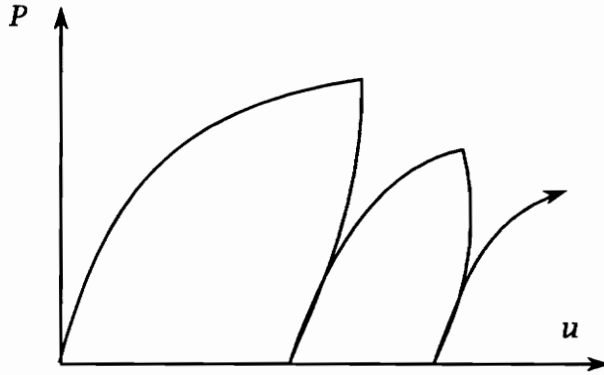
Maldonado et al. (1987) and Casciati (1987) observed that the most serious drawback in the original Bouc-Wen model (i.e., the nondegrading, nonpinching type) was its inability to form a small loop during partial loading-unloading (see Fig. 3.12). Instead, the model softens during reloading without stress reversal. Most materials, including wood, demonstrate hysteresis loops in loading situations without stress reversal. This unwanted model behavior, however, is of relatively minor consequence in seismic analysis because seismic ground motions induce stress reversals on structures. Seismic ground action is often treated as a zero mean random process. For other loadings (e.g., wind) where this mechanical behavior needs to be modeled properly for analysis, a modification to the Bouc-Wen model was proposed by Casciati (1987). Two terms are added in the hysteretic constitutive equation so that the stiffness at the beginning of reloading, when there is no stress reversal, is greater than the one at the end of unloading. These terms disappear during unloading.

Casciati's modification of the Bouc-Wen model will not be considered in the present work. Dynamic analysis will be limited, for now, to wood structural systems under earthquake loading.

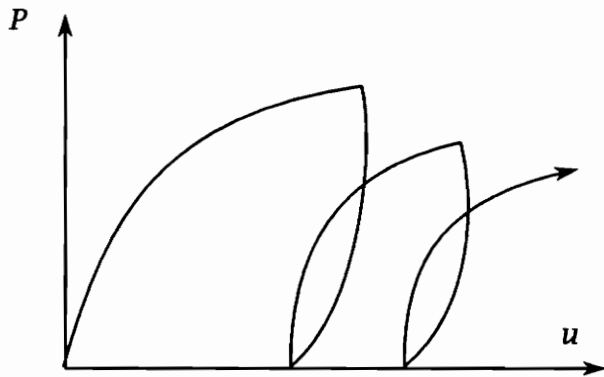
3.5 Pinching of Wood Systems

3.5.1 Experimental Observations

A closer examination of the pinching behavior of wood subassemblies in Fig. 2.4 and the nailed sheathing joint in Fig. 2.5c shows that the pinching function should have the following features (illustrated in Fig. 3.13):



(a) Bouc-Wen hysteresis behavior



(b) behavior of most materials (including wood)

Figure 3.12: Hysteresis during partial loading-unloading

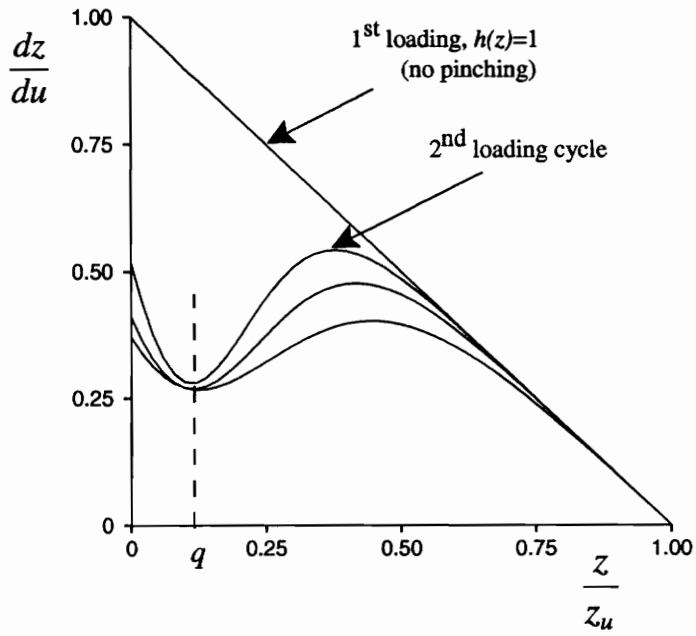


Figure 3.13: Pinching of wood systems (dz/du vs. z/z_u)

- In initial loading (starting from rest), no pinching occurs.
- In the second loading cycle, pinching starts: dz/du drops at $z=0$ and continues to decrease until it reaches a minimum at $z = \text{some fraction of } z_u$, or qz_u . Then the stiffness increases relatively rapidly as z increases, slowing down as the original slope is approached. As z finally approaches ultimate value, the slope sharply decreases and reaches zero at z_u .
- In the third and successive cycles, the drop of dz/du at $z=0$ slows down but the stiffness reaches a minimum at qz_u again. Medearis and Young (1964) first noticed this on cyclic tests of plywood shear walls and called qz_u the *invariant point*. Others call it the *residual force*.

3.5.2 Pinching Function Development

Baber and Noori (1986) introduced the use of dz/du vs. z curves to develop hysteresis models. Here, the object is to obtain mathematical functions that would provide the dz/du behavior shown in Fig. 3.13 and listed in section 3.5.1. To do this, the tangent stiffness function, given earlier in Eq. 3.6 as

$$\frac{dz}{du} = h(z) \left\{ \frac{1 - \nu(\beta \operatorname{sgn}(\dot{u}) |z|^{n-1}z + \gamma |z|^n)}{\eta} \right\}, \quad (3.30)$$

is examined.

To get the desired pinching, the pinching function, $h(z)$, should be a small value at $z=0$ and reach a minimum at $z = qz_u$; this makes dz/du minimum at this level as well. As z increases, $h(z)$ should approach 1 to allow dz/du to return to the original stiffness path. During unloading, $h(z)$ should not cause pinching even at $z = qz_u$. Thus, pinching should be induced during loading only, that is, when $z\dot{u} > 0$ or $\operatorname{sgn}(z) \cdot \operatorname{sgn}(\dot{u})$ is positive [see Eq. (3.20)].

Several modifications of Baber and Noori's (1986) original function, defined by

Eqs. (3.27), (3.28) and (3.29), were investigated. One that meets the foregoing requirements with the least modification of Baber and Noori's function is

$$h(z) = 1.0 - \zeta_1 e^{[-(z \operatorname{sgn}(\dot{u}) - qz_u)^2 / \zeta_2^2]} \quad (3.31)$$

where q is a constant that sets a fraction of z_u as the pinching level and all other parameters are as previously defined. Eq. (3.31) is a generalization of Baber and Noori's pinching function; that is, when $q=0$, the model reverts back to Baber and Noori's original function. It is desired that as little modification as possible is introduced to Baber and Noori's equation in the hope that the new model will maintain the original form's compatibility with statistical linearization during random vibration analysis. Although random vibration analysis is not performed in the present work, this is the goal of the project's next phase.

Figure 3.14 shows $h(z)$ as a function of z and $\operatorname{sgn}(\dot{u})$, where $\zeta_1=0.85$, $\zeta_2=0.02$, $q=0.15$ and $z_u=1.0$. Its effect on dz/du satisfies the pinching requirements for wood systems and produces a dz/du vs. z/z_u plot similar to that in Fig. 3.13.

3.6 Summary

The Bouc-Wen-Baber-Noori (BWBN) hysteresis model was used as the basis of a general model for wood joints and structural systems. The mechanical model consisted of three parallel elements: (1) a linear viscous damping, (2) a linear spring and (3) a hysteretic element. The hysteretic element was defined by a nonlinear first-order differential equation with a form similar to that in the endochronic theory of plasticity. The hereditary nature of the constitutive relations satisfied the requirement that the response depends not only on instantaneous displacement but also on its past history (or memory).

The form and properties of the original Bouc-Wen model and its extensions were presented. The pinching capability of the BWBN model was modified so that it would

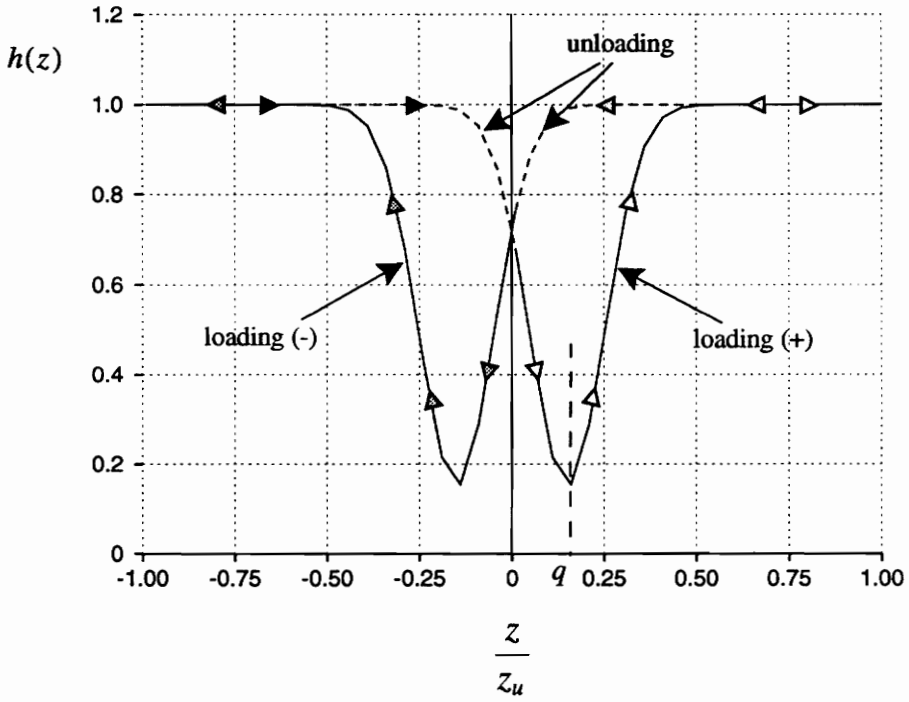


Figure 3.14: Behavior of the proposed pinching function for wood systems

represent pinching in dowel-type wood joints more accurately. The generalized pinching capability enhanced the model's versatility. The modified BWBN model is, in fact, applicable to structures made of other materials, such as steel and reinforced concrete, that exhibit pinching similar to that observed in dowel-type wood joints and plywood shear walls. In summary, the modified BWBN hysteresis model incorporates all the experimentally observed characteristics of timber structures that were identified in the previous chapter. It has: (1) a nonlinear, inelastic load-displacement relationship without a distinct yield point, (2) stiffness degradation, (3) strength degradation, (4) pinching, and (5) memory.

Chapter 4

Dynamic Modeling of Wood Structures

4.1 General

Structures are continuous systems and as such have an infinite number of degrees of freedom. For analytical purposes, the structure is simplified by means of *spatial discretization* of the continuum. The following discretization methods can be used in the dynamic modeling of structures (Clough and Penzien 1993): (1) concentrated mass method, (2) generalized displacements method, and (3) finite element method. Use of any of these methods results in a discretized structural model with a finite number of degrees of freedom. The present work will concentrate on the concentrated mass method only.

The basis, form and properties of a general hysteresis model for wood joints and structural systems were presented in the previous chapter. Here, the complete form of the modified Bouc-Wen-Baber-Noori (BWBN) model for SDF wood systems will be summarized, a model for MDF systems will be derived, methods for parameter estimation will be briefly discussed, model behavior will be compared with a selected number of experimental hysteresis results and its potential applications for future studies in dynamic analysis and design of wood structures and structural systems will be presented.

4.2 Proposed Model for Wood Structural Systems

4.2.1 Model for SDF Systems

While very few real structures are accurately modeled by SDF models, such models

may still be used for preliminary dynamic analyses of many types of structures. In some cases, a SDF model is sufficient to obtain a basic understanding of the dynamic behavior of the structural system. Fig. 4.1 shows a SDF dynamic model idealization of a trussed wood-frame and a wood shear wall. The structural mass is assumed to be concentrated in the direction of the displacement. Stewart (1987) and Kamiya (1988) performed time history analyses of wood-sheathed shear walls using a SDF model that incorporates their hysteresis models presented in section 2.4.2. Stewart obtained hysteresis parameters from full-scale cyclic tests of the walls, while Kamiya obtained model parameters from pseudo-dynamic tests. Gavrilović and Gramatikov (1991) also used a SDF model to compute the dynamic response of a trussed-frame wood structure.

The hysteresis model developed and described in the previous chapter will now be summarized for SDF wood systems. The equation of motion is

$$\ddot{u} + 2\xi_o\omega_o\dot{u} + \alpha\omega_o^2u + (1 - \alpha)\omega_o^2z = f(t) . \quad (4.1)$$

So that α is the ratio of the final tangent stiffness to the initial stiffness (see section 3.4.3.1), A will be set to unity ($A=1$) in the hysteretic constitutive relations. Then, the constitutive law, Eq. (3.3), becomes

$$\dot{z} = h(z) \left\{ \frac{\dot{u} - \nu(\beta|\dot{u}||z|^{n-1}z + \gamma\dot{u}|z|^n)}{\eta} \right\} \quad (4.2)$$

with pinching function

$$h(z) = 1.0 - \zeta_1 e^{[-(z \operatorname{sgn}(\dot{u}) - qz_u)^2 / \zeta_2^2]} \quad (4.3)$$

where

$$\zeta_1(\varepsilon) = \zeta_{1o} [1.0 - e^{(-p\varepsilon)}] \quad (4.4)$$

$$\zeta_2(\varepsilon) = (\psi_o + \delta_\psi \varepsilon) (\lambda + \zeta_1) . \quad (4.5)$$

Strength and stiffness degradation are modeled, respectively, by

$$\nu(\varepsilon) = 1.0 + \delta_\nu \varepsilon \quad (4.6)$$

$$\eta(\varepsilon) = 1.0 + \delta_\eta \varepsilon .$$

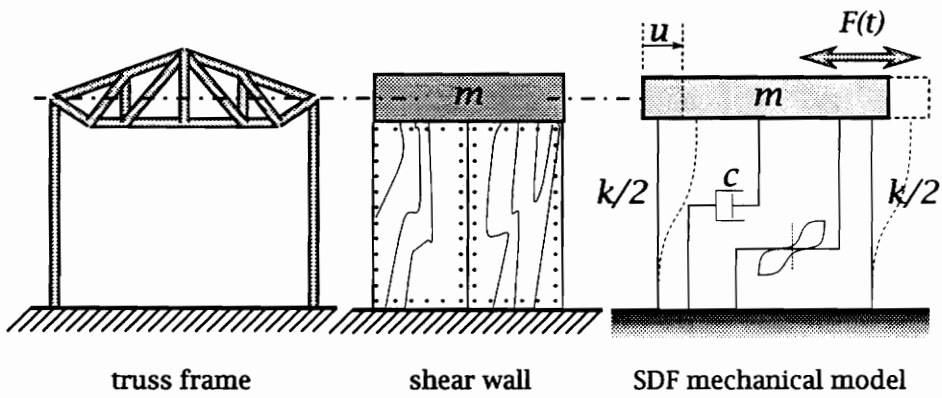


Figure 4.1: SDF idealization of wood structural systems

Note that parameter A is now treated as a constant (in this case $A=1$). Pinching, and strength and stiffness degradation are controlled by the hysteretic energy dissipation

$$\varepsilon = (1 - \alpha)\omega_0^2 \int_{t_0}^{t_f} z\dot{u} dt . \quad (4.7)$$

All variables are as previously defined.

The foregoing model satisfies all the experimentally observed features of hysteretic behavior of wood joints and structural systems, namely, (1) nonlinear hysteresis, (2) stiffness degradation, (3) strength degradation, (4) pinching and (5) memory (see section 2.3.2). The constitutive law takes into account the dependence of wood joints' response on their past history.

4.2.2 Model for MDF Systems

4.2.2.1 Shear Building Model

Multi-storey buildings have been commonly treated as "shear-beam" or, simply, shear buildings in most earthquake engineering studies. A shear building model, the simplest MDF model possible, is based on the following assumptions (Paz 1991): (1) the total mass of the structure is concentrated at the levels of the floors (or the roof, at the top floor), (2) the girders on the floors are infinitely rigid as compared to the columns, and (3) the deformation of the structure is independent of the axial forces present in the columns. The structure will now only have as many degrees of freedom as it has lumped masses at the floor levels. With the second assumption, rotation at the girder-to-column joint is suppressed. The third assumption means that the rigid girders remain horizontal during ground motion.

While many wood structures may not be ideal candidates as shear building models, these models may still provide enhancements that make them more preferable than alternative SDF models. A two-storey wood building shown in Fig. 4.2a, for example, may be better represented by a three-degree-of-freedom shear building than by a SDF model. The first mass, m_1 , is assumed to be concentrated at the floor of the first

storey. Corresponding hysteretic properties are obtained from the floor-to-foundation connections. The second mass, m_2 , is concentrated on the second-storey floor. Corresponding hysteretic properties are obtained from the columns (or walls) connecting the first and second storey floor systems. The trussed-roof structure carries m_3 , with corresponding hysteretic properties obtained from the columns (or walls) connecting the second storey floor system and the roof system. Sakamoto and Ohashi (1988) used the shear building model to compute the seismic response of one-, two- and three-storey conventional Japanese wood houses. Fig. 4.3 shows the lumped mass model that they used.

Generally, a shear building model may have up to r lumped masses and, thus, r degrees of freedom. Considering the shear building model in Fig. 4.2b, the relative displacement of the i^{th} mass with respect to the ground displacement is indicated by x_i . Interstorey drift, or the relative displacement between floors, is denoted by $u_i = x_i - x_{i-1}$. When dynamically loaded, the i^{th} mass is acted upon by the forces shown in Fig. 4.2c, where \ddot{x}_i^A is the absolute acceleration, $\ddot{x}_i^A = \ddot{x}_i + \ddot{x}_g$, and Q_i is the total restoring force of the i^{th} mass given as

$$Q_i = c_i(\dot{x}_i - \dot{x}_{i-1}) + \alpha_i k_i(x_i - x_{i-1}) + (1 - \alpha_i)k_i z_i \quad (4.8)$$

or, in terms of u_i ,

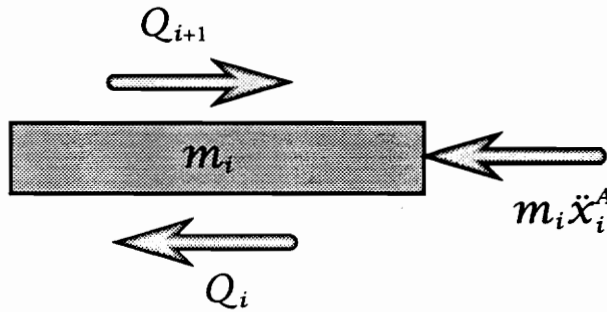
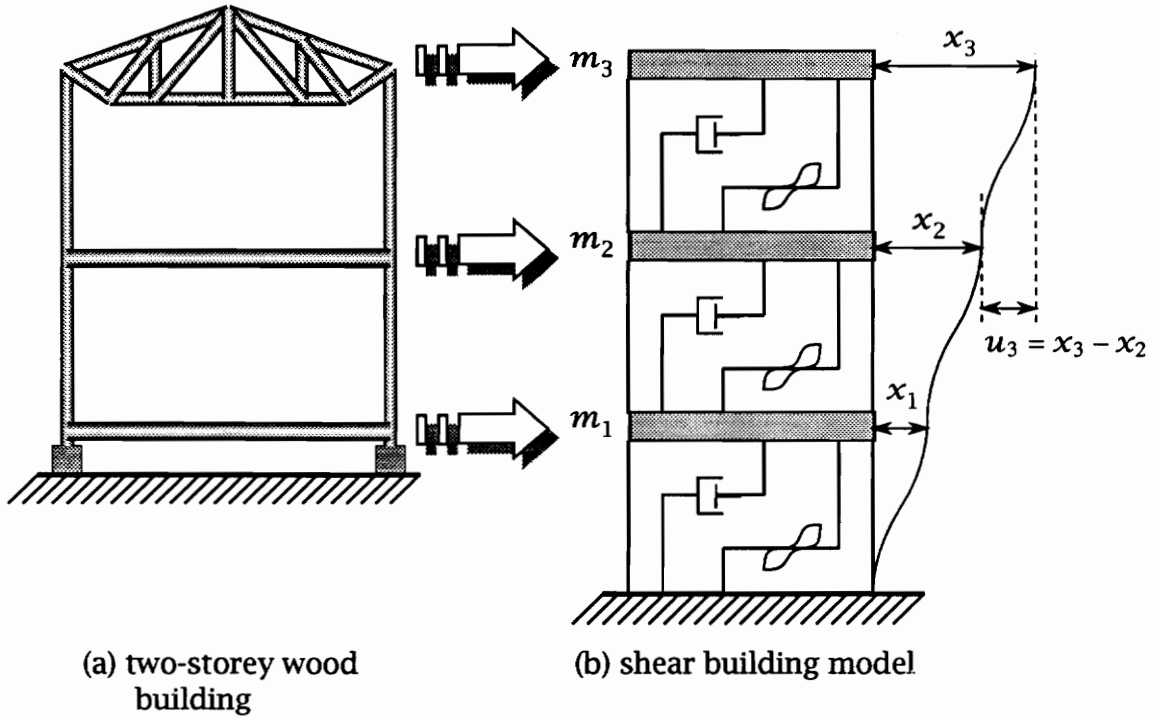
$$Q_i = c_i \dot{u}_i + \alpha_i k_i u_i + (1 - \alpha_i)k_i z_i . \quad (4.9)$$

Using D'Alembert's principle, the equation of motion is obtained as

$$m_i \ddot{x}_i^A + Q_i - Q_{i+1} = 0 \quad (4.10)$$

or, after substituting \ddot{x}_i^A and Eq. (4.8) and rearranging,

$$\begin{aligned} m_i \ddot{x}_i - c_i \dot{x}_{i-1} + (c_i - c_{i+1})\dot{x}_i + c_{i+1}\dot{x}_{i+1} - \\ \alpha_i k_i x_{i-1} + (\alpha_i k_i - \alpha_{i+1} k_{i+1})x_i + \alpha_{i+1} k_{i+1} x_{i+1} + \\ (1 - \alpha_i)k_i z_i - (1 - \alpha_{i+1})k_{i+1} z_{i+1} = -m_i \ddot{x}_g \end{aligned} \quad (4.11)$$



(c) forces acting on i^{th} mass

Figure 4.2: MDF idealization of multi-storey wood buildings

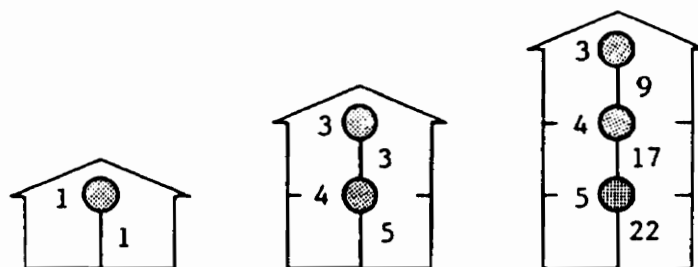


Figure 4.3: Sakamoto and Ohashi's (1988) MDF idealization of multi-storey conventional Japanese houses

where $i = 1, 2, \dots, r$. The assemblage of equations of motion for all r masses gives the following matrix equation:

$$[M]\{\ddot{X}\} + [C]\{\dot{X}\} + [K^\alpha]\{X\} + [H^\alpha]\{Z\} = -[M]\{T\}\ddot{x}_g \quad (4.12)$$

where $\{X\}$ is the relative displacement vector, $\{Z\}$ is the vector for the hysteretic component of the displacement and $\{T\}$ is the influence vector (all entries are 1, in this case).

The hysteretic displacement, z_i , of the i^{th} mass is related to the relative displacement between floors, u_i , through the following first-order nonlinear differential equation:

$$\dot{z}_i = h(z_i) \left\{ \frac{\dot{u}_i - v_i(\beta_i |\dot{u}_i| |z_i|^{n_i-1} z_i + \gamma_i \dot{u}_i |z_i|^{n_i})}{\eta_i} \right\} \quad (4.13)$$

where the parameters are the same as in the SDF model except that they are now defined for each element. That is,

$$h(z_i) = 1.0 - \zeta_{1i} e^{[-(z_i \operatorname{sgn}(\dot{u}_i) - a_i z_i u_i)^2 / \zeta_{2i}^2]} \quad (4.14)$$

$$\zeta_{1i}(\varepsilon_i) = \zeta_{1oi} [1.0 - e^{(-p_i \varepsilon_i)}] \quad (4.15)$$

$$\zeta_{2i}(\varepsilon_i) = (\psi_{oi} + \delta_{\psi_i} \varepsilon_i) (\lambda_i + \zeta_{1i}) \quad (4.16)$$

$$v_i(\varepsilon_i) = 1.0 + \delta_{v_i} \varepsilon_i \quad (4.17)$$

$$\eta_i(\varepsilon_i) = 1.0 + \delta_{\eta_i} \varepsilon_i \quad (4.18)$$

$$\varepsilon_i = (1 - \alpha_i) \omega_{oi}^2 \int_{t_0}^{t_f} z_i \dot{u}_i dt. \quad (4.19)$$

Note that $u_i = x_i - x_{i-1}$ and $i = 1, 2, \dots, r$.

All the matrices in Eq. (4.12) have dimension $(r \times r)$. $[M]$ is the diagonal mass matrix. $[C]$ is the damping matrix with the following nonzero entries:

$$[C] = \begin{bmatrix} (c_1 + c_2) & -c_2 & & & & \\ -c_2 & (c_2 + c_3) & -c_3 & & & \\ & \ddots & \ddots & \ddots & & \\ & & & c_{n-1} & (c_{n-1} + c_n) & -c_n \\ & & & & -c_n & c_n \end{bmatrix}. \quad (4.20)$$

The linear part of the stiffness matrix, $[K^\alpha]$, has the following nonzero entries:

$$[K^\alpha] = \begin{bmatrix} (k_1^\alpha + k_2^\alpha) & -k_2^\alpha & & & & \\ -k_2^\alpha & (k_2^\alpha + k_3^\alpha) & -k_3^\alpha & & & \\ & \ddots & \ddots & \ddots & & \\ & & & k_{n-1}^\alpha & (k_{n-1}^\alpha + k_n^\alpha) & -k_n^\alpha \\ & & & & -k_n^\alpha & k_n^\alpha \end{bmatrix} \quad (4.21)$$

where $k_i^\alpha = \alpha_i k_i$. Matrix $[H^\alpha]$ contains the hysteretic elements with the following nonzero entries:

$$[H^\alpha] = \begin{bmatrix} h_1^\alpha & -h_2^\alpha & & & & \\ & h_2^\alpha & -h_3^\alpha & & & \\ & & \ddots & \ddots & & \\ & & & & h_{n-1}^\alpha & -h_n^\alpha \\ & & & & & h_n^\alpha \end{bmatrix} \quad (4.22)$$

where $h_i^\alpha = (1 - \alpha_i)k_i$.

The model for MDF shear buildings is now complete and is described by Eqs. (4.12) to (4.22). There are a total of $2r$ unknowns: r unknowns in vector $\{X\}$ plus r unknowns in $\{Z\}$. There are r equations in (4.12) and another r equations to define the constitutive relations of each deforming element, Eqs. (4.13) to (4.19). If we are interested in the behavior and performance of the i^{th} mass, its hysteresis may be plotted in the z_i - u_i plane. Note that u_i is the interstorey drift, or the relative displacement between floors, calculated as $(x_i - x_{i-1})$.

If it is desired to obtain u_i directly, the equations of motion should be formulated in terms of u_i . Substituting $\ddot{x}_i^A = \ddot{x}_i + \ddot{x}_g = \sum_{j=1}^i \ddot{u}_j + \ddot{x}_g$ into Eq. (4.10) and dividing by m_i ,

$$\sum_{j=1}^i \ddot{u}_j + \ddot{x}_g + \frac{Q_i}{m_i} - \frac{Q_{i+1}}{m_i} = 0 \quad (4.23)$$

The relative accelerations are decoupled by subtracting the $(i-1)^{\text{th}}$ equation from the i^{th} equation (except when $i=1$) to obtain

$$\ddot{u}_i - (1 - \delta_{i1}) \frac{Q_{i-1}}{m_{i-1}} + \left[1 + (1 - \delta_{i1}) \frac{m_i}{m_{i-1}} \right] \frac{Q_i}{m_i}$$

$$-(1 - \delta_{ir}) \frac{Q_{i+1} m_{i+1}}{m_{i+1} m_i} = -\delta_{i1} \ddot{x}_g \quad (4.24)$$

where δ_{i1} , δ_{ir} are Kronecker deltas (i.e., $\delta_{ir} = 1$ when $i = r$, 0 otherwise) introduced so that the equation will be valid for the first mass ($i = 1$) and last mass ($i = r$), as well as all the intermediate masses. The complete model is now described by Eqs. (4.24) and (4.13) to (4.19).

4.2.2.2 Alternatives to the Shear Building Model

Other structural models may be used instead of the simple shear building model given above. Related work will be cited but no other model that specifically incorporates the modified BWBN hysteresis model will be formulated.

Takizawa (1975) proposed a structural modeling technique that considers the interaction of inelastic storey drifts. His approach required that the structural mechanism producing the inelastic response deformations be known or assumed. The post-yield degrees of freedom are then based on the frame yield mechanism, with the pre-yield stiffness based upon the natural frequency. His approach sometimes leads to a SDF system. Baber (1980) reviewed other modeling techniques and chose the discrete hinge concept, normally used in deterministic analysis of yielding structures, to model plane frame structures. Yielding was confined to discrete hinge regions that incorporate the non-pinching BWBN constitutive relations. Baber (1980; 1986a; 1986b) performed zero and non-zero mean random vibration analyses of hysteretic frames using this approach. Fig. 4.4 shows a typical discrete hinge model of a planar frame. Maldonado (1992) used a similar approach in developing a response spectrum method for plane frames with potential plastic hinges modeled by the non-pinching non-deteriorating BWBN constitutive law.

Previous work have, thus, shown that incorporation of the BWBN hysteresis model into analytical structural models is not limited to shear type buildings. If desired, it can be used with other structural modeling techniques.

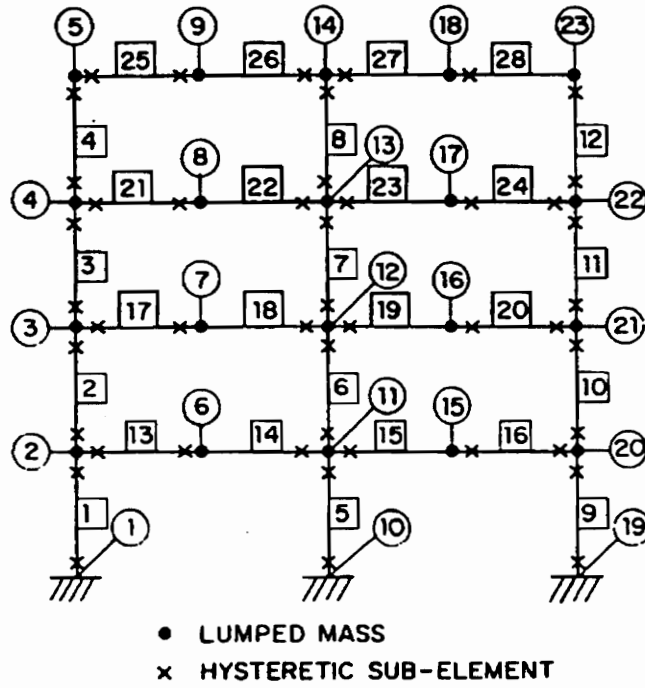


Figure 4.4: Hysteresis frame discrete hinge model (from Baber 1986b)

4.3 Parameter Estimation

There are typically two steps in constructing a mathematical model from measured data (Ljung and Söderström 1983): (1) selecting a family of candidate models that represents the general behavior of the physical system, and (2) choosing a particular member of this family that best describes the observed data. A general hysteresis model has just been proposed for wood structural systems. The model then needs to be explicitly defined for a particular set of system materials and configurations. This is specifically known as a *parameter estimation* problem, or generally as a *system identification* problem.

System identification is defined as “a process for constructing a mathematical description or model of a physical system when both the input to the system and the corresponding output are known” (Yao 1985). The general topic of system identification originated from mechanical control theory and electrical engineering but has since been used in many branches of science and engineering. For structural engineering applications, the input is usually a forcing function and the output is displacement, velocity, or acceleration response of the structure to this force. Thus, the particular model obtained from the identification process should produce a response that closely matches the system output, given the same input (Yao 1985).

Ideally, one should use system identification techniques such as Newton’s iterative algorithm, Gauss method, or Extended Kalman Filtering technique to systematically determine the hysteresis model parameters from experimental data (e.g., Sues et al. 1988; Maruyama et al. 1989). But this is a major project by itself and is beyond the scope of the present work. For the purpose of this thesis, a practical, albeit nonsystematic, approach will be used.

Properties needed in the equation of motion are estimated from the physical system. The system’s natural frequency, ω_o , is computed as $\sqrt{k_i/m}$, where m is the estimated mass of the system and k_i is its initial stiffness. From the system’s experimental hysteresis, the nonlinear weighting constant, α , is computed as the ratio of

the final tangent stiffness, k_f , to initial stiffness, k_i . Since system nonlinearity, hysteretic damping, and the non-viscous energy dissipation property are modeled by the hysteretic element, the value of the *linear* damping ratio, ξ_o , is not critical and may be arbitrarily chosen within the range 0.01 and 0.05 (Yeh et al. 1971; Chui and Smith 1989) for all wood systems.

Hysteresis shape parameter values for β and γ should be chosen such that

$$\beta + \gamma > 0 \text{ and } \gamma - \beta \leq 0.$$

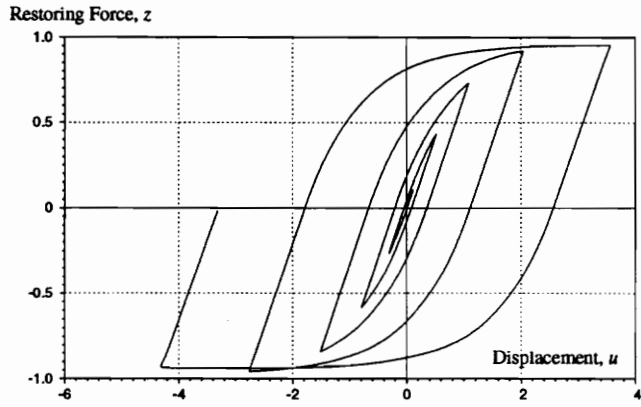
Note that, to obtain positive energy dissipation, $\beta > 0$. The pinching level constant, q , is determined from the experimental hysteresis as the ratio of the residual force (at invariant point) to the maximum restoring force. The pinching and degradation parameters, p , ζ_{1o} , λ , ψ_o , δ_ψ , δ_v and δ_η , are obtained by experimentation. That is, they are assigned certain values, the response is computed using the computer program that is described in the next chapter and the model hysteresis is plotted and compared with experimental hysteresis. This is repeated until the basic hysteresis shape is satisfactorily reproduced.

4.4 Comparison With Experimental Hysteresis

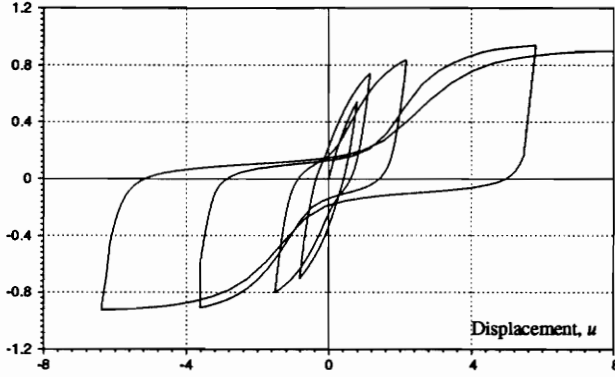
Model parameters of three common wood joints, to represent the major hysteresis types for timber structures that Dowrick (1986) identified (see section 2.3.1), were estimated. Figures 4.5a, b and c show the hysteresis shapes produced by the model.

For a SDF wood system, with $\omega_o=9.425$ rad/s, $\xi_o=0.05$, $\alpha=0.25$, whose behavior is governed by joints with yielding plates, the hysteresis parameters are: $\beta=0.5$, $\gamma = 0.5$, $q=0$, $h(z)=1.0$, $\delta_v=0$ and $\delta_\eta = 0$ (Fig. 4.5a). Model parameters for a system, with $\omega_o=6.283$ rad/s, $\xi_o=0.05$, $\alpha=0.10$ and joints with yielding nails, are: $\beta=1.5$, $\gamma = -0.5$, $q=0.10$, $\zeta_{1o}=0.97$, $\lambda=0.10$, $p=1$, $\psi_o=0.20$, $\delta_\psi=0.002$, $\delta_v=0.005$ and $\delta_\eta = 0.05$ (Fig. 4.5b). For a wood structural system, with bolted joints and $\omega_o=3.0$ rad/s, $\xi_o=0.05$, $\alpha=0.35$,

(a) model for joint with yielding plate



Restoring Force, z



(b) model for joint with yielding nail

(c) model for joint with yielding bolt

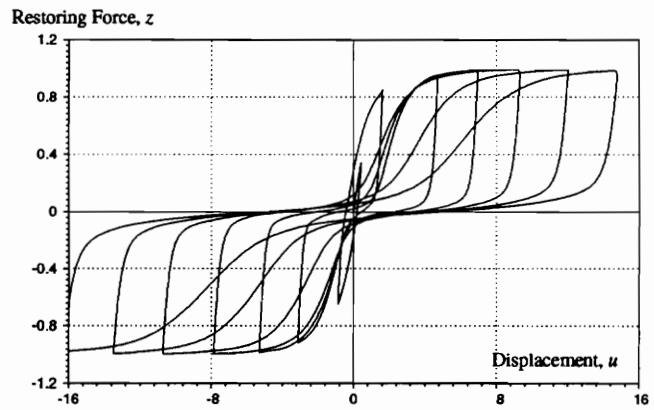


Figure 4.5: Hysteresis loops produced by the modified BWN model

the model parameters are: $\beta=2.0$, $\gamma = -1.0$, $q=0$, $\zeta_{1o}=0.98$, $\lambda=0.10$, $p=2.0$, $\psi_o=0.20$, $\delta_\psi=0.004$, $\delta_v=0.0$ and $\delta_\eta = 0.025$ (Fig. 4.5c). Note that to get the exact hysteresis shapes and response values as shown in Fig. 2.5, complete information about connection materials, test set-up and the forcing function that was used for testing are needed. Since most of these are not known, the focus should only be on modeling the basic hysteresis shape of the joints in Fig. 2.5; thus, no specific force and displacement units are considered.

Comparison of model hysteresis (Fig. 4.5) with experimental hysteresis (Fig. 2.5) shows that the proposed model reasonably mimics the basic hysteresis shape of test data. The slight discrepancy in the hysteresis shapes of the yielding bolt joints (Fig. 2.5c vs. Fig. 4.5c) may be largely attributed to different forcing functions used in the test and the analysis. Even then, the basic behavior of the actual bolt joint can be observed in the model hysteresis.

The model is very flexible and can actually produce a wide variety of hysteresis shapes if the parameters are varied.

4.5 Potential

Although some practical guidance has been presented to obtain hysteresis parameters for any wood system, it is ideal that system identification techniques be used to estimate the parameters of the proposed model. This will allow us to: (1) systematically obtain a system model from laboratory or field data for predicting the structural response of similar real-world systems under adverse environmental loadings such as earthquakes or winds, and (2) estimate the existing conditions of structures for the assessment of damage and deterioration. The latter may be used to obtain an “improved” or “updated” mathematical model that better represents the characteristics of the existing structure. The updated model may then be used to assess safety and reliability of the existing structure. Maruyama et al. (1989) have performed system identification of the non-pinching BWBN model using the Extended Kalman Filter algorithm. If the same

technique can be successfully applied to the proposed model, hysteresis parameters of any system configuration and material combination can be systematically estimated as long as hysteresis data are available.

The non-pinching BWBN model has been shown to adequately model the dynamic behavior of concrete and steel structures (Sues et al. 1988) and has been used in random vibration analysis and stochastic seismic performance evaluation of buildings under natural hazard loadings. If the proposed model for wood systems, which is a modified BWBN model, proves to be similarly suited for random vibration analysis, it would help narrow the gap between advances in general structural dynamics and those in wood engineering. It has the potential to open up future research opportunities, in the league of those in other structural materials, in the area of analysis and design of timber structures against natural hazards.

For example, Ang (1988) and his associates used the Bouc-Wen model (or the non-degrading, non-pinching BWBN model) to develop a reliability-based damage-limiting seismic design procedure for reinforced concrete buildings. Structural damage was quantified using a damage index expressed as a combination of maximum displacement and hysteretic energy dissipation. Both quantities can also be obtained from random vibration analysis of hysteretic wood systems using the proposed model. Following Ang's work, random vibration analysis of wood structural systems using the proposed hysteresis model could provide a method for (1) cumulative damage model development for, and (2) safety and damage assessment of, wood structures subjected to dynamic loading. A host of other random vibration problems in wood structures and structural systems, such as those related to the transport of goods on wooden pallets and containers, can also be addressed.

4.6 Summary

The complete form of the modified Bouc-Wen-Baber-Noori (BWBN) model proposed

for SDF wood systems was summarized. A model for MDF shear buildings was formulated; alternative models for planar frames were reviewed. Previous work have shown that incorporation of the BWBN hysteresis model into analytical structural models need not be limited to shear type buildings. It may be used with other spatial discretization methods.

The topic of system identification and parameter estimation was introduced. A general set of rules for identifying hysteresis model parameters for wood systems was given. Comparison of model hysteresis with experimental hysteresis showed that the proposed model reasonably mimics the basic hysteresis shape of test data. Potential research topics for future work were cited.

Chapter 5

Nonlinear Dynamic Analysis

5.1 General

General purpose dynamic analysis programs have long been used in the analysis and design of reinforced concrete and steel structures. These programs have, however, seen very limited use in the analysis of wood structures because the available material models and finite elements are inadequate to model wood system response. It was not until the start of the 1980's that hysteresis models specifically derived for wood systems surfaced in the literature (see the review in section 2.4.2). (Note that all the models for wood have only been proposed in the past 13 years or so.) The models for wood have been incorporated into either existing commercial programs (e.g., DRAIN-2D) or new programs written to solve a specific problem. The availability of various types of hysteresis models for wood structures allowed researchers and engineers to perform dynamic analyses of wood structures and structural systems. The problems considered and the types of analysis so far employed can be found in Gupta and Moss (1991). It is clear, however, that a gap between advances in general structural dynamics and the dynamic analysis of wood structures remains.

A major requirement for any hysteresis model is that it should provide as realistic a description of the actual structure's behavior as possible. Accuracy of the computed response depends on the accuracy of the mathematical model used to describe the actual system. But to be of any use, the model should also be readily incorporated into some kind of dynamic analysis procedure. The last two chapters showed that the proposed hysteresis model for wood systems, the modified Bouc-Wen-Baber-Noori (BWBN)

model, reasonably mimics the basic hysteresis shape of test data. It incorporates all the experimentally observed characteristics of timber structures, namely (1) nonlinear, inelastic behavior, (2) stiffness degradation, (3) strength degradation, (4) pinching, and (5) memory. To demonstrate its analytical capability, the model will now be incorporated into a nonlinear dynamic analysis computer program. It is sufficient to limit the present analysis to a single-degree-of-freedom (SDF) wood system.

5.2 Preliminary Considerations

5.2.1 Governing Equations

The complete set of equations that governs the dynamic behavior of a SDF wood system were given in section 4.2.1. The equation of motion and constitutive law are given as

$$\ddot{u} + 2\xi_o\omega_o\dot{u} + \alpha\omega_o^2u + (1 - \alpha)\omega_o^2z = f(t) \quad (5.1)$$

$$\dot{z} = h(z) \left\{ \frac{\dot{u} - \nu(\beta|\dot{u}||z|^{n-1}z + \gamma\dot{u}|z|^n)}{\eta} \right\} \quad (5.2)$$

where the hysteretic pinching, $h(z)$, and degradation parameters, ν and η , are functions of the energy dissipated by the system, previously given in Eq. (4.7). The rate of change of the hysteretic energy dissipation may be written as

$$\dot{\epsilon} = (1 - \alpha)\omega_o^2z\dot{u} . \quad (5.3)$$

All parameters are as previously defined.

5.2.2 Overview of Numerical Solution Methods

The governing equations may be solved using any of the available algorithms for nonlinear structural dynamics. Time derivatives are usually approximated by difference equations involving one or more increments of time. (A *differential equation* involves functions and their derivatives defined on some continuous interval, while a *difference equation* involves functions and their differences defined at discrete points.)

Discrete systems of difference equations are solved using step by step methods, which may be classified as either *single step* or *multistep*. A single step method requires information about the solution (i.e., displacement, velocity or acceleration) from a single preceding step to obtain the solution at the current point in time. A multistep method requires information from several preceding steps.

If a given step formula expresses the response at time t only in terms of the previously obtained solution at times before t , it is called an *explicit* method. If the response at time t depends also on the solution at time t , then the method is *implicit*.

When at least two equations, in a set of difference equations, have very different scales of the independent variable on which the dependent variables are changing, the set of equations is said to be *stiff*. This is often encountered in many physically important situations or systems. When this occurs, one is “required to follow the variation in the solution of the shortest length scale to maintain stability of the integration, even though accuracy requirements allow a much larger stepsize” (Press et al. 1992). Special algorithms addressing this issue should be used to solve a stiff set of equations.

Adeli et al. (1978) evaluated several commonly used explicit and implicit numerical integration techniques in nonlinear structural dynamics and compared their accuracy, stability and efficiency as applied to a plane stress problem. They concluded that, among the explicit methods they considered, the central difference predictor is better than the two-cycle iteration with the trapezoidal rule and the fourth-order Runge-Kutta method. Among the implicit methods, the Park stiffly-stable method was rated better than the Newmark-Beta method and Houbolt's procedure. Comparing the Park stiffly-stable method to the central difference method, they found that the Park method is better for elastoplastic analysis, especially when there are geometric nonlinearities. Park's method is based on a class of time integrators originally proposed by Gear (1971).

Several new solution algorithms have been proposed for structural dynamic problems since Adeli et al.'s study. An excellent review of the new methods can be found in Allahabadi (1987). He chose the constant average acceleration (CAA) method, a special

case of the Newmark-Beta method, with some enhancements as the solution algorithm for DRAIN-2DX. Detailed properties of the Newmark method, including five other traditional methods for nonlinear dynamic analysis, are given in Barbat and Canet (1989).

5.2.3 Solution Approach

Let us consider a vector \mathbf{y} defined as

$$\mathbf{y} = \begin{Bmatrix} y_1 \\ y_2 \\ y_3 \\ y_4 \end{Bmatrix} = \begin{Bmatrix} u \\ \dot{u} \\ z \\ \varepsilon \end{Bmatrix} \quad (5.4)$$

Then, Eqs. (5.1), (5.2) and (5.3) may be rearranged into a set of 4 first-order nonlinear ordinary differential equations,

$$\dot{y}_1 = y_2 \quad (5.5)$$

$$\dot{y}_2 = -\alpha\omega_o^2 y_1 - 2\xi_o\omega_o y_2 - (1 - \alpha)\omega_o^2 y_3 + f(t) \quad (5.6)$$

$$\dot{y}_3 = h(z) \left\{ \frac{y_2 - \nu(\beta|y_2||y_3|^{n-1}y_3 - \gamma y_2|y_3|^n)}{\eta} \right\} \quad (5.7)$$

$$\dot{y}_4 = (1 - \alpha)\omega_o^2 y_2 y_3 \quad (5.8)$$

This arrangement results in a stiff set of equations. Thus, a stiffly-stable method, known as Gear's Backward Differentiation Formula (BDF) (Gear 1971; IMSL 1987), was used to solve for \mathbf{y} . Gear's BDF method is an implicit multistep method. A simple computer program, incorporating the IMSL subroutine for Gear's BDF method, was written to compute the response time histories of SDF wood systems subjected to arbitrary dynamic loading.

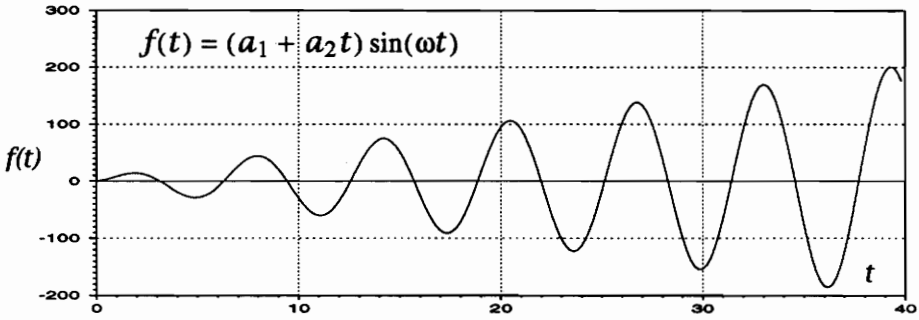
5.3 Response to General Cyclic Loading

The computer program accepts the following types of loading: (1) a single sinusoidal function of the form $f(t) = (a_1 + a_2 t) \sin(\omega t)$, where the a_i 's are specified

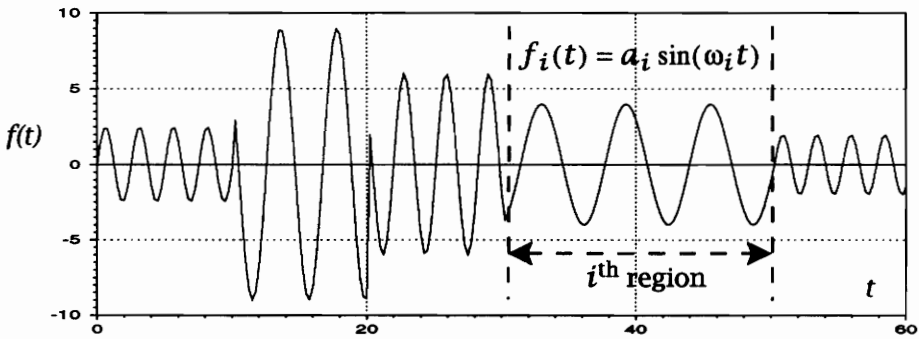
constants, (Fig. 5.1a); (2) a series of sinusoidal functions as shown in Fig. 5.1b where $f_i(t) = a_i \sin(\omega_i t)$ for each region, $t_{i-1} < t < t_i$, $i = 1, 2, \dots, 5$ and where amplitude a_i and frequency ω_i for each region are specified independently; and (3) an arbitrary acceleration input such as the ground acceleration record shown in Fig. 5.1c.

Loading types (1) and (2) are used to verify the program and check the basic capability of the proposed hysteresis model. They are also used to compare model hysteresis with experimental hysteresis (e.g., section 4.4). Most available hysteresis data of wood joints and systems have been obtained from static cyclic load tests, where the test specimen is subjected to a predetermined number of displacement controlled loading cycles. The displacement pattern is normally increasing as shown in Fig. 5.2a. Since the experimental hysteresis loops in Fig. 2.5 were obtained in this manner, the hysteretic response of common wood joints in Fig. 4.5 (section 4.4) using the proposed model were obtained, using the dynamic analysis program, with input defined by loading type (1) shown in Fig. 5.1a.

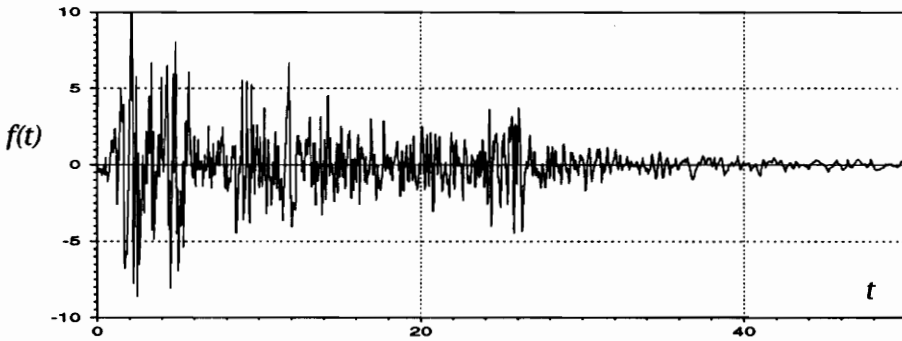
The use of tests with increasing amplitude pattern alone to model hysteresis behavior of wood systems has been criticized (Moss 1991; Reyer and Oji 1991), however, and a test procedure with increasing-decreasing-increasing loading pattern, producing hysteresis inner loops from the smaller amplitude loading, is currently being proposed in ASTM (Fig. 5.2b). Current hysteresis models proposed for wood, with the exception of that proposed by the UBC researchers shown in Fig. 2.12, did not consider the hysteresis inner loops produced from the smaller amplitude loading cycles. Fig. 5.3 shows that the modified BWN model produces small hysteresis loops similar to the behavior of dowel-type fasteners, modeled by the UBC model, when subjected to a loading pattern similar to loading type (2). The hysteresis plots were obtained with load histories having different combinations of amplitude and frequency for each region as shown in the side plots in Fig. 5.3. The SDF system used in all hysteresis plots has the following properties: $\omega_o=3.0$ rad/s, $\xi_o=0.05$, $\alpha=0.10$, $\beta=1.5$, $\gamma = -0.5$, $q=0.10$, $\zeta_{1o}=0.97$, $\lambda=0.10$, $p=1$, $\psi_o=0.20$, $\delta_\psi=0.002$, $\delta_v=0.005$ and $\delta_\eta = 0.05$.



(a) Load type 1 : increasing amplitude sinusoidal load

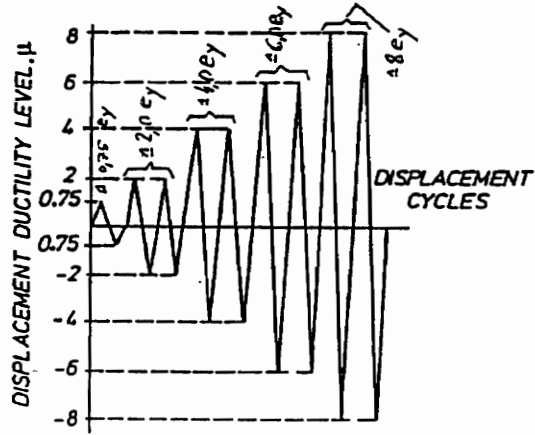


(b) Load type 2 : general cyclic load

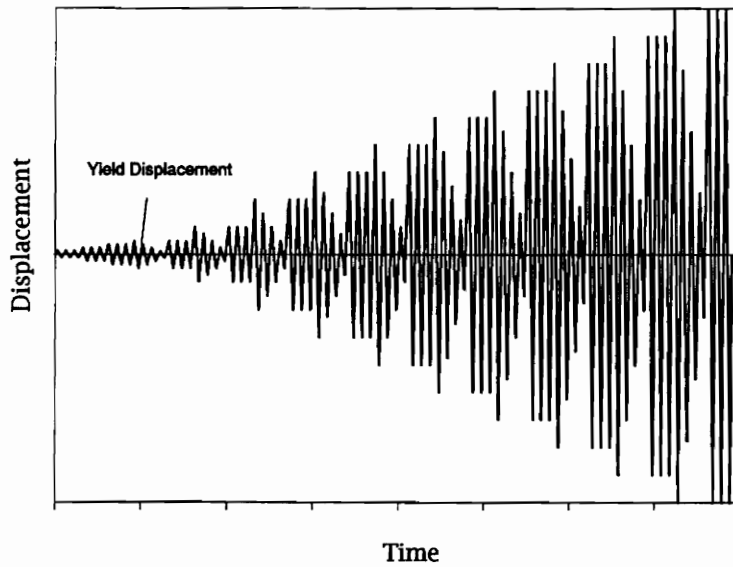


(c) Load type 3 : arbitrary dynamic load

Figure 5.1: Loading types handled by the computer program



(a) displacement-controlled loading cycles (increasing amplitude pattern)



(b) amplitude pattern proposed in ASTM

Figure 5.2: Cyclic loading patterns for tests of wood joints and structural systems

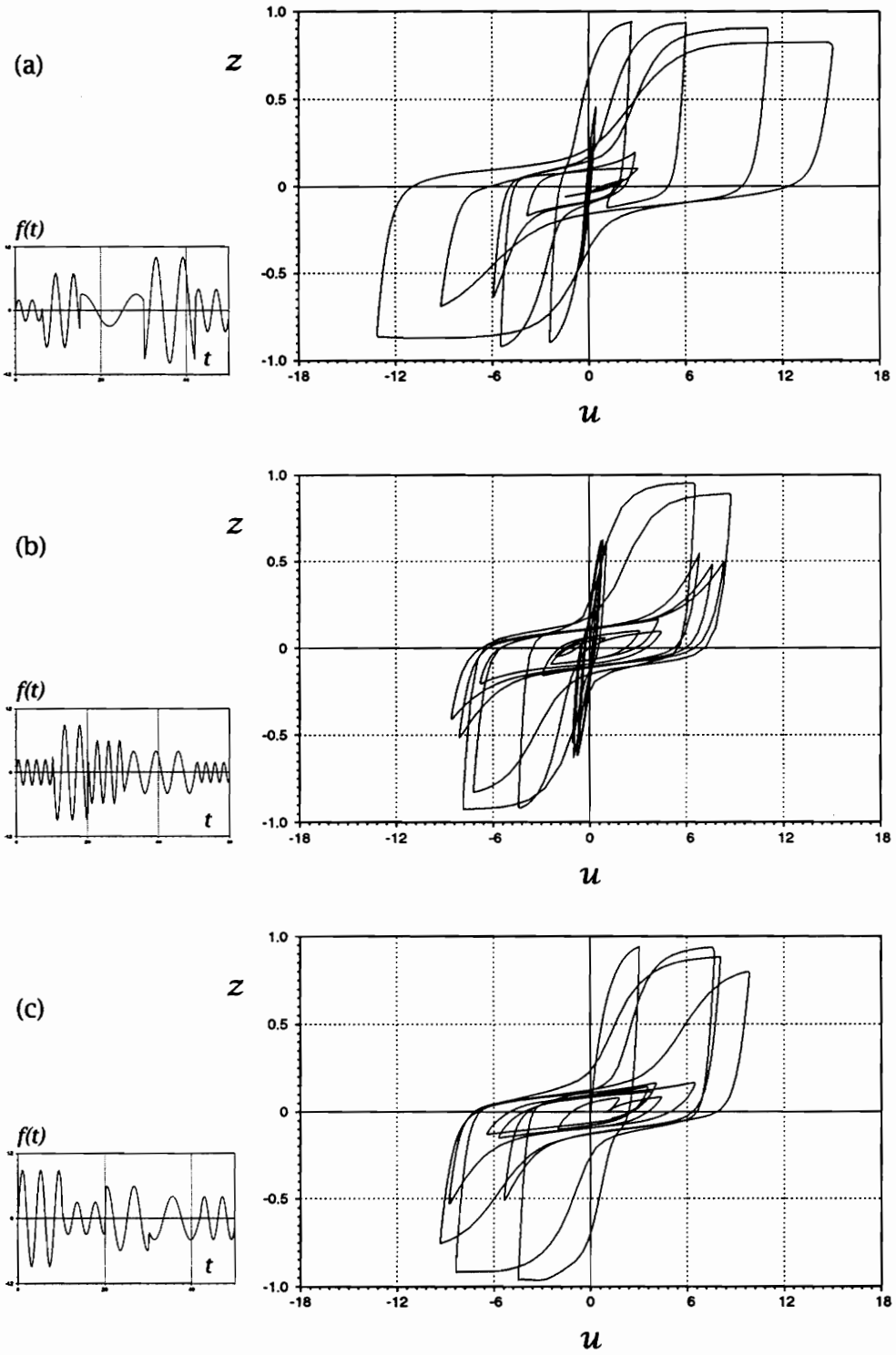


Figure 5.3: Modified BWN response to general cyclic load

Including loading type (2) as an option for load input in the program, therefore, allowed investigation of model response to general cyclic loading. This will assume greater importance if the ASTM test procedure proposal is passed and adopted. If desired, a specialized loading pattern based on the proposed standard may be added as another load input option to the program.

After the model was verified and validated (this was discussed in section 4.4), loading type (3) was added as a load input option. Response of SDF wood systems under arbitrary dynamic loading is discussed next.

5.4 Time History Analysis

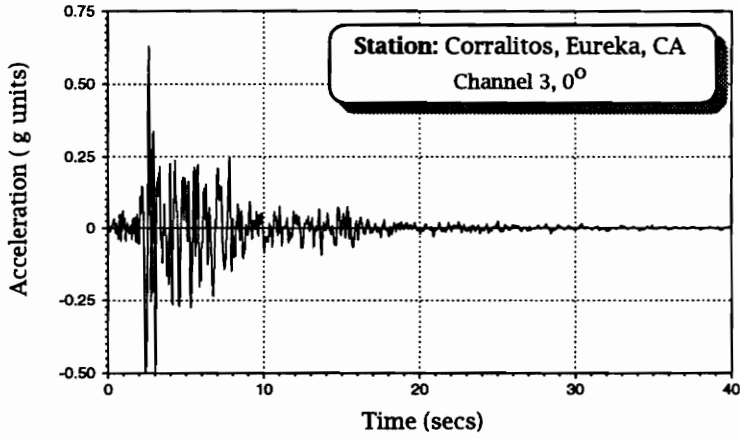
5.4.1 Ground Accelerogram

Since we are primarily interested in the seismic response of wood structures and structural systems, earthquake accelerogram data will be used for $f(t)$ in time history analysis. For illustration purpose, only the Loma Prieta accelerogram record will be used (Fig. 5.4a). It is the ground acceleration record of the earthquake that occurred in the San Francisco Bay Area in California in October 17, 1989. The epicenter of the 7.1 Richter scale earthquake was located at the Loma Prieta peak in the Santa Cruz Mountains, about 60 miles (97 km) southeast of San Francisco. The accelerogram was recorded in Eureka, California and has a peak horizontal acceleration of $0.63g$, where g is the acceleration of gravity. It was estimated that a ground acceleration of about $0.3g$ occurred in the bay mud area (Turner et al. 1990).

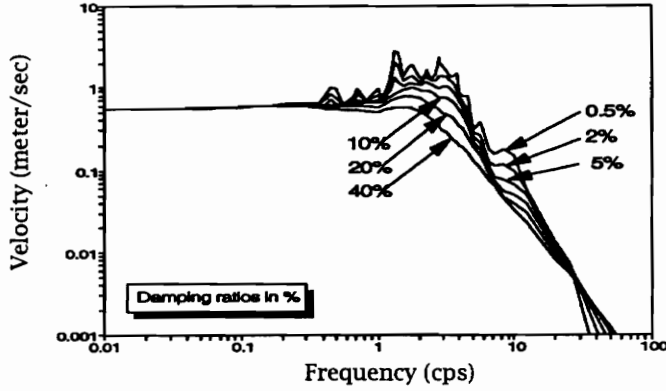
The relative velocity and pseudo acceleration spectra of the Loma Prieta earthquake are shown in Figs. 5.4b and c, respectively.

5.4.2 Seismic Response

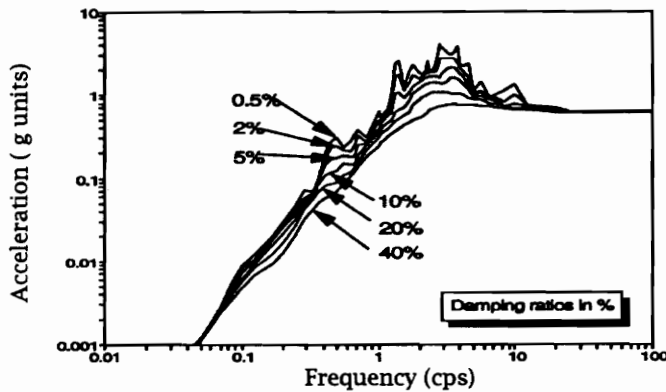
Consider three hypothetical simple wooden buildings in Eureka, CA at the time of the Loma Prieta earthquake. How would they have behaved if the ground where they



(a) acceleration record



(b) relative velocity spectra



(c) pseudo acceleration spectra

Figure 5.4: The Loma Prieta earthquake ground acceleration

stand moved horizontally with acceleration shown in Fig. 5.4a?

Modeling the buildings as SDF systems, to simplify the analysis, and using the proposed hysteresis model for wood structures to represent the three buildings, their global response time history (i.e., solution of y for the entire time duration under consideration) can be computed as described earlier. As an illustration of response computations, no specific units of force, displacement, velocity and energy are considered. Additionally, the hysteresis parameter values used in response computations should *not* be viewed as realistic representation of any physical system.

5.4.2.1 Trussed-frame Building

The first building is a trussed-frame structure whose behavior was primarily governed by metal plate connections that have hysteresis behavior given by that in Fig. 4.5a. The SDF system model was assumed to have the following properties (these were taken to be the same as those in section 4.4 and Fig. 4.5a): $\omega_o=9.425$ rad/s, $\xi_o=0.05$, $\alpha=0.25$; the hysteresis parameters are: $\beta=0.5$, $\gamma = 0.5$, $q=0$, $h(z)=1.0$, $\delta_v=0$ and $\delta_\eta = 0$.

The hysteresis response of this trussed-frame building to the Loma Prieta accelerogram is given in Fig. 5.5. Response time histories are shown in Fig. 5.6.

5.4.2.2 Building with Plywood Shear Walls

The other building had plywood shear walls to resist lateral loads. The shear walls governed the building behavior and have hysteresis loops given by that in Fig. 4.5b for nailed sheathing joints. The model parameters for the system are assumed as: $\omega_o=6.283$ rad/s, $\xi_o=0.05$, $\alpha=0.10$, $\beta=1.5$, $\gamma = -0.5$, $q=0.10$, $\zeta_{1o}=0.97$, $\lambda=0.10$, $p=1$, $\psi_o=0.20$, $\delta_\psi=0.002$, $\delta_v=0.005$ and $\delta_\eta = 0.05$.

The building governed by plywood shear walls would respond to the Loma Prieta accelerogram as shown in Figs. 5.7 and 5.8.

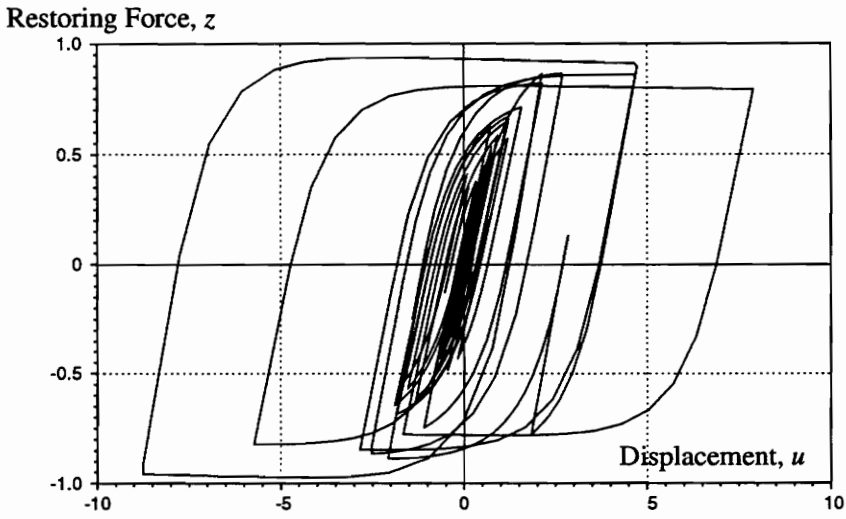
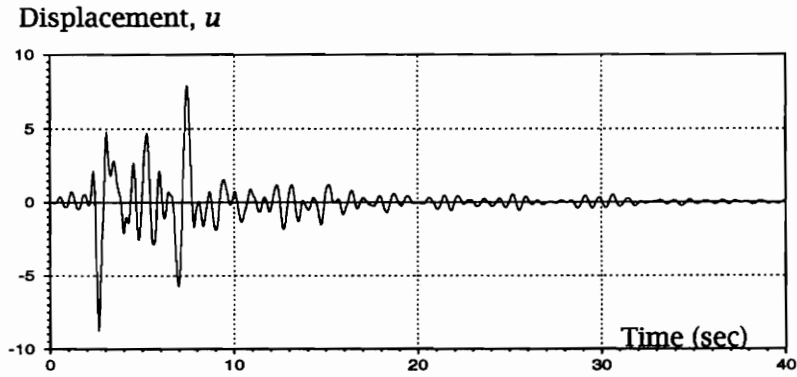
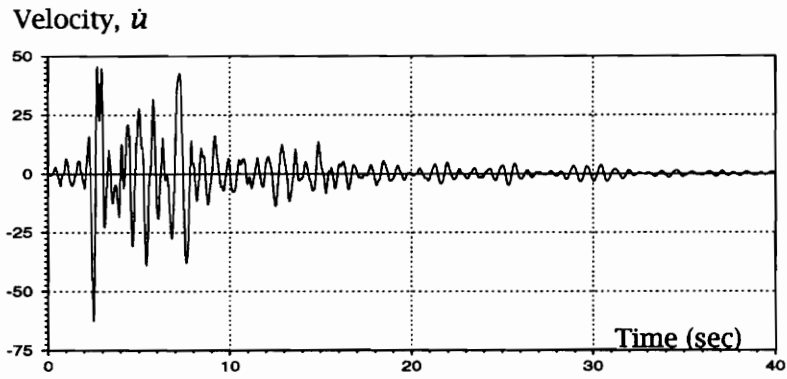


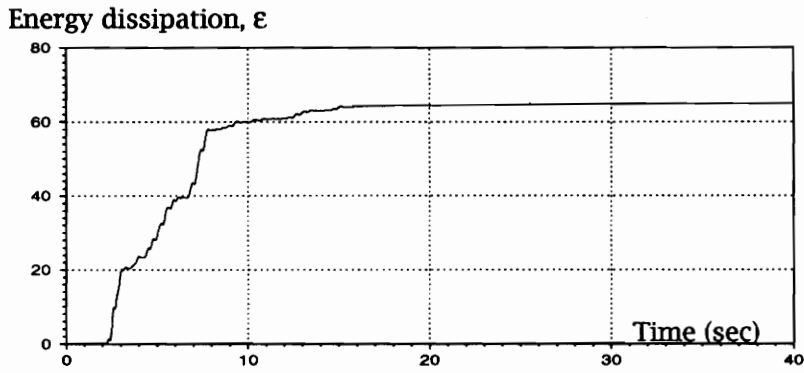
Figure 5.5: Hysteresis response of a trussed-frame building to the Loma Prieta accelerogram



(a) displacement time history



(b) velocity time history



(c) hysteretic energy dissipation time history

Figure 5.6: Response time histories of a trussed-frame building to the Loma Prieta accelerogram

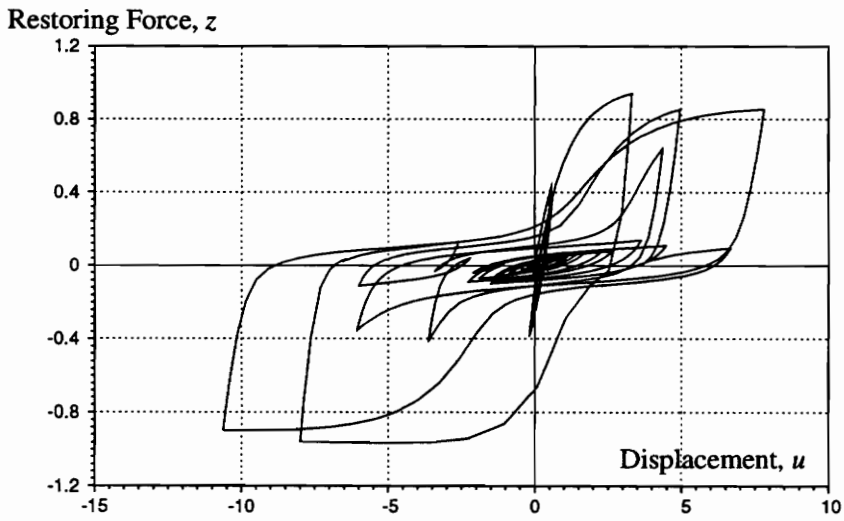
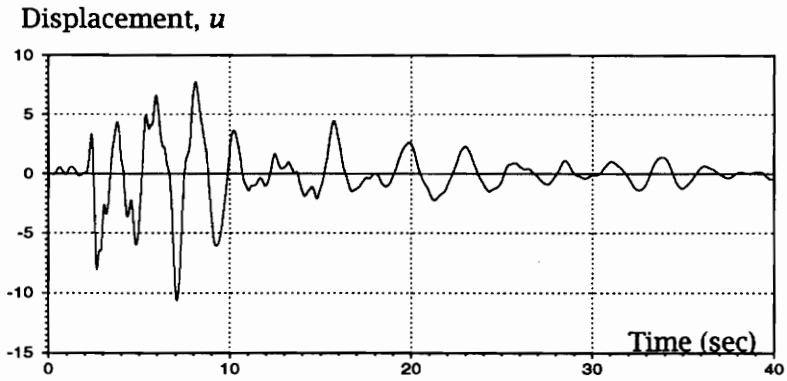
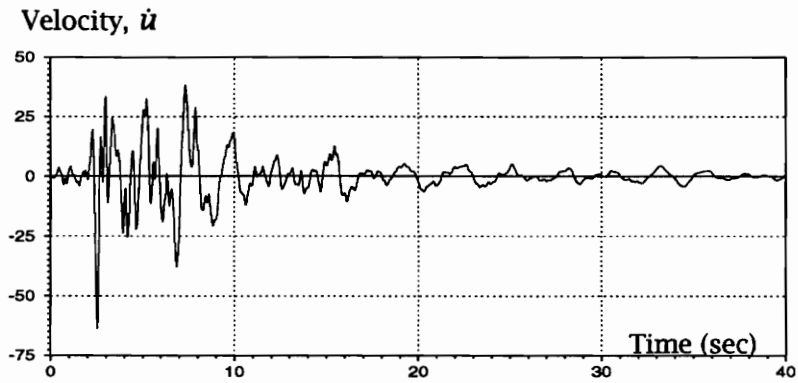


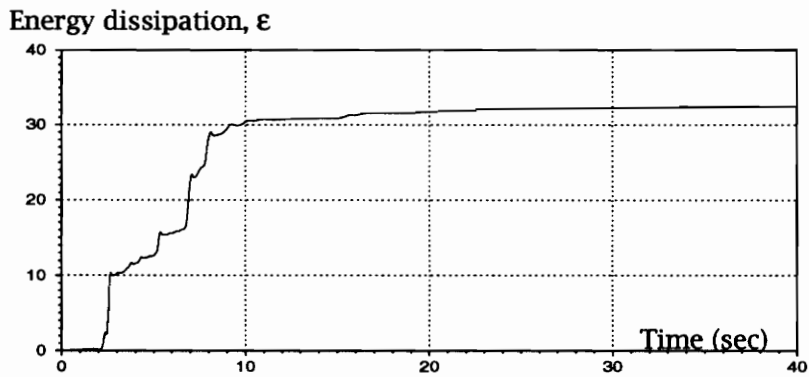
Figure 5.7: Hysteresis response of a building with plywood shear walls to the Loma Prieta accelerogram



(a) displacement time history



(b) velocity time history



(c) hysteretic energy dissipation time history

Figure 5.8: Response time histories of a building with plywood shear walls to the Loma Prieta accelerogram

5.4.2.3 Heavy Timber Building

The third building is of heavy timber construction. The members are primary held together by bolted joints that behave like the one in Fig. 4.5c. The SDF system properties are assumed as: $\omega_o=3.0$ rad/s, $\xi_o=0.05$, $\alpha=0.35$, $\beta=2.0$, $\gamma = -1.0$, $q=0$, $\zeta_{1o}=0.98$, $\lambda=0.10$, $p=2.0$, $\psi_o=0.20$, $\delta_\psi=0.004$, $\delta_v=0.0$ and $\delta_\eta = 0.025$.

This building would have a hysteretic behavior due to the Loma Prieta accelerogram as shown in Fig. 5.9. The response time histories are shown in Fig. 5.10.

5.5 Comments

Recall that the purpose of performing time history analyses of the hypothetical wooden buildings is to demonstrate the analytical capability of the proposed modified BWBN model. If the SDF system properties were obtained from actual tests using an appropriate system identification method, we can comment on seismic performance and safety of these buildings based on the computed response. Key dynamic properties, including ductility, can be obtained from hysteresis plots similar to those shown in Figs. 5.5, 5.7 and 5.9. Various types of sensitivity and parametric studies, like those mentioned by Stalnaker and Gramatikov (1991), can be performed using the model, without the need for additional physical testing. Model parameters that critically affect the ductility, serviceability and safety of the wood structure under study can be identified.

The computer program is presently limited to dynamic analysis of SDF systems. For a more refined analysis, multi-degree-of-freedom (MDF) models can be constructed to represent various types of wood structures and structural systems, where each degree-of-freedom is modeled by the hysteretic behavior of its governing connection. (See section 4.2.2 for the formulation for shear building models.) The proposed hysteresis model can be included as an alternative subroutine to existing nonlinear dynamic analysis programs. It can also be incorporated into finite element models in dynamic

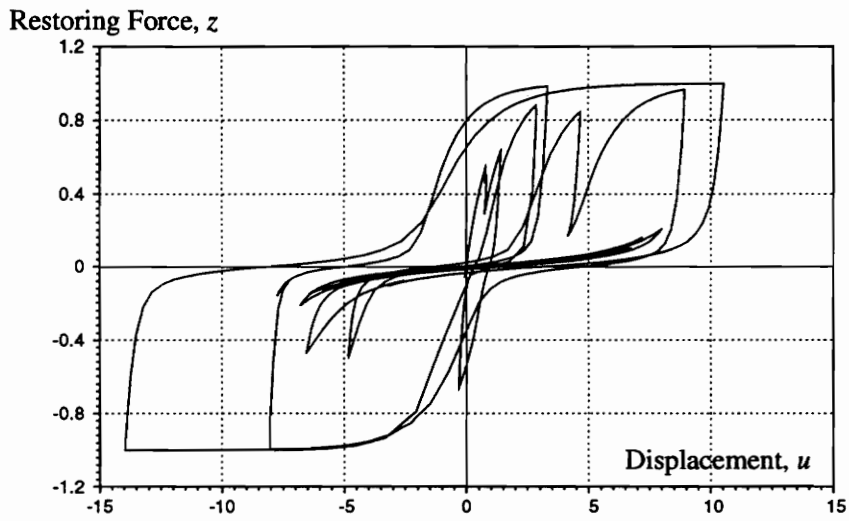
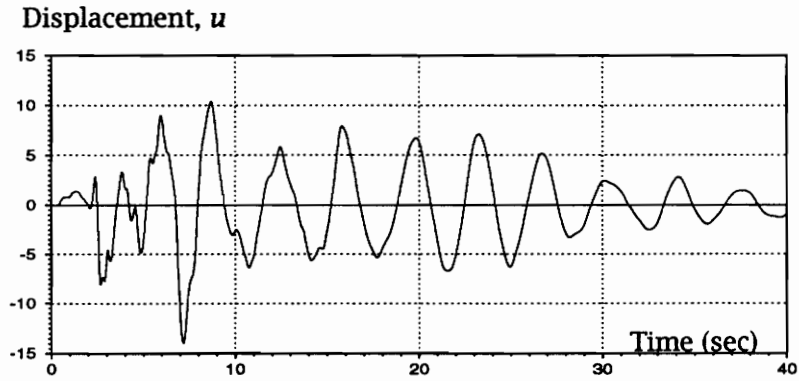
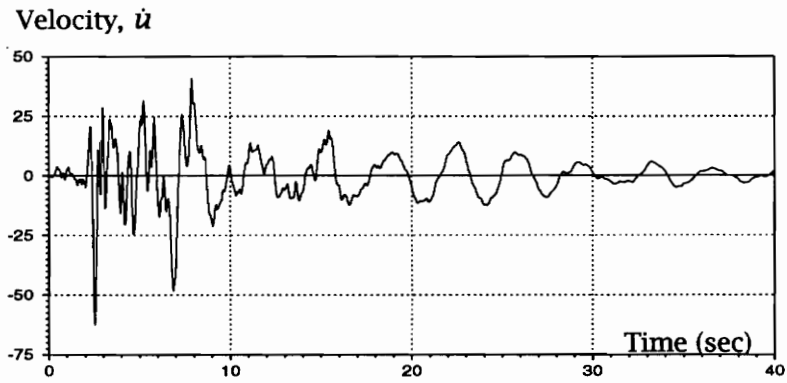


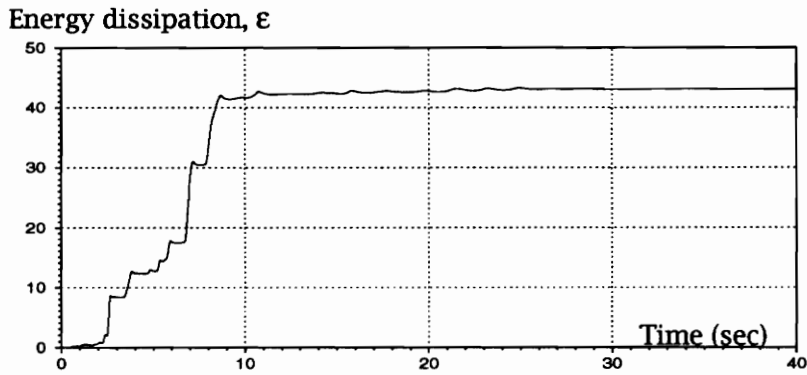
Figure 5.9: Hysteresis response of a heavy timber building to the Loma Prieta accelerogram



(a) displacement time history



(b) velocity time history



(c) hysteretic energy dissipation time history

Figure 5.10: Response time histories of a heavy timber building to the Loma Prieta accelerogram

analysis.

With currently available hysteresis models for wood joints and structural systems, one subroutine for each connection type, that defines its hysteretic behavior, has to be implemented. Incorporating a new model for a specific connection set-up into a commercial dynamic analysis program, such as DRAIN-2D or its latest version DRAIN-2DX, is a major undertaking (Dowrick 1986). Thus, analytical study of a wood structural system that requires several models of hysteresis behavior is very laborious. Because of the general nature of the proposed model, however, only one subroutine for hysteretic constitutive relations needs to be written for the whole gamut of wood products, fastener types and configurations that are currently used in construction. Only the model parameters have to be changed for the desired hysteresis shape. Thus, with the proposed general hysteresis model, analytical study of MDF wood structural systems that need to be modeled by several different hysteresis shapes is simplified.

5.6 Summary

The modified BWBN model was implemented in a nonlinear dynamic analysis program for single-degree-of-freedom (SDF) systems. Incorporation of the model into the program was relatively straightforward. System response from arbitrary dynamic loading, such as cyclic or earthquake-type loadings, can be computed. Three SDF wood systems were subjected to the Loma Prieta accelerogram to obtain their hysteresis loops and response time histories. Advantages of using the proposed model over currently available models in nonlinear dynamic analysis of more complex wood structural systems were identified.

The program allows response computations of a wide variety of wood structures and structural systems that can be modeled as SDF systems, as long as hysteresis parameters for these systems are known. The program may be extended to handle dynamic analysis of multi-degree-of-freedom (MDF) systems; an MDF shear building model incorporating the proposed hysteresis model has already been formulated in

section 4.2.2.1.

Conclusions and Recommendations

6.1 Summary and Conclusions

A general hysteresis model for wood joints and structural systems was developed and incorporated into a nonlinear dynamic analysis program. It is a modification of the Bouc-Wen-Baber-Noori (BWBN) model. The hysteretic constitutive law, based on the endochronic theory of plasticity and characterized by a single mathematical form, produces a versatile, smoothly varying hysteresis that models previously observed behavior of wood joints and structural systems, namely, (1) nonlinear, inelastic behavior, (2) stiffness degradation, (3) strength degradation, (4) pinching, and (5) memory. The constitutive law takes into account the experimentally observed dependence of wood joints' response to their past history (i.e., the input and response at earlier times, or memory).

Practical guidelines to estimate the hysteresis parameters of any wood joint or structural system were given. Hysteresis shapes produced by the proposed model were shown to compare reasonably well with experimental hysteresis of wood joints with: (1) yielding plate, (2) yielding nails, and (3) yielding bolts.

The model is versatile and can actually model a wide variety of hysteresis shapes, degradations, and pinching behavior to cover a whole gamut of possible combinations of materials and joint configurations in wood systems. Continued evolution of wood-based products, fasteners, and use of wood-based products need not be a problem, as long as hysteresis data from tests of representative wood joints or structural systems are available, from which model parameters can be estimated.

The proposed model was implemented in a nonlinear dynamic analysis program for single-degree-of-freedom (SDF) systems. System response from arbitrary dynamic loading, such as cyclic or earthquake-type loadings, can be computed. Three SDF wood systems were subjected to the Loma Prieta accelerogram to obtain their response time histories. Advantages of using the proposed model over currently available models in nonlinear dynamic analysis of more complex systems were identified. A multi-degree-of-freedom (MDF) shear building model incorporating the proposed hysteresis model was formulated but not implemented on a computer.

6.2 Recommendations for Future Work

Research on dynamic analysis of wood structures has lagged behind advances in general structural dynamics mainly because of (1) many factors affecting the collection of test data and (2) difficulties in characterizing the dynamic behavior of wood joints and structural systems. The latter hindered investigations into their performance under dynamic loading. The present work attempted to address this problem and succeeded in (1) deriving a general hysteresis model for wood structures, and (2) incorporating the model into a simple computer program for nonlinear dynamic analysis of SDF systems. It is clear, however, that this is just the first step. Much work remains to be done. The following topics are recommended for future work:

1. *System Identification* - although some practical guidance has been presented to obtain hysteresis parameters for any wood system, it is ideal that system identification techniques be used to estimate the parameters of the proposed model. This will allow us to: (a) systematically obtain a system model from laboratory or field data for predicting the structural response of similar real-world systems during earthquake or wind events, and (b) estimate the existing conditions of structures for the assessment of damage and deterioration. If successful, hysteresis

parameters of any system configuration and material combination can be systematically estimated as long as hysteresis data are available. Furthermore, various types of sensitivity and parametric studies, like those mentioned by Stalnaker and Gramatikov (1991), can be performed using the model, without the need for additional physical testing. Model parameters that critically affect the ductility, serviceability and safety of the wood structure under study can be identified.

2. *Multidegree-of-freedom Systems* - the model for MDF shear buildings that was formulated in the present work should be implemented numerically. The proposed hysteresis model should also be incorporated in the formulation of discrete hinge and finite element models for wood structural systems. Incorporation of the hysteresis model to commercial dynamic analysis programs should also be explored. The modified BWBN model is, in fact, applicable to structures made of other materials, such as steel and reinforced concrete, and may also be used for dynamic analysis of these structures.
3. *Random Vibration Analysis* - the original BWBN model has been used in random vibration analysis. The modification to generalize its pinching behavior does not guarantee that equivalent linearization of the governing equations would work as it did for the parent form. Random vibration analyses of SDF and MDF wood systems would allow researchers to investigate the performance of wood structures under natural hazards, with the loading modeled as random processes. With a reliable estimate of response statistics, one may then design a structure based on accepted levels of safety, measured in terms of probability of failure.
4. *Seismic Damage Analysis* - structural damage due to a seismic event may be quantified using a damage index expressed as a combination of maximum displacement and hysteretic energy dissipation. Both quantities can be obtained from random vibration analysis of hysteretic wood systems using the proposed model.

Following Ang's (1988) work, random vibration analysis of wood structural systems using the proposed hysteresis model could provide a method for (a) cumulative damage model development for, and (b) safety and damage assessment of, wood structures subjected to dynamic loading.

The foregoing list of potential research topics shows that with the proposed hysteresis model for wood structural systems, a number of future research opportunities in the area of analysis and design of timber structures against natural hazards have opened up. All this will hopefully help wood engineering research catch up with advances in general structural dynamics.

Bibliography

- [1] Adeli, H., J.M. Gere and W. Weaver Jr. 1978. "Algorithms for nonlinear structural dynamics." *Journal of the Structural Division ASCE* 104(ST2):263-280.
- [2] Ang, A. H-S. 1988. "Seismic damage assessment and basis for damage-limiting design." *Probabilistic Engineering Mechanics* 3(3): 559-583.
- [3] Ang, A. H-S. and Y-K. Wen. 1982. "Prediction of structural damage under random earthquake excitations." *Earthquake Ground Motion and Its Effects on Structures ASME, AMD Vol. 53: 91-107.*
- [4] Allahabadi, R. 1987. "Seismic response and damage assessment for 2D Structures." PhD Thesis, Dept. of Civil Eng., Univ. of California, Berkeley, CA.
- [5] Baber, T.T. 1980. "Stochastic equivalent linearization for hysteretic, degrading, multistory structures." PhD Thesis, Dept. of Civil Eng., Univ. of Illinois at Urbana-Champaign, Urbana, IL.
- [6] Baber, T.T. 1986a. "Modal analysis for random vibration of hysteretic frames." *Earthquake Engineering and Structural Dynamics* 14:841-859.
- [7] Baber, T.T. 1986b. "Nonzero mean random vibration of hysteretic frames." *Computers and Structures* 23:265-277.
- [8] Baber, T.T. and M.N. Noori. 1986. "Modeling general hysteresis behavior and random vibration application." *Journal of Vibration, Acoustics, Stress and Reliability in Design ASME* 108: 411-420.
- [9] Baber, T.T. and Y-K. Wen. 1981. "Random vibration of hysteretic degrading systems." *Journal of the Engineering Mechanics Division ASCE* 107(EM6):1069-1089.

- [10] Barbat, A.H. and J.M. Canet. 1989. *Structural Response Computations in Earthquake Engineering*. Pineridge Press, Swansea, U.K.
- [11] Bhatti, M.A. and K.S. Pister. 1981. "Transient response analysis of structural systems with nonlinear behavior." *Computers and Structures* 13:181-188.
- [12] Bouc, R. 1967. "Forced vibration of mechanical systems with hysteresis", Abstract. Proc. Fourth Conference on Nonlinear Oscillations, Prague, Czechoslovakia.
- [13] Buchanan, A.H. and J.A. Dean. 1988. "Practical design of timber structures to resist earthquakes." Proc. 1988 International Conference on Timber Engineering, Seattle, WA 1: 813-822.
- [14] Casciati, F. 1987. "Nonlinear stochastic dynamics of large structural systems by equivalent linearization." In *Reliability and Risk Analysis in Civil Engineering 2*, N.C. Lind, ed., University of Waterloo, Canada. pp.1165-1172 .
- [15] Ceccotti, A. and A. Vignoli. 1990. "Engineered timber structures: An evaluation of their seismic behavior". Proc. 1990 International Timber Engineering Conference, Tokyo, Japan , 946-953.
- [16] Cheung, K.C., R.Y. Itani and A. Polensek. 1988. "Characteristics of wood diaphragms: Experimental and parametric studies." *Wood and Fiber Science* 20(4):438-456
- [17] Chou, C. 1987. "Modeling of nonlinear stiffness and nonviscous damping in nailed joints between wood and plywood." PhD Thesis, Dept. of Forest Products, Oregon State Univ., Corvallis, OR.
- [18] Chui, Y. H. and I. Smith. 1989. Quantifying damping in structural timber components. Proc. Second Pacific Timber Engineering Conference, Auckland, New Zealand .

- [19] Clough, R.W. and J. Penzien 1993. *Dynamics of Structures*, Second Edition. McGraw-Hill Book Co., New York, NY.
- [20] Conner, H.W., D.S. Gromala, and D.W. Burgess. 1987. "Roof connections in houses: key to wind resistance". *Journal of Structural Engineering ASCE* 113(12):2459-2474.
- [21] Crandall, S.J. 1970. "The role of damping in vibration theory". *Journal of Sound and Vibration* 11(1):3-18.
- [22] Dean, J. A., B. L. Deam, and A. H. Buchanan. 1989. "Earthquake resistance of timber structures". *NZ Journal of Timber Construction* 5(2):12-16.
- [23] Diekmann, E.D. 1989. Diaphragms and Shear Walls. in *Wood Engineering and Construction Handbook*, K. Faherty and T. Williamson, eds., McGraw-Hill Pub. Co., New York, NY.
- [24] Dolan, J.D. 1989. "The dynamic response of timber shear walls". PhD thesis, Dept. of Civil Engineering. Univ. of British Columbia, Vancouver, BC, Canada.
- [25] Dowrick, D.J. 1986. "Hysteresis loops for timber structures". *Bulletin of New Zealand National Society of Earthquake Engineering* 19(20):143-152.
- [26] Ewing, R.D., T.J. Healey and M.S. Agbabian. 1980. "Seismic analysis of wood diaphragms in masonry buildings." Proc. Workshop on Design of Horizontal Wood Diaphragms, Applied Technology Council, Berkeley, CA, 253-276.
- [27] Falk, R.H. and L.A. Soltis. 1988. "Seismic behavior of low-rise wood framed buildings". *The Shock and Vibration Digest* 20(12):3-7.
- [28] Filiatrault, A. and R.O. Foschi. 1991. "Static and dynamic tests of timber shear walls fastened with nails and wood adhesive". *Canadian Journal of Civil Engineering* 18:749-755.

- [29] Gavrilović, P. and K. Gramatikov. 1991. "Experimental and theoretical investigations of wooden truss-frame structures under quasi-static and dynamic loads." Proc. Workshop on Full-scale Behavior of Wood-Framed Buildings in Earthquakes and High Winds, Watford, United Kingdom, XXVI-1-37.
- [30] Gear, C.W. 1971. *Numerical Initial Value Problems in Ordinary Differential Equations*. Prentice-Hall, Englewood Cliffs, NJ.
- [31] Gupta, A.K. and P.J. Moss, eds. 1991. Proc. Workshop on Full-scale Behavior of Wood-Framed Buildings in Earthquakes and High Winds, Watford, United Kingdom.
- [32] Hirashima, Y. 1988. "Analysis of observed earthquake response of post-and-beam wood structure." Proc. 1988 International Conference on Timber Engineering, Seattle, WA 2:235-242.
- [33] Iemura, H. 1977. "Earthquake response of stationary and deteriorating hysteretic structures." Dept. of Civil Engineering, Kyoto University, Kyoto, Japan.
- [34] Iwan, W.D. 1969. "Application of nonlinear analysis techniques." In *Applied Mechanics in Earthquake Engineering*, W.D. Iwan, ed., ASME, New York, NY. pp.135-161.
- [35] Iwan, W.D. 1977. "The response of simple stiffness degrading structures." Proc. Sixth World Conf. on Earthquake Engineering, New Delhi, India, Vol. 2:1094-1099.
- [36] IMSL. 1987. *User's manual: Math/Library*. International Mathematical and Statistical Library, Inc., Houston, TX.
- [37] Jennings, P.C. 1965. "Response of yielding structures to stationary generated ground motion." Proc. Third World Conf. on Earthquake Engineering, Auckland, New Zealand, Vol. 2:783-796.

- [38] Kaldjian, M.J. and W.R.S. Fan. 1968. "Earthquake response of a Ramberg-Osgood structure". *Journal of the Structural Division ASCE* 94(ST10): 2451-2465.
- [39] Kamiya, F. 1988. "Nonlinear earthquake response analysis of sheathed wood walls by a computer-actuator on-line system." Proc. 1988 International Conference on Timber Engineering, Seattle, WA 1:838-847.
- [40] Kivell, B.T., P.J. Moss and A.J. Carr. 1981. "Hysteretic modeling of moment resisting nailed timber joints". *Bulletin of New Zealand Nat. Soc. for Earthquake Eng.* 14(4): 233-245.
- [41] Lazan, B.J. 1968. *Damping of Materials and Members in Structural Mechanics*. Pergamon Press, London, Great Britain.
- [42] Lee, C-S. 1987. "A composite-beam finite element for seismic analysis of wood-framed buildings." PhD Thesis, Dept. of Civil Engineering, Oregon State Univ. Corvallis, OR.
- [43] Ljung, L. and T. Söderström. 1983. *Theory and Practice of Recursive Identification*. The MIT Press, Cambridge, MA.
- [44] Loh, C. and R. Ho. 1990. "Seismic damage assessment based on different hysteretic rules". *Earthquake Engineering and Structural Dynamics* 19: 753-771.
- [45] Maldonado, G.O. 1992. "Stochastic and seismic design response of linear and nonlinear structures." PhD Dissertation, Dept. of Engineering Science and Mechanics, Virginia Polytechnic Inst. and State Univ., Blacksburg, VA.
- [46] Maldonado, G.O., M.P. Singh, F. Casciati and L. Faravelli. 1987. "Stochastic response of single degree of freedom hysteretic oscillators." Technical Report of Research Supported by the National Science Foundation (Grant CEE-8412830), Dept. of Engineering Science and Mechanics, Virginia Polytechnic Inst. and State Univ., Blacksburg, VA.

- [47] Maruyama, O., C-B. Yun, M. Hoshiya and M. Shinozuka. 1989. "Program EXKAL2 for identification of structural dynamic systems." Technical Report NCEER-89-0014, National Center for Earthquake Eng. Research, State Univ. of New York, Buffalo, NY.
- [48] Medearis, K. and D.H. Young. 1964. "Energy absorption of structures under cyclic loading." *Journal of the Structural Division ASCE* 90(ST1): 61-91.
- [49] Meirovitch, L. 1985. *Introduction to Dynamics and Control*. John Wiley & Sons Inc., New York, NY.
- [50] Meirovitch, L. 1986. *Elements of Vibration Analysis*. McGraw-Hill Book Co., New York, NY.
- [51] Miyazawa, K. 1990. "Study on nonlinear static and dynamic structural analysis of wooden wall-frame buildings subjected to horizontal force." Proc. Thirteenth Symposium on Computer Technology of Information, Systems and Applications, A.I.J., Japan.
- [52] Moss, P.J. 1991. "The performance of low-rise timber buildings in New Zealand when subjected to seismic, wind and snow loads." Proc. Workshop on Full-scale Behavior of Wood-Framed Buildings in Earthquakes and High Winds, Watford, United Kingdom, XVII-1-64.
- [53] Noori, M.N. 1984. "Random vibration of degrading systems with general hysteretic behavior." PhD Dissertation, Dept. of Civil Engineering, Univ. of Virginia, Charlottesville, VA.
- [54] Paz, M. 1991. *Structural Dynamics: Theory and Computations*, Third Edition. Van Nostrand Reinhold, New York, NY.
- [55] Polensek, A. 1988. "Effects of testing variables on damping and stiffness of nailed wood-to-sheathing joints." *ASTM Journal of Testing and Evaluation* 16(5): 474-480.

- [56] Polensek, A. and K.J. Bastendorff. 1987. "Damping in nailed joints of light-frame wood buildings." *Wood and Fiber Science* 19(2): 110-125.
- [57] Polensek, A. and H.I. Laursen. 1984. "Seismic behavior of bending components and intercomponent connections of light framed wood buildings." Final Report to the National Science Foundation (Grant CEE-8104626), Dept. of Forest Products, Oregon State Univ., Corvallis, OR.
- [58] Polensek, A. and B.D. Schimel. 1991. "Dynamic properties of light-frame wood subsystems". *Journal of Structural Engineering ASCE* 117(4): 1079-1095.
- [59] Press, W.H., B.P. Flannery, S.A. Teukolsky and W.T. Vetterling. 1992. *Numerical Recipes in FORTRAN: The Art of Scientific Computing*, Second Edition. Cambridge University Press, Cambridge, United Kingdom.
- [60] Reyer, E. and O.A. Oji. 1991. "A testing procedure for phenomenological modeling of timber joints and members under cyclic loading." Proc. Workshop on Full-scale Behavior of Wood-Framed Buildings in Earthquakes and High Winds, Watford, United Kingdom, XIII-1-22.
- [61] Sakamoto, I. and Y. Ohashi. 1988. "Seismic response and required lateral strength of wooden dwellings" Proc. 1988 International Conference on Timber Engineering, Seattle, WA 2:243-247.
- [62] Soltis, L.A. 1984. "Low-rise timber buildings subjected to seismic, wind and snow loads." *Journal of Structural Engineering ASCE* 110(4): 744-753.
- [63] Sozen, M.A. 1974. "Hysteresis in structural elements." In *Applied Mechanics in Earthquake Engineering*, W.D. Iwan, ed., ASME, New York, NY. pp.63-98.
- [64] Srinivasan, P. 1982. *Mechanical Vibration Analysis*. Tata McGraw-Hill Pub. Co. Ltd., New Delhi, India.

- [65] Stalnaker, J. and K.K. Gramatikov. 1991. "Modeling." Proc. Workshop on Full-scale Behavior of Wood-Framed Buildings in Earthquakes and High Winds, Watford, United Kingdom, VI-1-3.
- [66] Stewart, W.G. 1987. "The seismic design of plywood-sheathed shear walls". PhD thesis, Univ. of Canterbury, Christchurch, New Zealand.
- [67] Sues, R.H., S.T. Mau and Y-K. Wen. 1988. "System identification of degrading hysteretic restoring forces." *Journal of Engineering Mechanics ASCE* 114(5):833-846.
- [68] Takizawa, H. 1975. "Non-linear models for simulating the dynamic damaging process of low-rise reinforced concrete buildings during severe earthquakes." *Earthquake Engineering and Structural Dynamics* 4: 73-94.
- [69] Touliatos, P.G. 1989. "Report on Greek experiences." Proc. Workshop on Structural Behavior of Timber Construction in Seismic Zones, Florence, Italy , 267-296.
- [70] Turner, L.S., F. Stewart and K.C.K. Cheung. 1990. "Performance of wood structures: Loma Prieta earthquake aftermath." *Wood Design Focus* 1(4):14-16.
- [71] Uang, C. and V.V. Bertero. 1990. "Evaluation of seismic energy in structures." *Earthquake Engineering and Structural Dynamics* 19: 77-90.
- [72] UBC. 1993. "Timber engineering software." Dept. of Civil Engineering, Univ. of British Columbia, Vancouver, BC, Canada.
- [73] Wen, Y-K. 1976. "Method for random vibration of hysteretic systems." *Journal of the Engineering Mechanics Division ASCE* 102(EM2):249-263.
- [74] Wen, Y-K. 1980. "Equivalent linearization for hysteretic systems under random excitation." *Journal of Applied Mechanics ASME* 47:150-154.
- [75] Weyerhaeuser. 1990. "The lateral resistance of OSB and plywood under cyclic shear loads." Material Testing Services, Weyerhaeuser Company, Tacoma, WA.

- [76] Whale, L.R.J. 1988. "Deformation characteristics of nailed or bolted timber joints subjected to irregular short or medium term lateral loading." PhD Thesis, Polytechnic of the South Bank, CNAA, U.K.
- [77] Yao, J.T.P. 1985. *Safety and Reliability of Existing Structures*. Pitman Publishing Inc., Boston, MA.
- [78] Yasumura, M., I. Nishiyama, T. Murota, and N. Yamaguchi. 1988. "Experiments on a three-storied wooden frame building subjected to horizontal load." Proc. 1988 International Conference on Timber Engineering, Seattle, WA 2: 262-275.
- [79] Yeh, T.C., B.J. Hartz and C.B. Brown. 1971. "Damping sources in wood structures." *Journal of Sound and Vibration* 19(4): 411-419.

Vita

(June, 1993)

Greg, born on June 18, 1964, received a Bachelor of Science degree in Civil Engineering in 1984 from the Mapua Institute of Technology in Manila, Philippines. He obtained a professional civil engineering license the following year. From 1985 to 1987, he worked as a researcher at the Philippine Forest Products Research and Development Institute. He was a three-time Philippine representative to seminar-workshops sponsored by the United Nations Development Program (UNDP/UNIDO) related to building materials, technologies and construction systems. He performed damage assessment surveys on houses damaged by typhoons or tropical cyclones and helped interested professionals to organize a national technical team for typhoon damage assessment.

He came to the United States as a graduate student at Virginia Polytechnic Institute and State University (Virginia Tech) in September 1987. He taught some laboratory classes on mechanical properties of wood for the Department of Wood Science and Forest Products and an introductory class on microcomputing in natural resources for the School of Forestry and Wildlife Resources. He received a Master's degree in Wood Mechanics and Engineering in November 1989 and continued studies in the PhD program. His master's research on the strength capacity of notched wood beams generated positive interest from timber code authorities and design practitioners, and is currently being considered as the basis for notched wood beam design in the United States.

Greg received the 1993 A.B. Massey Award, given by the School of Forestry and Wildlife Resources at Virginia Tech, for superior performance and professionalism as a graduate student.

A handwritten signature in black ink, appearing to read "Greg Pliente". The signature is written in a cursive style with a horizontal line extending to the left and another to the right.